Optimisation of thermal treatment of invasive alien plants (IAPs) for char production for use in combustion applications

by

Jhonnah Mundike

Dissertation presented for the Degree

of

DOCTOR OF PHILOSOPHY
(Chemical Engineering)

in the Faculty of Engineering
at Stellenbosch University

Supervisor
Prof. Johann Görgens

Co-Supervisor
Dr. François-Xavier Collard

March 2018

Declaration

By submitting this dissertation electronically, I declare that the entirety of the work contained therein is my own, original work, that I am the sole author thereof (save to the extent explicitly otherwise stated), that reproduction and publication thereof by Stellenbosch University will not infringe any third-party rights and that I have not previously in its entirety or in part submitted it for obtaining any qualification.

Date: March 2018

This dissertation includes [02] original papers published in peer-reviewed journals or books and [01] unpublished publications. The development and writing of the papers (published and unpublished) were the principal responsibility of myself and, for each of the cases where this is not the case, a declaration is included in the dissertation indicating the nature and extent of the contributions of co-authors.

Abstract

Due to the popular worldwide demand for need to use cleaner fuels, lignocellulosic-derived char is gaining importance as a possible component in co-firing with coal. In order to avoid deforestation of indigenous forests in Zambia for char production, possibilities of using alternative feedstocks from invasive alien plants (IAPs) were investigated.

In the present study, torrefaction and slow pyrolysis were used for char production from IAPs for energy applications. Both processes were optimised individually at milligram-scale in a thermogravimetric analyser (TGA) for char yield and higher heating value (HHV), through manipulation of the temperature, heating rate and holding time. Two IAPs, namely *Lantana camara* (LC) and *Mimosa pigra* (MP), from Zambia were used as feedstock materials. The feedstock particle size distribution (PSD) used was from 425 to 600 µm. The optimisation results for torrefaction and slow pyrolysis showed that temperature majorly influenced char yield and HHV. In case of torrefaction, operating at temperatures ≤ 300 ˚C, heating rate and hold time also influenced char HHV, while neither parameters had a statistically-significant influence on char yield and HHV during slow pyrolysis.

During torrefaction at 300 ˚C, LC recorded a higher char yield of 43 wt.%, and a corresponding HHV of 27.0 MJ kg^{-1}, mainly due to increased hemicelluloses content, compared with MP that had a char yield of 52 wt.% with HHV of 24.4 MJ kg^{-1}. In case of slow pyrolysis, MP recorded the highest char HHV of 31.0 MJ kg^{-1} at 580 ˚C, due to increased lignin, in comparison with LC that had a highest char HHV of 30.0 MJ kg^{-1} at 525 ˚C.

Based on optimised conditions from milligram-scale, LC and MP samples of PSD from 850 to 2800 µm were used for char production at gram-scale in a bench-scale reactor. Scaling-up promoted secondary char formation due to mass and heat transfer limitations in larger particles and increased sample size, thereby increasing char yields for both biomasses. Char yields were increased by 4 and 2 wt.% for MP and LC, respectively, due to scale-up. The highest HHVs at bench-scale were 30.8 MJ kg^{-1} (614 ˚C) and 31.6 MJ kg^{-1} (698 ˚C) for LC and MP, respectively.

For the purposes of coal substitution and co-firing, a combustion study was conducted in a TGA reactor using LC and MP chars (torrefied and pyrolysed) from gram-scale of PSD from 850 to 2800 µm. LC and MP chars were blended with three South African coals between 5 to 90 wt.% (biomass char). The combustion characteristic results showed that LC chars were more reactive than MP chars, with significantly lower combustibility temperatures than the coals. During co-combustion, the combustion indices for blends < 30% were similar to those of the individual coals, showing that partial coal substitution could be done without significant modifications to existing equipment. There was better combustion performance through increased combustion indices for blends > 60%, though probably with a likelihood of modifications to existing reactors that were initially designed for coal combustion, as the conversion was much faster.

In summary, this study has shown that LC and MP IAPs could be valorised through torrefaction and slow pyrolysis to produce char for direct energy applications and co-firing with coal. LC samples torrefied at 300 ˚C were found to be equivalent to high volatile bituminous *C* coal, while pyrolysed chars for LC and MP were equivalent to high volatile bituminous *B* coal. To confirm the practicality of co-firing possibilities, it is recommended that scale-up studies to pilot-scale be conducted in order to assess overall energy efficiency, techno-economics, operating conditions of industrial reactors and a life cycle assessment.

Opsomming

Weens die populêre, wêreldwye behoefte om skoner brandstof te gebruik, is daar 'n toename in die belangrikheid van houtskool afkomstig vanaf lignosellulose as 'n moontlike komponent in die gesamentlike-verbranding met steenkool. Om ontbossing van inheemse bosse in Zambië vir houtskool produksie te voorkom, die moontlikheid om indringer uitheemse plante as grondstof te gebruik, is ondersoek.

In die huidige studie is die lae-temperatuur rooster, ook bekend as torrefaksie, en stadige pirolise benut vir die produksie van houtskool wat in energietoepassings gebruik kan word. Die eerste teiken was om houtskool produksie deur torrefaksie en stadige pirolise vir energietoepassings te optimeer, deur die houtskool-opbrengs en hoër-verhittings-waarde (HVW) te maksimeer, deur die optimering van temperatuur, verhittingstempo, en hou-tyd op milligram-skaal in 'n termo-gravimetriese analiseerder (TGA). Twee indringer uitheemse plante in Zambië, naamlik *Lantana camara* (LC) en *Mimosa pigra* (MP), was as grondstof gebruik. Vir die grondstof was 'n partikel-grootte-verspreiding (PGV) van 425 tot 600 µm gebruik. Die optimiserings-resultate vir torrefaksie en stadige pirolise het getoon dat temperatuur 'n groot invloed op houtskool-opbrengs en HVW gehad het. In die geval van torrefaksie was dit bevind dat vir temperature $\leq$ 300 ˚C, die verhittingstempo en hou-tyd ook die houtskool-HVW beïnvloed, terwyl vir stadige pirolise het beide veranderlikes geen statistiese merkbare invloed op die houtskool-opbrengs of HVW gehad nie.

Gedurende torrefaksie by 300 ˚C het LC 'n hoër houtskool-opbrengs van 43 massa% en 'n ooreenstemmende HVW van 27.0 MJ kg^{-1} gehad, grootliks as gevolg van die verhoogde hoeveelheid hemisellulose. Dit is in vergelyking met MP wat 'n houtskool-opbrengs van 52 massa% en 'n HVW van 24.4 MJ kg^{-1} gehad het. In die geval van stadige pirolise het MP 'n hoër maksimum HVW van

31.0 MJ kg^{-1} by 580 ˚C getoon as gevolg van verhoogde lignien inhoud. Dit is in vergelyking met LC wat ’n optimale houtskool HVW van 30.0 MJ kg^{-1} by 525 ˚C gehad het.

Gebaseer op die ge-optimiseerde kondisies op milligram-skaal, was LC en MP monsters met PGV van 850 tot 2800 µm gebruik vir houtskool produksie op gram-skaal in ’n laboratoriumskaal reaktor. Opskalering het sekondêre-houtskool-produksie bevorder as gevolg van massa-en-hitte-oordrag beperkinge in groter partikels en groter monster-groottes en gevolglik het beide monsters verhoogde houtskool-opbrengs getoon. Verhoogde houtskool-opbrengs verskille tot 4 en 2 massa% was verkry vir MP en LC onderskeidelik. Die opgeskaleerde optimale HVW resultate was 30.8 MJ kg^{-1} (614 ˚C) en 31.6 MJ kg^{-1} (698 ˚C) vir LC en MP onderskeidelik.

’n Verbrandingstudie was gedoen op LC en MP houtskool (vanaf torrefaksie en pirolise) met gram-skaal-PGV van 850 tot 2800 µm in ’n TGA reaktor met die doel van steenkool substitusie. LC en MP houtskool was gemeng met drie Suid-Afrikaanse steenkool in ’n verhouding van 5 tot 90 massa% (biomassa houtskool). Die verbrandingseienskappe-resultate het getoon dat LC houtskool meer reaktief is as MP houtskool, aangesien dit die verbrandingstemperatuur van al die steenkool aansienlik verlaag het. Gedurende gesamentlike-verbranding was dit bevind dat vir mengsels < 30% is die verbrandingsindekse soortgelyk was die van die individuele steenkool, wat wys dat gedeeltelike substitusie moontlik is sonder om merkbare veranderinge aan die bestaande toerusting hoef te maak. Vir mengsels > 60% was die verbrandings-bedrywe beter met verhoogde verbrandingsindekse, maar aangesien die verbranding baie vinniger was, sal daar waarskynlik veranderinge aan die bestaande toerusting gemaak moet word.

In opsomming, die studie het gewys dat indringer uitheemse plante, veral LC en MP, gebruik kan word deur torrefaksie en stadige pirolise om houtskool te produseer vir direkte energietoepassings deur gesamentlike-verbranding met steenkool. Dit was bevind dat LC monsters van torrefaksie by 300 ˚C, gelykwaardig is aan hoogsvlugtige bitumeniese *C* steenkool, terwyl gepiroliseerde houtskool van LC en MP gelykwaardig was aan hoogsvlugtige bitumeniese *B* steenkool. Om die praktiese moontlikehede van gesamentlike verbranding te bevestig, word dit voorgestel dat studies rakende die opskalering na loodskaal gedoen word om die algehele energie-doeltreffendheid, tegno-ekonomiese, en bedryftoestande van industriële reaktore te evalueer, sowel as ’n lewens-siklus-evaluasie.

Dedication

This thesis work is dedicated to my family, who have been very supportive during the entire long journey!

Acknowledgements

Primarily, I would like to thank my supervisor Prof. Johann Görgens for the professional and technical guidance as well as the opportunity given for me to enrol for this work. I am especially indebted to my co-supervisor Dr. François-Xavier Collard for his guidance, encouragement and support throughout the course of this degree.

I would like to thank the Department of Process Engineering at Stellenbosch University and the Copperbelt University from Zambia for their financial support which added value to this research work. For all the various laboratory analyses conducted, I would like to thank the following technical staff; Hanlie Botha, Levine Simmers and Alvin Petersen of Process Engineering, Cynthia Sanchez-Garrido of Soil Science and Henry Solomon of Forestry and Wood Science.

Finally, but not the least, special thanks to the thermochemical process development research group for all the memorable experiences we have had, good and bad, frustrating and up-lifting, they all added value to this work. A special friendly thank you to David Naron, Frank Nsaful, Logan Brown, Malusi Mkize and Angelo JJ Ridout (Dr.), who we shared technical and professional experiences in our research group as we journeyed through this period of study.

Special thanks to Salomie Van der Westhuizen for the translation of the English version of the abstract into Afrikaans.

Table of contents

List of Figures

List of Tables

List of acronyms and abbreviations

AC	Ash content
AFT	Ash fusion temperature
ANOVA	Analysis of variance
ASTM	American Standards for Testing of Materials
BET	Brunauer, Emmet and Teller
Bρ	Bulky density
CCD	Central composite design
C_i	Combustion index
DoE	Design of experiments
DTG	Derivative thermogravimetric
DTG_{max}	Maximum combustion rate
DTG_{mean}	Average or mean combustion rate
EnY	Energy yield
FAO	Food and Agriculture Organisation
FC	Fixed carbon
GC-MS	Gas chromatography-mass spectrometery
HAA	Hydroxyacetaldehyde
HHV	Higher heating value
HR	Heating rate
HT	Hold time
IAPs	Invasive alien plants
LC	*Lantana camara*
MP	*Mimosa pigra*
NIST	National Institute for Standards and Technology

PSD	Particle size distribution
RSD	Relative standard deviation
R^2	R-squared
R^2 adj	R-squared adjusted
TAPPI	Technical Association for Pulp and Paper Industries
T_{bo}	Burnout temperature
TGA	Thermogravimetric analyser
T_{ig}	Ignition temperature
T_{pk}	Peak temperature
VM	Volatile matter
Ychar	Char yield

Chapter 1 **Introduction**

1.1 Contextual background

Of the 78% of the global energy supply that is comprised of fossil energy [1], coal represents about 40%, especially for power generation [2]. Due to the challenges of negative environmental impacts from the use of fossil fuels and their ultimate depletion, lignocellulose-based energy-carriers are one of the main alternative and renewable sources of energy to substitute fossil fuels [3,4]. In Zambia, the main types of urban solid fuels are fire-wood (61%), charcoal (25%) and coal (14%) [5,6]. Firewood and charcoal are mainly domestic fuels, while coal is used for industrial applications. In case of charcoal as a domestic fuel, it is more popular than fire-wood because it requires less space for storage with longer storage time, has higher energy content and releases less smoke when burning [7].

However, charcoal is mainly linked to deforestation of indigenous forests, land degradation, promotes global climate change and its production is energy inefficient, with close to half of the input energy lost during the production process [7–10]. Charcoal has long been made from traditional, low-efficiency earth-kilns with minimal industrialization and mechanisation of the charcoal production process [11]. Zambia's high deforestation rate is mainly associated with subsistence agriculture and charcoal production impacting mainly indigenous trees [12].

The proliferation of invasive alien plants (IAPs) worldwide is of major concern to affected natural ecosystems [13–17]. Globally, IAP proliferation is a serious threat to affected agricultural land and natural ecosystems [13–17]. Man is responsible for the global increase of IAPs in most regions [18], with some of these IAPs intentionally introduced for restorative purposes, while other IAPs were unintentionally introduced [19,20]. Whether intentionally or unintentionally introduced, IAPs are a serious threat to various ecosystems worldwide. In South Africa for example, the most negatively affected ecosystems due to presence of IAPs are

pastures for grazing, surface and groundwater resources, agricultural land, forestry and fishery resources [21–24].

The motivations for seeking alternative solutions for management and control of IAPs differ from one country or region to another. Zambia, like many other countries worldwide, has not been spared from the invasion of terrestrial IAPs. Out of the many IAPs found in Zambia, *Lantana camara* (LC) and *Mimosa pigra* (MP) are the most notable [25–27], impacting different types of ecosystems including agricultural land in most parts of the country. For instance, by 2005, more than 29, 000 hectares of land had been covered by MP along one section of the Kafue Flood Plains [26]. The main control methods for IAPs globally are mechanical, chemical and biological. Mechanical methods use physical means; chemical methods employ the use of herbicides, while biological methods utilise biocontrol agents or living organisms [17,28]. The management and control strategies of IAPs can be costly in terms of human resources and capital investments [22,23] with little or no returns [29,30].

However, these IAPs could be viable feedstock materials for producing value-added products like good quality char (commonly called charcoal), in particular, which is a potential substitute for domestic and industrial use with coal, possibly through co-firing [31,32]. Zambian charcoal is mainly produced from indigenous trees that are fast being depleted due to increased demand for charcoal use domestically [8,9,12]. For the Zambian scenario, use of IAP lignocellulose for charcoal production could provide environmental benefits, not only due to mitigation of deforestation, but also through the use of efficient production methods with high conversions and low emissions [33], compared with the less efficient traditional earth-kiln method presently used [9]. Furthermore, production of char from IAP lignocellulosic biomass will support the continued clearing of bush encroachment, ultimately freeing up land for other productive activities like crop and animal farming, while finding a renewable and alternative solid fuel as

a substitute for coal and as a domestic fuel. In this way, mechanically harvested IAP lignocellulosic biomass could be valorised. This approach would also be in line with the increasing demand for cleaner fuels worldwide, which has been directed towards the use of renewable feedstocks [3].

The present project will consider the conversion of IAP lignocelluloses into char that can serve as a (partial) substitute for coal in industrial processes. Coal from Zambia, is generally of low or medium grade, mainly used for various industrial processes [34]. Despite the environmental and health impacts, the industrial energy market is still dominated by coal as the main solid fuel [1,35]. Coal use significantly impacts the environment, such as air pollution from oxides of sulphur and other greenhouse gas emissions, for example CO_2 [2]. The co-utilisation of coal and lignocellulosic biomass in energy applications offers environmental benefits through partial mitigation of pollutant emissions [32,36] and reduced CO_2 greenhouse gas emissions [37].

Coal substitution or replacement using renewable energy sources still poses challenges in terms of the quantity and quality of the possible substitutes. Although lignocellulosic biomass appears to be a credible alternative, renewable energy resource to coal, it suffers one main disadvantage, that is, that of low energy content [3]. Lignocellulosic biomass needs to be modified or converted into char/charcoal, in order to provide fuel properties more similar to coal. The main thermal technologies that could modify and maximise char from lignocellulosic biomass are torrefaction [4,38] and slow pyrolysis [29,39], which could become bioenergy technologies for the diversification of the Zambian energy sector.

The main goal of this study is to optimise the production of char from two IAPs of LC and MP from Zambia for energy applications in industrial processes, in particular by considering the desired quality of the char required for partial coal substitution through industrial co-firing. The

char product from torrefaction or slow pyrolysis could be used as a biofuel for heat energy generation through combustion [40], as well as co-combustion [36,41–43]. Co-combustion involves the blending of lignocellulosic biomass and/or lignocellulose-derived char with coal. Though most studies on co-combustion have focused on blending coal with raw lignocellulose [32,36,42], with some on torrefied lignocellulosic biomass [41,44] and pyrolysis char [45], rare works on assessing the influence of torrefied and pyrolysed char on coal blends have been reported. In the current work, torrefied and pyrolysed char from LC and MP will be blended with coal in order to assess the effect of each pre-treatment on the performance of various blending ratios under combustion conditions.

1.2 Thesis outline

This dissertation consists of 9 chapters. **Chapter 2** outlines the motivation behind the use of IAP lignocellulose as feedstock materials for char especially for energy applications using thermal technologies of torrefaction and slow pyrolysis. The chapter further discusses quality control parameters, which could be useful in defining char quality as a possible substitute for coal. In addition, the chapter also presents the process conditions of temperature, heating rate and hold time applicable to torrefaction and slow pyrolysis for producing char for energy use. C**hapter 3** presents the specific objectives developed after reviewing literature and identifying existing gaps in order to justify the current work. **Chapter 4** includes the materials and main methods used in conducting key experimental works detailed in **Chapters 5-7** of this study. **Chapter 5** discusses the results from the feedstock characterisation and optimisation of process parameters for torrefaction using the two IAPs, LC and MP at milligram-scale in a thermogravimetric analysis (TGA) reactor. **Chapter 6** details the slow pyrolysis of LC and MP at milligram-scale, by investigating the influence of temperature, heating rate and hold time on char yield and HHV. The chapter further assess the influence of scale-up on the char properties

by comparing TGA with gram-scale results. **Chapter 7** describes the combustion characteristics of parent fuels and blended fuel samples. The parent fuels include torrefied and pyrolyzed LC and MP chars produced at gram-scale and three South African coals. **Chapter 8** contains the potential application of chars produced from LC and MP. The main conclusions and recommendations of the entire study are contained in **Chapter 9.**

1.3 References

[1] Energy Information Administration (EIA). International Energy Outlook 2016. vol. 484. Washington, DC 20585: 2016.

[2] International Energy Agency (IEA). Energy, Climate Change & Environment. Paris: 2016.

[3] Garcia R, Pizarro C, Lavin AG, Bueno JL. Characterization of Spanish biomass wastes for energy use. Bioresour Technol 2012;103:249–58.

[4] Basu P. Biomass Gasification, Pyrolysis and Torrefaction: Practical Design and Theory. second ed. London: Academic Press; 2013.

[5] Munyeme G, Jain P. Energy scenario of Zambia: Prospects and constraints in the use of renewable energy resources. Renew Energy 1994;5:1363–70.

[6] Ministry of Energy & Water Development. National Energy Policy-2008. vol. 1. Lusaka: 2008.

[7] Adam JC. Improved and more environmentally friendly charcoal production system using a low-cost retort–kiln (Eco-charcoal). Renew Energy 2009;34:1923–5.

[8] Chidumayo EN. Forest degradation and recovery in a miombo woodland landscape in Zambia: 22 years of observations on permanent sample plots. For Ecol Manage 2013;291:154–61.

[9] Chidumayo EN, Gumbo DJ. The environmental impacts of charcoal production in tropical ecosystems of the world: A synthesis. Energy Sustain Dev 2013;17:86–94.

[10] Kammen DM, Lew DJ. Review of Technologies for the Production and Use of Charcoal Table of Contents : California: 2005.

[11] Chidumayo EN. A survey of wood stocks for charcoal production in the Miombo

woodlands of Zambia. For Ecol Manage 1987;20:105–15.

[12] Vinya R, Syampungani S, Kasumu E, Monder C, Kasubika R. Preliminary Study on the Drivers of Deforestation and Potential for REDD+ in Zambia. 2011.

[13] Baars J-R. Geographic range, impact, and parasitism of lepidopteran species associated with the invasive weed Lantana camara in South Africa. Biol Control 2003;28:293–301.

[14] Baars J-R, Urban AJ, Hill MP. Biology, host range, and risk assessment supporting release in Africa of Falconia intermedia (Heteroptera: Miridae), a new biocontrol agent for Lantana camara. Biol Control 2003;28:282–92.

[15] Forsyth GG, Le Maitre DC, O'Farrell PJ, van Wilgen BW. The prioritisation of invasive alien plant control projects using a multi-criteria decision model informed by stakeholder input and spatial data. J Environ Manage 2012;103:51–7.

[16] Richardson DM, Rejmánek M. Trees and shrubs as invasive alien species - a global review. Divers Distrib 2011;17:788–809.

[17] Vardien W, Richardson DM, Foxcroft LC, Thompson GD, Wilson JRU, Le Roux J. Invasion dynamics of Lantana camara L. (sensu lato) in South Africa. South African J Bot 2012;81:81–94.

[18] Mack RN, Simberloff D, Lonsdale MW, Evans H, Clout M, Bazzaz F. Biotic Invasions: Causes, Epidemiology, Global Consequences, and Control. Ecol Appl 2000;10:689–710.

[19] Eviner VT, Garbach K, Baty JH, Hoskinson S. Measuring the Effects of Invasive Plants on Ecosystem Services: Challenges and Prospects. Invasive Plant Sci Manag 2012;5:125–36.

[20] Barney JN. Bioenergy and Invasive Plants: Quantifying and Mitigating Future Risks.

Invasive Plant Sci Manag 2012;5:125–36.

[21] Enright WD. The effect of terrestrial invasive alien plants on water scarcity in South Africa. Phys Chem Earth, Part B Hydrol Ocean Atmos 2000;25:237–42.

[22] Le Maitre DC, van Wilgen BW, Gelderblom CM, Bailey C, Chapman RA, Nel J. Invasive alien trees and water resources in South Africa: case studies of the costs and benefits of management. For Ecol Manage 2002;160:143–59.

[23] McConnachie MM, Cowling RM, van Wilgen BW, McConnachie DA. Evaluating the cost-effectiveness of invasive alien plant clearing: A case study from South Africa. Biol Conserv 2012;155:128–35.

[24] van Wilgen BW, Reyers B, Le Maitre DC, Richardson DM, Schonegevel L. A biome-scale assessment of the impact of invasive alien plants on ecosystem services in South Africa. J Environ Manage 2008;89:336–49.

[25] Nang'alelwa MM. Effects of treatment on Lantana camara (L.) and the restoration potential of riparian seed banks in cleared areas of the Victoria Falls World Heritage Site, Livingstone, Zambia. Rhodes, 2010.

[26] Shanungu GK. Management of the invasive Mimosa pigra L. in Lochinvar National Park, Zambia. Biodiversity 2009;10:56–60. doi:10.1080/14888386.2009.9712844.

[27] Mumba M, Thompson JR. Hydrological and ecological impacts of dams on the Kafue Flats floodplain system, southern Zambia. Phys Chem Earth, Parts A/B/C 2005;30:442–7.

[28] Zalucki MP, Day MD, Playford J. Will biological control of Lantana camara ever succeed? Patterns, processes & prospects. Biol Control 2007;42:251–61.

[29] Liao R, Gao B, Fang J. Invasive plants as feedstock for biochar and bioenergy production. Bioresour Technol 2013;140:439–42.

[30] van Wilgen BW, Forsyth GG, Le Maitre DC, Wnnenburgh A, Kotze JDF, van den Berg E, Henderson L. An assessment of the effectiveness of a large, national-scale invasive alien plant control strategy in South Africa. Biol Conserv 2012;148:28–38.

[31] Van Loo J, Koppejan S. The handbook of biomass combustion & co-firing. first ed. Washington, DC: Earthscan; 2008.

[32] Kubacki ML, Ross AB, Jones JM, Williams A. Small-scale co-utilisation of coal and biomass. Fuel 2012;101:84–9.

[33] Tripathi M, Sahu JN, Ganesan P. Effect of process parameters on production of biochar from biomass waste through pyrolysis: A review. Renew Sustain Energy Rev 2016;55:467–81.

[34] Bennett JD. Review of Lower Karoo coal basins and coal resource development in parts of central and southern Africa with particular reference to northern Malawi Keyworth , Nottingham British Geological Survey 1989. Nottingham: 1989.

[35] Schweinfurth SP. An introduction to coal quality. Virginia: 2009.

[36] Smajevic I, Kazagic A, Music M, Becic K, Hasanbegovic I, Sokolovic S, Delihasanovic N, Skopljak A, Hodzic N. Co-firing bosnian coals with woody biomass: Experimental studies on a laboratory-scale furnace and 110 MW e power unit. Therm Sci 2012;16:789–804.

[37] Mellin P, Wei W, Yang W, Salman H, Hultgren A, Wang C. Biomass availability in Sweden for use in blast furnaces. Energy Procedia 2014;61:1352–5.

[38] Pimchuai A, Dutta A, Basu P. Torrefaction of agriculture residue to enhance combustible properties. Energy and Fuels 2010;24:4638–45.

[39] Lee Y, Eum P-R-BRB, Ryu C, Park Y-KK, Jung J-HH, Hyun S. Characteristics of biochar produced from slow pyrolysis of Geodae-Uksae 1. Bioresour Technol

2013;130:345–50.

[40] Di Blasi C. Combustion and gasification rates of lignocellulosic chars. Prog Energy Combust Sci 2009;35:121–40.

[41] Liu Z, Hu W, Jiang Z, Mi B, Fei B. Investigating combustion behaviors of bamboo, torrefied bamboo, coal and their respective blends by thermogravimetric analysis. Renew Energy 2016;87:346–52.

[42] Moon C, Sung Y, Ahn S, Kim T, Choi G, Kim D. Effect of blending ratio on combustion performance in blends of biomass and coals of different ranks. Exp Therm Fluid Sci 2013;47:232–40.

[43] Aho M, Gil A, Taipale R, Vainikka P, Vesala H. A pilot-scale fireside deposit study of co-firing Cynara with two coals in a fluidised bed. Fuel 2008;87:58–69.

[44] Sahu SG, Sarkar P, Chakraborty N, Adak AK. Thermogravimetric assessment of combustion characteristics of blends of a coal with different biomass chars. Fuel Process Technol 2010;91:369–78.

[45] Kastanaki E, Vamvuka D. A comparative reactivity and kinetic study on the combustion of coal-biomass char blends. Fuel 2006;85:1186–93.

Chapter 2 **Literature review**

This chapter outlines a general overview of the literature on the use of invasive alien plants (IAPs) as solid biofuels in energy applications, and the composition of lignocellulosic biomass. The chapter also details the main thermal technologies (torrefaction and slow pyrolysis) for producing char from lignocellulosic biomass. The process conditions of temperature, heating rate and hold time, which ultimately influence the fuel properties of the desired product, are also considered.

2.1 General overview

The advantages of using lignocellulosic biomass resources for energy applications over fossil fuels are mainly renewability, environmental benefits and socio-political gains [1]. Torrefaction and slow pyrolysis of IAP lignocellulose could be a means of valorisation for mechanically harvested IAPs. Therefore, lignocellulosic char from torrefaction or slow pyrolysis should be of good and competitive quality to compete with coal that has been well-established. This implies that the quality of char should be well defined and established so that the required standards of the desired char can be guaranteed [2]. Several analytical techniques are required for establishing char quality control. The techniques for characterising char for its chemical composition, energy content and reactivity during combustion, are detailed in a specific section (2.2.2 below).

The main composition of lignocellulosic biomass is cellulose and hemicelluloses (carbohydrate polymers) and lignin, with minor components like extractives and inorganics (minerals) [1,3]. Pyrolysis/torrefaction is the thermal conversion of a carbonaceous feedstock material (lignocellulosic biomass) in inert environments into gas, bio-oil and char [1]. The proportions of the pyrolysis products are related to the type of lignocellulosic biomass as well as the parameters of conversion

(temperature, heating rate, pressure, particle size) [4]. It is well accepted that relatively low heating rates ($\leq 20^{\circ}C\ min^{-1}$) promote the production of char [5–8], generally with final temperatures in the range (300-800˚C) [7,9,10] according to the reactor configurations. When slow pyrolysis is performed under a relatively low temperature (T < 300˚C), the conversion process to char is not completed, resulting in a distinct char product, in a process known as torrefaction. Although the energy density of the char obtained by torrefaction is intermediate between lignocellulose and pyrolysis-char, such char could also be considered for energy applications, for instance for use in co-combustion with coal [11]. Vacuum pyrolysis is a modified type of slow pyrolysis that utilises an operating vacuum atmosphere, while heating rates and temperature ranges are similar to slow pyrolysis. While slow pyrolysis will typically give the highest char yield, char obtained from vacuum pyrolysis have specific properties [5,12–14], which make them more applicable for soil amendments and biomaterials [12,15]. When compared with slow pyrolysis using sugar cane bagasse, vacuum pyrolysis was reported to have reduced calorific value of the char (measured as the higher heating value, HHV) [7]. Since there are challenges with maintaining vacuum conditions at industrial scale, vacuum pyrolysis technology was rendered unsuitable for this study.

The most commonly known fuel properties applicable to lignocellulosic char include proximate analysis, reported in terms of fixed carbon, volatile matter and ash [16], as well as elemental composition, with emphasis on carbon, hydrogen and oxygen [16,17]. HHV constitutes the energy content per unit mass of the fuel [1,18]. The high oxygen content of lignocellulosic biomass generally lowers its HHV [19]. The other fuel properties include bulk density that is useful in transportation and storage, ash fusion temperature in furnaces and pore surface area in terms of oxygen diffusion during combustion [7,20]. Most, if not all, of the fuel properties of char are influenced by process conditions during thermal conversion of lignocellulosic biomass, as well as the properties of the biomass raw materials.

2.2 Use of IAPs as feedstock materials for char production

Invading weeds on land or water have globally affected various ecosystems due to the easy and free movement of people worldwide. The global proliferation of IAPs is of concern as it does threaten biodiversity [21–24]. Globally, IAPs could be linked to negative impacts that affect economic, environmental and social aspects of human life [25]. The economic impacts can be directly linked to financial losses, environmental impacts are those that bring unexpected changes to biodiversity and may be linked to climate change [26], while social impacts are those that may affect human quality of life in terms of health and safety [25,27].

Lantana camara (LC) is a global IAP found mainly in tropical regions [28,29]. In Zambia, LC is mainly found in most eucalyptus and pine forest plantations, within Mosi-O-Tunya National Park, near the Victoria Falls in Livingstone as well as general bush and farm-land encroachment countrywide [30]. *Mimosa pigra* (MP) originates from the tropical regions of central America whose impacts are prevalent in most tropical countries of the world [31–33]. In Zambia MP is mainly found in Lochinvar National Park of the Kafue Flood Plains, threatening the grazing pastures of the black lechwe and other herbivorous animals [32,34]. MP is also found along the Zambezi River in western and southern provinces of the country. As a way of controlling and managing IAPs, biological, chemical and mechanical strategies have been used [28,35–38], even though Liao et al. [6] reported that these management strategies have recorded minimal success in their use as control measures. Standardised control and management methods have so far not emerged worldwide for most IAPs, despite their significant economic and ecological impacts [28,39].

Of late, some works have investigated the opportunity of thermally converting IAP lignocellulosic biomass for solid bioenergy applications [6,12]. In particular Wongsiriamnuay and Tippayawong [40,41] considered the utilisation of MP in Thailand and studied its conversion at milligram-scale in

oxidative and inert environments. In India, Sharma et al. [42] reported the use of LC for biogas production and further proposed the burning of dried LC as firewood, while Kumar and Chandrashekar [43] studied the combustion behaviours of LC wood char.

Therefore, the proposed use of IAP lignocellulose as feedstock material for thermal conversion, to produce char as an energy-carrier, is expected to offer an option towards value-addition to the management strategies of IAPs. This approach will further add value to land-use patterns, as more cleared land will be readily available for other viable economic activities like animal husbandry and cash crop farming, ultimately improving food security and boosting tourism in case of affected game national parks. Moreover, the use of IAPs could minimise depletion of indigenous trees, an environmental impact that, is closely linked to traditional charcoal production [44], especially in Zambia. In the Zambia context, where coal is largely (48%) used for energy production in industrial processes and 37% in the mining sector [45], its substitution through co-firing with char produced from IAP feedstocks appears as a promising opportunity. The use of IAPs as feedstocks for char production using torrefaction and slow pyrolysis will promote the concept of relatively cleaner energy compared with coal. Another application for char produced from IAP could be meeting the domestic charcoal market demands. In this way, the depletion of indigenous trees that are directly linked to traditional charcoal production [44,46], especially in Zambia, could be minimised.

2.2.1 Lignocellulosic biomass for torrefaction and pyrolysis

Lignocelluloses come mainly from virgin terrestrial and aquatic plants [1]. Lignocellulosic biomass, the oldest source of energy, is mainly composed of lignin, hemicellulose and cellulose materials that are not starch but fibrous components of the plant material [1,47,48]. The main classes of lignocelluloses are softwood, hardwood and herbaceous plants as summarized in Table 2-1. As

indicated in Table 2-1 on a weight dry basis, cellulose constitutes at least half of lignocelluloses followed by hemicelluloses or lignin depending on the biomass type. Softwoods contain relatively more lignin than hardwoods, and vice-versa for hemicelluloses.

Table 2-1: Composition of different lignocellulose (% dry weight)

Biomass	Cellulose	Hemicelluloses	Lignin	Reference
Herbaceous plants	24-50	12-38	6-29	[3,49]
Softwoods	41-50	11-33	19-30	[3,49,50]
Hardwoods	39-53	19-36	17-24	[3,9,49]

2.2.1.1 Cellulose

The main structural component of plant cell wall is cellulose [49,51], forming up to 50 wt.% on dry basis (Table 2-1). Cellulose is made up of linearly linked cellobiose units through β–(1–4) glycosidic bonds, with degree of polymerisation ranging from 500 to 15, 000 glucose units [52,53]. The molecules of cellulose are linked together through hydrogen bonds (OH groups) [1]. Strong intra-molecular and inter-molecular hydrogen bonding agglomerate hydroxyl groups together forming the cellulose fibril structure [54]. The macro and micro-fibrils in the cellulose molecules form highly ordered patterns that provide plant cell walls with crystalline properties [55]. A simplified linearly linked cellobiose unit through β–(1–4) glycosidic bonds forming a cellulose polymer is shown in Figure 2-1.

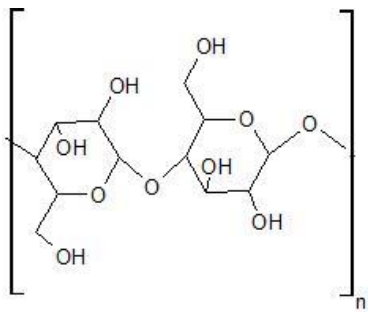

Figure 2-1: Cellulose polymer

(Source [56])

2.2.1.2 Hemicelluloses

On a dry basis, hemicelluloses form up to 30 wt.% of the main composition of lignocelluloses (Table 2-1). Hemicelluloses form shorter heterogeneous, highly branched and very amorphous molecules, compared to cellulose, with up to 200 interconnecting monosaccharide units joined linearly and/or branched [57,58]. The most common monosaccharide units found in hemicelluloses are D-galactose, D-glucose, D-glucuronic acid, D-xylose, D-mannose and L-arabinose, forming various types of alpha (α) and beta (β) bonds between them [52,59,60]. Figure 2-2a shows the structural arrangement of hemicelluloses monomers. The most common hemicelluloses branched polymer is xylan [47], as shown in Figure 2-2b. Xylan is mostly found in hardwoods (angiosperms) and annual plants like herbaceous plants and agricultural residues, while softwoods (gymnosperms) are mainly composed of glucomannans [57,61].

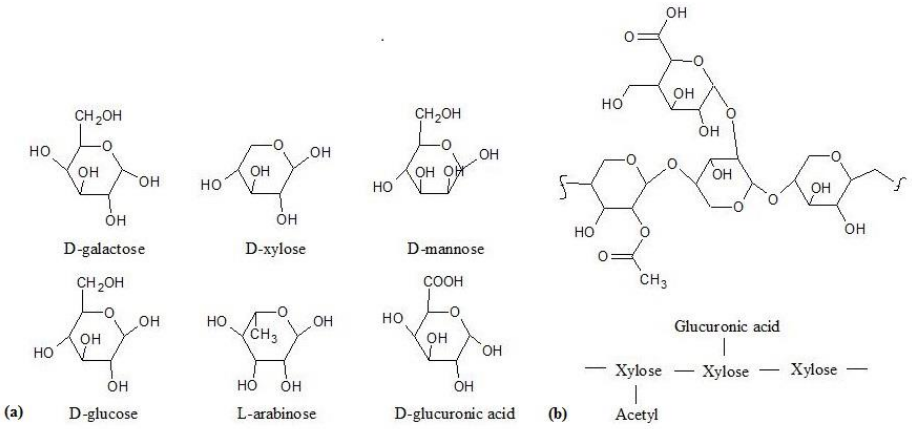

Figure 2-2: Structural arrangement of (a) hemicelluloses monomers (b) partial structure of xylan

(Source [56])

2.2.1.3 Lignin

On a dry basis, lignin consist of 15 to 35% of lignocelluloses [62]. Lignin is a complex three-dimensional heterogeneous natural polymer consisting of three benzene units, namely, guaiacyl (G),

p-hydroxyphenyl (H) and syringyl (S) [1,52]. Guaiacyl and synapyl monomers are predominantly found in hardwoods, while softwoods mainly consist of guaiacyl monomers [63]. The age of the plant as well as the local environment of growth can influence the lignin content [64]. The cross-linking and coupling of the different monomers through polymerisation in lignin result into a highly branched structure [1,52]. Lignin in lignocellulosic biomass is a fibrous natural binding agent shielding polysaccharides from destruction from fungi and bacteria [1]. The degree of polymerisation in lignin can vary between 450 to 500 units, mainly joined together by carbon-carbon and carbon-ether bonds [52], with benzene rings being the main monomeric units in the lignin polymer [65], as shown in Figure 2-3. Lignin also contains oxygenated compounds within its polymer, like alcohol, carboxylic acid and carbonyl [66,67].

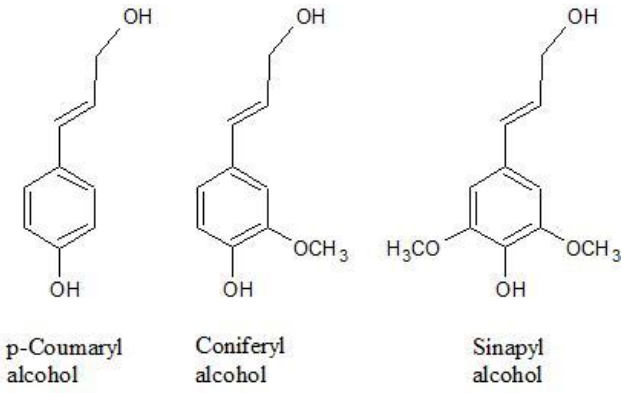

Figure 2-3: Structural arrangements of benzene rings found in lignin

(Source [56])

2.2.1.4 Extractives and inorganics

Extractives mainly consist of insoluble and soluble components like alkaloids, essential oils, fats, gums, glycosides, proteins, phenolics, pectins, resins, terpenes, waxes and simple sugars. They are mainly found between the plant fibres acting as a defence mechanism against microbes [47].

Inorganics or minerals are present in crystalline, semi-crystalline and amorphous solids mainly absorbed from the soil during plant growth [68]. These inorganics could be in the form of carbonates (Na/Mg), chlorides (Ca), oxy-hydroxides (Cu/Al), nitrates (K), phosphates, silicates, sulphates (Ca) and many others depending on the soil type [69]. The residue that remains after complete combustion is referred to as total inorganics or ash and varies according to the type of lignocellulosic biomass [53]. Inorganics in lignocellulosic biomass are known to have catalytic effects during pyrolysis [70]. The inorganics, hemicelluloses, cellulose and lignin compositions of raw biomass all collectively influence the product quality and properties of the resultant product of pyrolysis [71].

2.2.1.5 Thermal degradation of lignocellulosic biomass

The behaviour of lignocellulosic components in biomass during thermal treatment has been studied using pure samples of hemicelluloses, cellulose and lignin in a thermogravimetric analyser (TGA) [63]. [Analysis of the thermogravimetric (TG) and derivative thermogravimetric (DTG) curves shows that the weight loss in the lower temperature region of 200 to 350 ˚C, represents hemicelluloses decomposition, while a slightly higher temperature range of 260 to 430 ˚C represents cellulose weight loss, with lignin weight loss peak seen from 200 to 500 ˚C [63]. Between 310 to 330 ˚C, the DTG curves show an intersection, a temperature zone where maximum gas production occurs, mainly from hemicelluloses and cellulose [3,52,63].

As stated earlier, during thermal decomposition of lignocellulosic constituents, hemicelluloses decompose early from around 200 to 350 ˚C [40,52,61]. Xylans quickly break down at lower temperatures than glucomannans, mainly through dehydration reactions to form water [61,72,73].

Due to its crystalline nature, cellulose breaks down at slightly higher temperatures than hemicelluloses when thermally treated [74]. Cellulose thermally decomposes from 300 to 390 ˚C

[59,63,72]. As for lignin, when thermally treated, lignin cross-linkages may behave differently, mainly due to differences in chemical bond energies [75] . Therefore, lignin decomposes over a wider range of temperature, generally from 200 to 500 ˚C [40,52,63].

The main products during thermal degradation of lignocellulosic biomass in an inert environment are the solid char, tar and gases [1,18]. Temperature, heating rate and hold time play a major role in determining the products to be formed [18,40]. During pyrolysis of pure components, cellulose recorded the lowest char yields followed by hemicelluloses, while the highest char yields were obtained from lignin [63,76]. Similarly, lignin in lignocellulosic biomass feedstocks is mainly attributed to the production of increased char yields compared with hemicelluloses and cellulose [77,78]. Char from cellulose is mainly characterised with increased surface area than that from hemicelluloses and lignin [79].

Lignocellulose with generally a low HHV has been used as a fuel directly for a long time. Generally on a dry basis, raw lignocellulose contain on average 48% of carbon, 6% of hydrogen and 42% of oxygen, with an average HHV of 19 MJ kg^{-1} [79]. The relatively high amounts of oxygen is responsible for the low HHV, compared to fossil fuels such as coal [80]. In order to improve its energy density, there is need to convert raw lignocellulose to useful products such as lignocellulosic char [19].

Raw lignocellulosic biomass can be converted into fuel by means of thermochemical technologies [18]. In order to produce solid value-added products like char for coal substitution or co-combustion, thermal conversion (torrefaction and slow pyrolysis) of organic materials in inert environments (thermochemical) appears as the most suitable technologies [1,19]. Since lignocellulosic feedstock materials vary in type and composition [1,81], different quantities and qualities of char can be

obtained from torrefaction and slow pyrolysis. Moreover, the parameters of conversion (temperature, heating rate, hold time, particle size) also modify significantly the composition and yield of the end products [5,7,82]. Hence, prior to studying the thermal conversion of lignocellulose itself, there is need to determine, depending on the targeted use, the required quality of the char.

2.2.2 Quality of lignocellulosic char

Char production for energy use requires control of its quality, so that the required standards of the end-product can be assured [2]. In this way, the quality of the feedstock material used in the production process could be assessed in order to allow for variations.

After considering the mass yield of char, the most-frequently reported parameters of char characterisation are chemical analyses (ultimate and proximate) and HHV [83–87]. Other parameters rarely studied but of particular interest for industrial applications are ash fusion temperature (AFT), bulk density (Bρ), and Brunauer Emmett and Teller (BET) surface area. Recently several works reported the development of methods to study the combustion properties of a solid fuel using thermogravimetric analysis (TGA), some using biomass only [88]; others lignocellulosic char [43,89], while some have used coal blends with various lignocelluloses [11,90,91]. All or some of the above-mentioned parameters could be used as quality control measures in order to compare lignocellulosic char and coal properties for energy applications.

2.2.2.1 Char composition and higher heating value

The energy content of a fuel is generally estimated using a bomb calorimeter by measuring its HHV, which is the energy released by a unit weight of fuel when it undergoes complete combustion in an oxygen-rich environment. Proximate and ultimate analysis results are usually correlated with HHV.

Literature has shown that increased carbon content, in particular high fixed carbon, is linked to high energy content [79,92]. Fixed carbon and volatile matter positively influence HHV, while moisture and ash contents have a negative impact on char HHV [93,94]. For elemental analysis, carbon, hydrogen and sulphur do have positive influences, while oxygen and nitrogen negatively influence char HHV [18]. After thermal treatment of lignocellulosic biomass, a ratio of the preserved energy in the treated sample to that of the energy contained in the raw sample, is a measure of gross energy yield [17,95]. Energy yield (EnY; %) can be determined using the expression in equation 1:

$$EnY\ (\%) = \frac{Product\ weight\ x\ HHV_{product}}{Raw\ sample\ weight\ x\ HHV_{raw\ sample}}\ x\ 100 \quad \text{.....Equation 1.}$$

Where raw sample weight is the mass of the initial raw biomass, product weight is the mass of the resultant char and HHV is the higher heating value (MJ kg^{-1}).

2.2.2.2 Other parameters

Bρ determination is very useful for flow consistency, storage and transportation purposes as it translates to the weight of solid fuel per unit volume [80]. Lignocellulosic biomass Bρ is also useful in the iron ore sintering process where coal could be blended with lignocellulosic char , as the sinter quality in terms of abrasion strength reduces with increased char in the blend [96].

The temperature at which ash fuses (AFT) is an important process parameter in the design of industrial heat energy reactors. If the ash fuses during combustion of fuel in furnaces, fouling will build up with more concern on heat transfer surfaces, thereby reducing the equipment performance efficiency [20,97,98]. Despite the testing conditions not necessarily matching those found in practice, it has been found that a link does exist between laboratory fusion characteristics and those experienced in practice [2,20,97,98]. In literature, most of the studies on AFT have been reported on coal with minimal works on char.

BET surface area analysis has been developed to determine the porosity of the char. This determination is mainly used for application in activated carbon and soil amendments [14,15,99]. In the case of char combustion, the pores found in the char also constitutes a key parameter as it influences the diffusion of the oxygen and thus the reactivity of the char.

In trying to define char quality, AFT, BET surface area and Bρ amongst others could assist in further defining the quality of chars for various energy applications. However, minimal information has been reported on the influence of operational conditions on these parameters especially for the use of chars as energy carriers. Recently studies have shown that TGA can be used to study the combustion reactivity of fuels [43,89,100]. By monitoring the evolution of the mass of a fuel during its combustion under oxidising environments with a controlled flow of air, it is possible to determine the temperatures of ignition (at which conversion rate rises to one weight percent per minute of the original sample (1wt.% min^{-1}) and burnout (conversion rate starts to diminish to 1wt.% min^{-1}) [100]. Further Xiong et al. [89] proposed that the performance of any carbonaceous fuel (char) when burned in oxygen-rich environments can be evaluated by combustion index (C_i), a combustion characteristic index, as expressed in equation 2 below.

$$C_i = \frac{(\frac{dw}{dt})_{max}\,(\frac{dw}{dt})_{mean}}{T_{ig}^2\,T_{bo}} \quad \text{.....Equation 2}$$

Where T_{ig} is the ignition temperature; T_{bo} is the final or burnout temperature; $\left(\frac{\mathrm{dw}}{\mathrm{dt}}\right)$mean is the percentage average combustion rate per minute; $\left(\frac{\mathrm{dw}}{\mathrm{dt}}\right)$max is the percentage maximum combustion rate per minute and C_i is the index that measures combustion performance characteristics of the fuel [100]. The C_i can be useful in setting up quality control standards for char. Char that is more reactive than coal will have a higher C_i than coal [89,101]. Studies on co-combustion of coal with lignocellulosic biomass have attracted attention mainly due to their environmental benefits [90,91,102,103].

Few studies on co-combustion of coal with lignocellulosic biomass have been conducted, especially investigating the influence of biomass pre-treatment such as torrefaction and pyrolysis on combustion behaviour.

2.2.2.3 Zambian coal specifications

Coal is a fossil fuel mainly made up of inorganic and organic complex compounds [104]. Carbon, hydrogen, oxygen, sulphur and nitrogen are the bulk materials that constitute the organic fraction of coal, with a combination of other trace elements [104]. Coal can be ranked in three major categories, with lignite being the lowest (HHV range of 14.7 to 19.3 MJ kg^{-1}), sub-bituminous (19.3 to 26.7 MJ kg^{-1}), high volatile A, B and C bituminous coal (26.7 to 32.6 MJ kg^{-1}), while medium and low volatile bituminous coals are ranked in terms of fixed carbon (69.0 to 78.0%), with anthracitic coal occupying the top position (fixed carbon $\geq$ 86%), as the best ranked coal [105]. Coal in Zambia lies between sub-bituminous and bituminous, whose ash content is generally high (16-29%). It is a non-coking coal of medium quality with energy content in the range of 24-29 MJ kg^{-1} [105]. Coal is mainly used in the mining sector (37%), manufacturing, brewing industry and the rest (63%) [45,106]. The annual coal consumption is about 240, 000 tonnes, supplied by the local coal mines. Zambia's major industries as well as the mining sector utilise coal with fixed carbon from 50% upwards (see Table 2-2).

Three companies named A, B, C from Zambia have provided the coal specification requirements, which they utilise in their processes that will be used for comparisons in **Chapter 8** with the produced char from LC and MP. The coal specifications are detailed in Table 2-2. Based on American Standard for Testing of Materials (ASTM) D388, the coal specifications provided in Table 2-2 can be group ranked as being between sub-bituminous *B* coal up to high volatile bituminous *B* coal [105]. The

names of the companies have been withheld for ethical reasons. Coal in Zambia is mostly used for combustion purposes (heat).

Table 2-2: Coal specifications from three Zambian companies

Company	A	B	C
Moisture content (%)	1.3 – 5.0	<3.5	<4.0
Volatile Matter (%)	<19.0	22.0 – 27.0	28.0 – 40.0
Fixed carbon (%)	>64.0	50.0 – 62.0	>56.0
Ash content (%)	<16.0	<30.0	14.0 – 20.0
Higher heating value (MJ kg^{-1})	>27.0	23.4 – 26.3	20.0 – 22.0
Sulphur (%)	<1.03	<3.0	<2.5
Ash fusion temperature (˚C)	-	-	1387.0
Particle size (mm)	10.0 – 20.0	-	14.0 – 21.0

From the coal specifications provided by the three Zambian companies in Table 2-2, it is justifiable to proceed with this study since the fixed carbon content and HHVs are comparable with results obtained from torrefied lignocellulosic biomass in literature [107–109] as well as pyrolysis char [43,89]. Lignocellulosic biomass generally contains less sulphur (0.1%) [79], compared to coal that mainly has increased amounts of sulphur (organic and/or inorganic), ranging from trace amounts up to as high as 12% [110,111]. This makes lignocellulosic char a relatively less polluter than coal in terms of sulphur related emissions.

2.2.3 Production of char by torrefaction and pyrolysis

Thermochemical conversion technologies employ heat energy to convert raw lignocelluloses into three main products of gas, liquid and solid [18,112]. Generally, pyrolysis utilises inert environments by heating raw lignocellulose at generally low-heating-rate [1] to a maximum temperature, thereafter holding reactor contents at a pre-determined time (hold time). During the production of volatiles, the

time they are contained in the hot part of the reactor is called residence time. The design of the pyrolyser influences pyrolysis products [1,7], as well as lignocellulosic composition and reactor operating conditions [7].

2.2.3.1 Types of torrefaction and pyrolysis reactors

Torrefaction and slow pyrolysis have been conducted in different reactor designs made from various construction materials. In case of conventional slow pyrolysis reactors, fixed bed batch types are mostly used with a maximum temperature of up to 600 ˚C and hold time in the range of 5 to 30 min, maximising on char production [1]. Similar type of reactors at lab-scale are employed. Stainless steel is the most common construction material, usually in horizontal or vertical positions, varying from small millimeter to meter-sized reactors in terms of internal diameter and length [6,109,113,114]. At milligram-scale, TGA reactor is a simulation of a batch reactor applicable for torrefaction and slow pyrolysis.

The choice of the stainless steel horizontal fixed bed reactor used at gram-scale in this work is in agreement with most basic industrial applications. The details of the stainless steel reactor are detailed in **Chapter 4.**

Several works [40,115,116] have used TGA to study the pyrolysis of lignocellulosic biomass. The advantage of such analytical technique is that it allows the monitoring of the evolution of the mass of the sample during the process of conversion [40,89,116]. At milligram-scale, TGA is useful, though later on, scale-up would be necessary to account for heat and mass transfer effects on increased sample size and bed. Scaling-up works from milligram-scale to gram-scale have rarely been reported.

2.2.3.2 Reactor temperature

Of late, torrefaction has attracted attention as a viable thermal technology for lignocellulosic char production, commonly referred to as torrefied lignocellulosic biomass [80,117–119]. Torrefaction operates in inert environments under relatively low temperatures of 200-300 ˚C [1,17,117,120]. Several torrefaction studies have reported that temperature plays a key role in determining the final char yield [80,107,121,122] as well as the char energy content [17,79,80,123]. The higher the torrefaction temperature, the lower the char yield and the higher the char HHV. The torrefied lignocellulosic biomass has reduced moisture content [95,118] with lower ratios of O/C and H/C [121,124], mainly due to decomposition of hemicelluloses [52,61]. The torrefied char also has increased fixed carbon than the raw lignocellulose [80,107,123], consequently resulting into increased HHV [95,123,124]. Generally, char yields at 250 ˚C range from 75 to 90 wt.%, while those at 300 ˚C range from 40 to 60 wt.%, with corresponding char HHV increases of 1 to 3 and 3 to 7 MJ kg^{-1}, respectively [79,121].

Slow pyrolysis temperature starts where torrefaction ends, at 300 ˚C. Temperature during pyrolysis is the most significant factor determining char yield and its energy content [7,43,89]. Various slow pyrolysis studies have reported a temperature range of 300-600 ˚C [5–7], while others have reported higher temperatures (> 700 ˚C) that tend to decrease the HHV while the quality of the char increases with reduced char yields [59,125,126]. The improvement in the char properties is observed in fixed carbon and BET surface area [5,15,99]. Lignocellulosic char yields in the range of 34-39 wt.% are obtained between 300-500 ˚C, with HHVs in the range of 26-29 MJ kg^{-1} [43,89,127]. For temperatures above 500 ˚C, char yields in the range of 26-35 wt.% have been obtained corresponding to HHVs > 29 MJ kg^{-1} [5,43,89,127]. Concerning lignocellulosic char HHV, literature has compared with char HHV obtained between 500-600 ˚C, with no reported explanation for the HHV decrease. Concerning lignocellulosic char HHV, literature has shown that there is an increase in HHV between 500-600 ˚C

[127–129], while other works have shown decreases in HHV for some pyrolysis conversion temperatures > 600 ˚C [43,89,128,129], with no reported explanation for the HHV decrease.

2.2.3.3 Reactor heating rate

Reactor process heating rate is that of the reactor internal environment [130]. Torrefaction and slow pyrolysis use similar heating rates, generally up to 20 ˚C min^{-1} [5,6,122,131]. Most works on torrefaction have utilised single heating rates, ranging from 2-20 ˚C min^{-1} [122,131–133]. The influence of heating rate during torrefaction has rarely been reported [134]. However, during slow pyrolysis of pine wood at 300 ˚C (severe torrefaction temperature), char yields of 53.8, 55.6, 58.0 and 60.8% were obtained from variable heating rates of 5, 20, 40 and 80 ˚C min^{-1}, respectively. [125]. These results showed that heating rate could have an influence on char yield, though the char HHV was not considered.

Slow pyrolysis is a suitable technology for char production, which involves thermal decomposition of lignocellulosic biomass in an inert environment at temperatures ≥ 300 ˚C [5]. Various works have reported that slow pyrolysis for char maximisation is characterised by slow heating rates in the range of 1-20 ˚C min^{-1} [5–7,89]. Generally, slow heating rates promote increased mass yields [7,129] as secondary char formation reactions are promoted [7]. By decreasing heating rate from 20 to 5 ˚C min^{-1}, at 500 ˚C, char yields of almond shell increased by 4.2 wt.% [129]. Some studies have reported the influence of heating rate on char yield during slow pyrolysis [7,129], while the influence of heating rate on char HHV have been scarcely described [127,129].

2.2.3.4 Reactor hold time

Hold time is an isothermal stage during torrefaction or slow pyrolysis where reactor contents are held in the reactor at the process maximum temperature, thereafter, followed by cooling. As for torrefaction hold time, generally, longer hold time ensures that there is enough time for the evolution of oxygenated volatiles, ultimately resulting into lower char yield and increased HHV [80,123]. Variable hold times during torrefaction have been used, ranging from several minutes up to more than an hour [80,123,135,136]. For instance using pine, an increase in hold time from 2 to 3 h at 280 ˚C, lowered the char yields from 72.1 to 69.0 wt.%, while the char HHV increased from 22.3 to 22.7 MJ kg^{-1} [137].

Under slow pyrolysis, literature has reported holding lignocellulosic biomass samples at the maximum temperature for 30 min [89,138–140], while other works have used longer hold times [7,141]. As the hold time is increased, the char yields decrease, while the char HHV increases [139,142]. For example, at 450 ˚C, char yields from cherry sawdust reduced by 1.8 wt.% as the hold time was prolonged from 5 to 30 min, while under the same conditions, char HHV increased by 1.5 MJ kg^{-1}[139]. However, the effect of hold time seems to have less influence on char yields and HHV as the conversion temperature increases. For instance, at 600 ˚C, pyrolysed wood samples recorded a char yield decrease from 24.4 to 23.3 wt.%, while the char HHV remained constant at 34.4 MJ kg^{-1}, as hold time was increased from 10 to 60 min [142]. Use of hold times beyond 30 min during pyrolysis for char production may not be suitable.

2.3 Conclusion

Though literature has reported the use of LC from India [43,88] and MP from Thailand [32] for energy applications, both lignocelluloses, in this case from a different geographical region of Africa, in

particular Zambia, have not been reported in literature. The production of valuable char from mechanically harvested IAPs appears as a promising option for IAPs management. Such char could be used to partially substitute coal in energy applications. To determine the potential of torrefaction or slow pyrolysis for the production of valuable fuel products from such feedstocks, an optimisation study would be required. The main influential factors identified are temperature, heating rate and hold time. Following production of chars with acceptable HHV, further study is required to confirm the char product can be used in actual plants using coal. Recently developed TGA methods appears as suitable to study the combustion behaviours of solid fuels. They can be used to study the conversion of individual fuels but also of blends in order to estimate how much biomass char could be added without affecting significantly the conversion efficiency.

2.4 References

[1] Basu P. Biomass Gasification, Pyrolysis and Torrefaction: Practical Design and Theory. second ed. London: Academic Press; 2013.

[2] Hollingdale R, Krishnan A. P, Robinson AC. A handbook of charcoal production. second ed. Kent: Commonwealth Science Council; 1999.

[3] Limayem A, Ricke SC. Lignocellulosic biomass for bioethanol production : Current perspectives , potential issues and future prospects. Prog Energy Combust Sci 2012;38:449–67.

[4] Gomez N, Rosas JG, Cara J, Martinez O, Alburquerque JA, Sanchez ME. Slow pyrolysis of relevant biomasses in the Mediterranean basin. Part 1. Effect of temperature on process performance on a pilot scale. J Clean Prod 2014;120:181–90.

[5] Lee Y, Eum P-R-BRB, Ryu C, Park Y-KK, Jung J-HH, Hyun S. Characteristics of biochar produced from slow pyrolysis of Geodae-Uksae 1. Bioresour Technol 2013;130:345–50.

[6] Liao R, Gao B, Fang J. Invasive plants as feedstock for biochar and bioenergy production. Bioresour Technol 2013;140:439–42.

[7] Carrier M, Hugo T, Gorgens J, Knoetze H. Comparison of slow and vacuum pyrolysis of sugar cane bagasse. J Anal Appl Pyrolysis 2011;90:18–26.

[8] Elyounssi K, Blin J, Halim M. High-yield charcoal production by two-step pyrolysis. J Anal Appl Pyrolysis 2010;87:138–43.

[9] Noumi ES, Blin J, Rousset P. Optimization of Quality of Charcoal for Steelmaking using Statistical Analysis Approach. 5th Int Conf Eng Waste Biomass Valoris 2014:1–14.

[10] Manyà JJ, Ruiz J, Arauzo J. Some peculiarities of conventional pyrolysis of several agricultural residues in a packed bed reactor. Ind Eng Chem Res 2007;46:9061–70.

[11] Liu Z, Hu W, Jiang Z, Mi B, Fei B. Investigating combustion behaviors of bamboo, torrefied bamboo, coal and their respective blends by thermogravimetric analysis. Renew Energy 2016;87:346–52.

[12] De Jongh WA, Carrier M, Knoetze JHH. Vacuum pyrolysis of intruder plant biomasses. J Anal Appl Pyrolysis 2011;92:184–93.

[13] Garcìa-Pérez M, Chaala A, Pakdel H, Kretschmer D, Roy C. Vacuum pyrolysis of softwood and hardwood biomass. J Anal Appl Pyrolysis 2007;78:104–16.

[14] Lua AC, Yang T. Effects of vacuum pyrolysis conditions on the characteristics of activated carbons derived from pistachio-nut shells. J Colloid Interface Sci 2004;276:364–72.

[15] Carrier M, Hardie AG, Uras Ü, Görgens J, Knoetze JH. Production of char from vacuum pyrolysis of South-African sugar cane bagasse and its characterization as activated carbon and biochar. J Anal Appl Pyrolysis 2012;96:24–32.

[16] Pereira BCL, Carneiro ACO, Carvalho AMML, Colodette JL, Oliveira AC, Fontes M. Influence of Chemical Composition of Eucalyptus Wood on Gravimetric Yield and Charcoal Properties. BioResources 2013;3:4574–92.

[17] Pimchuai A, Dutta A, Basu P. Torrefaction of agriculture residue to enhance combustible properties. Energy and Fuels 2010;24:4638–45.

[18] Van Loo J, Koppejan S. The handbook of biomass combustion & co-firing. first ed. Washington, DC: Earthscan; 2008.

[19] Garcia R, Pizarro C, Lavin AG, Bueno JL. Characterization of Spanish biomass wastes for energy use. Bioresour Technol 2012;103:249–58.

[20] Weidong L, Ming L, Weifeng L, Haifeng L. Study on the ash fusion temperatures of coal and sewage sludge mixtures. Fuel 2010;89:1566–72.

[21] Mumba M. Biodiversity challenges for invaded wetland ecosystems in Africa: The case of

the Kafue Flats floodplain in southern Zambia. Proc a Glob Glob Synth Work Biodivers Loss Species Extinctions Manag Risk a Chang World 2002:1–8.

[22] Boy G, Witt A. Invasive Alien species and their Management in Africa. Nairobi: 2013.

[23] Keller R, Perrings C. International Policy Options to reduce the harmful impacts of Alien Invasive Species. Nairobi: 2010.

[24] Richardson DM, Rejmánek M. Trees and shrubs as invasive alien species - a global review. Divers Distrib 2011;17:788–809.

[25] Eviner VT, Garbach K, Baty JH, Hoskinson S. Measuring the Effects of Invasive Plants on Ecosystem Services: Challenges and Prospects. Invasive Plant Sci Manag 2012;5:125–36.

[26] International Energy Agency (IEA). Energy, Climate Change & Environment. Paris: 2016.

[27] Barney JN. Bioenergy and Invasive Plants: Quantifying and Mitigating Future Risks. Invasive Plant Sci Manag 2012;5:125–36.

[28] Vardien W, Richardson DM, Foxcroft LC, Thompson GD, Wilson JRU, Le Roux J. Invasion dynamics of Lantana camara L. (sensu lato) in South Africa. South African J Bot 2012;81:81–94.

[29] Ghisalberti EL. Lantana camara L. (Verbenaceae). Fitoterapia 2000;71:467–86.

[30] Nang'alelwa MM. Effects of treatment on Lantana camara (L.) and the restoration potential of riparian seed banks in cleared areas of the Victoria Falls World Heritage Site, Livingstone, Zambia. Rhodes, 2010.

[31] Heard TA, Paynter Q, Chan R, Mira A. Malacorhinus irregularis for biological control of Mimosa pigra: host-specificity, life cycle, and establishment in Australia. Biol Control 2005;32:252–62.

[32] Mumba M, Thompson JR. Hydrological and ecological impacts of dams on the Kafue Flats floodplain system, southern Zambia. Phys Chem Earth, Parts A/B/C 2005;30:442–7.

[33] Paynter Q, Flanagan GJ. Integrating herbicide and mechanical control treatments with fire and biological control to manage an invasive wetland shrub, Mimosa pigra. J Appl Ecol 2004;41:615–29.

[34] Shanungu GK. Management of the invasive Mimosa pigra L. in Lochinvar National Park, Zambia. Biodiversity 2009;10:56–60.

[35] Baars J-R, Urban AJ, Hill MP. Biology, host range, and risk assessment supporting release in Africa of Falconia intermedia (Heteroptera: Miridae), a new biocontrol agent for Lantana camara. Biol Control 2003;28:282–92.

[36] Broughton S. Review and Evaluation of Lantana Biocontrol Programs. Biol Control 2000;17:272–86.

[37] de Lange WJ, van Wilgen BW. An economic assessment of the contribution of biological control to the management of invasive alien plants and to the protection of ecosystem services in South Africa. Biol Invasions 2010;12:4113–24.

[38] Zalucki MP, Day MD, Playford J. Will biological control of Lantana camara ever succeed? Patterns, processes & prospects. Biol Control 2007;42:251–61.

[39] Reid AM, Morin L, Downey PO, French K, Virtue JG. Does invasive plant management aid the restoration of natural ecosystems? Biol Conserv 2009;142:2342–9.

[40] Wongsiriamnuay T, Tippayawong N. Non-isothermal pyrolysis characteristics of giant sensitive plants using thermogravimetric analysis. Bioresour Technol 2010;101:5638–44.

[41] Wongsiriamnuay T, Tippayawong N. Thermogravimetric analysis of giant sensitive plants under air atmosphere. Bioresour Technol 2010;101:9314–20.

[42] Sharma OMP, Makkar HPS, Dawra RK. A Review of the Noxious Plant Lantana camara. Toxicon 1988;26:975–87.

[43] Kumar R, Chandrashekar N. Study on chemical, elemental and combustion characteristics of

Lantana camara wood charcoal. J Indian Acad Wood Sci 2013;10:134–9.

[44] Chidumayo EN, Gumbo DJ. The environmental impacts of charcoal production in tropical ecosystems of the world: A synthesis. Energy Sustain Dev 2013;17:86–94.

[45] Ministry of Energy & Water Development. National Energy Policy-2008. vol. 1. Lusaka: 2008.

[46] Chidumayo EN. Forest degradation and recovery in a miombo woodland landscape in Zambia: 22 years of observations on permanent sample plots. For Ecol Manage 2013;291:154–61.

[47] De Wild P, Reith H, Heeres E. Biomass pyrolysis for chemicals. vol. 2. 2011.

[48] Manyà JJ. Pyrolysis for biochar purposes: a review to establish current knowledge gaps and research needs. Environ Sci Technol 2012;46:7939–54.

[49] Balat M. Production of bioethanol from lignocellulosic materials via the biochemical pathway : A review. Energy Convers Manag 2011;52:858–75.

[50] Chen WH, Lu KM, Tsai CM. An experimental analysis on property and structure variations of agricultural wastes undergoing torrefaction. Appl Energy 2012;100:318–25.

[51] Vandenbrink JP, Hilten RN, Das KC, Paterson AH, Feltus FA. Analysis of Crystallinity Index and Hydrolysis Rates in the Bioenergy Crop Sorghum bicolor 2012:387–97.

[52] Collard FX, Blin J. A review on pyrolysis of biomass constituents: Mechanisms and composition of the products obtained from the conversion of cellulose, hemicelluloses and lignin. Renew Sustain Energy Rev 2014;38:594–608.

[53] Yaman S. Pyrolysis of biomass to produce fuels and chemical feedstocks. Energy Convers Manag 2004;45:651–71.

[54] Bochek AM. Effect of Hydrogen Bonding on Cellulose Solubility in Aqueous and Nonaqueous Solvents 2003;76:1711–9.

[55] Schorr C, Muinonen M, Nurminen F. Torrefaction of biomass. Chem Eng 2010;117.

[56] Ridout CAM. Valorisation of paper waste sludge using pyrolysis processing. Stellenbosch, 2016.

[57] McKendry P. Energy production from biomass (Part 2): Conversion technologies. Bioresour Technol 2002;83:47–54.

[58] Sarkar N, Ghosh SK, Bannerjee S, Aikat K. Bioethanol production from agricultural wastes : An overview. Renew Energy 2012;37:19–27.

[59] Demirbas A. Products from Lignocellulosic Materials via Degradation Processes. Energy Sources 2007;30:27–37.

[60] Saha BC. Hemicellulose bioconversion. J Ind Microbiol Biotechnol 2003;30:279–91.

[61] Ciolkosz D, Pennsylvania T, Wallace R, Hamilton BA. A review of torrefaction for bioenergy feedstock 2011:317–29.

[62] Azadi P, Inderwildi OR, Farnood R, King DA. Liquid fuels , hydrogen and chemicals from lignin : A critical review. Renew Sustain Energy Rev 2013;21:506–23.

[63] Wang S, Guo X, Wang K, Luo Z. Influence of the interaction of components on the pyrolysis behavior of biomass. J Anal Appl Pyrolysis 2011;91:183–9.

[64] Toledano A, Erdocia X, Serrano L, Labidi J. Influence of Extraction Treatment on Olive Tree (Olea europaea) Pruning Lignin Structure 2013;32:1187–94.

[65] Neutelings G. Plant Science Lignin variability in plant cell walls : Contribution of new models. Plant Sci 2011;181:379–86..

[66] Gómez CJ, Mészáros E, Jakab E, Velo E, Puigjaner L. Thermogravimetry/mass spectrometry study of woody residues and an herbaceous biomass crop using PCA techniques. J Anal Appl Pyrolysis 2007;80:416–26.

[67] Shen DK, Gu S, Luo KH, Wang SR, Fang MX. Bioresource Technology The pyrolytic degradation of wood-derived lignin from pulping process. Bioresour Technol 2010;101:6136–46.

[68] Peng Y, Wu S. The structural and thermal characteristics of wheat straw hemicellulose. J Anal Appl Pyrolysis 2010;88:134–9.

[69] Rahbari M. Feasibility of Improving Biomass Combustion through Extraction of Nutrients. Ontario: 2011.

[70] Patwardhan PR, Satrio JA, Brown RC, Shanks BH. Influence of inorganic salts on the primary pyrolysis products of cellulose. Bioresour Technol 2010;101:4646–55.

[71] Mayer ZA, Apfelbacher A, Hornung A. A comparative study on the pyrolysis of metal- and ash-enriched wood and the combustion properties of the gained char. J Anal Appl Pyrolysis 2012;96:196–202.

[72] Prins MJ, Ptasinski KJ, Janssen FJJG. Torrefaction of wood. Part 1. Weight loss kinetics. J Anal Appl Pyrolysis 2006;77:28–34.

[73] Chen WH, Kuo PC. Isothermal torrefaction kinetics of hemicellulose, cellulose, lignin and xylan using thermogravimetric analysis. Energy 2011;36:6451–60.

[74] Kotilainen R, Zaman A, Ale R. Thermochemical behavior of Norway spruce (Picea abies) at 180 – 225 ° C 2002;36:163–71.

[75] Naron DR, Collard F, Tyhoda L, Görgens JF. Characterisation of lignins from different sources by appropriate analytical methods : Introducing thermogravimetric analysis-thermal desorption-gas chromatography – mass spectroscopy. Ind Crop Prod 2017;101:61–74.

[76] Miller RS, Bellan J. A Generalized Biomass Pyrolysis Model Based on Superimposed Cellulose , Hemicellulose and Liqnin Kinetics. Combust Sci Technol 1997;126:97–137.

[77] Elyounssi K, Collard FX, Mateke JAN, Blin J. Improvement of charcoal yield by two-step

pyrolysis on eucalyptus wood: A thermogravimetric study. Fuel 2012;96:161–7.

[78] Mok WSL, Antal MJ, Szabo P, Varhegyi G, Zelei B. Formation of charcoal from biomass in a sealed reactor. Ind Eng Chem Res 1992;31:1162–6.

[79] Giudicianni P, Cardone G, Ragucci R. Cellulose, hemicellulose and lignin slow steam pyrolysis: Thermal decomposition of biomass components mixtures. J Anal Appl Pyrolysis 2013;100:213–22.

[80] Neves D, Thunman H, Matos A, Tarelho L, Gómez-Barea A. Characterization and prediction of biomass pyrolysis products. Prog Energy Combust Sci 2011;37:611–30.

[81] Medic D, Darr M, Shah A, Potter B, Zimmerman J. Effects of torrefaction process parameters on biomass feedstock upgrading. Fuel 2012;91:147–54.

[82] Carrier M, Joubert J-E, Danje S, Hugo T, Görgens J, Knoetze JH. Impact of the lignocellulosic material on fast pyrolysis yields and product quality. Bioresour Technol 2013;150C:129–38.

[83] Shen J, Wang X-S, Garcia-Perez M, Mourant D, Rhodes MJ, Li C-Z. Effects of particle size on the fast pyrolysis of oil mallee woody biomass. Fuel 2009;88:1810–7.

[84] Apaydin-Varol E, Pütün E, Pütün AE. Slow pyrolysis of pistachio shell. Fuel 2007;86:1892–9.

[85] Lin TY, Kuo CP. Study of products yield of bagasse and sawdust via slow pyrolysis and iron-catalyze. J Anal Appl Pyrolysis 2012;96:203–9.

[86] Phan AN, Ryu C, Sharifi VN, Swithenbank J. Characterisation of slow pyrolysis products from segregated wastes for energy production. J Anal Appl Pyrolysis 2008;81:65–71.

[87] Şensöz S. Slow pyrolysis of wood barks from Pinus brutia Ten. and product compositions. Bioresour Technol 2003;89:307–11.

[88] Uçar S, Karagöz S. The slow pyrolysis of pomegranate seeds: The effect of temperature on

the product yields and bio-oil properties. J Anal Appl Pyrolysis 2009;84:151–6.

[89] Kumar R, Chandrashekar N, Pandey KK. Fuel properties and combustion characteristics of Lantana camara and Eupatorium spp. Curr Sci 2009;97:930–5.

[90] Xiong S, Zhang S, Wu Q, Guo X, Dong A, Chen C. Investigation on cotton stalk and bamboo sawdust carbonization for barbecue charcoal preparation. Bioresour Technol 2014;152:86–92.

[91] Aho M, Gil A, Taipale R, Vainikka P, Vesala H. A pilot-scale fireside deposit study of co-firing Cynara with two coals in a fluidised bed. Fuel 2008;87:58–69.

[92] Smajevic I, Kazagic A, Music M, Becic K, Hasanbegovic I, Sokolovic S, Delihasanovic N, Skopljak A, Hodzic N. Co-firing bosnian coals with woody biomass: Experimental studies on a laboratory-scale furnace and 110 MW e power unit. Therm Sci 2012;16:789–804.

[93] Antal MJ, Grønli M. The Art, Science, and Technology of Charcoal Production. Ind Eng Chem Res 2003;42:1619–40.

[94] Parikh J, Channiwala SA, Ghosal GK. A correlation for calculating HHV from proximate analysis of solid fuels. Fuel 2005;84:487–94.

[95] Sheng C, Azevedo JLT. Estimating the higher heating value of biomass fuels from basic analysis data. Biomass and Bioenergy 2005;28:499–507.

[96] Kim YH, Lee SM, Lee HW, Lee JW. Physical and chemical characteristics of products from the torrefaction of yellow poplar (Liriodendron tulipifera). Bioresour Technol 2012;116:120–5.

[97] Suopajärvi H, Kemppainen A, Haapakangas J, Fabritius T. Extensive review of the opportunities to use biomass-based fuels in iron and steelmaking processes. J Clean Prod 2017;148:709–34.

[98] Gupta SK, Wall TF, Creelman RA, Gupta R. Ash fusion temperatures and the

transformations of coal ash particles to slag. Fuel Process Technol 1998;56:33–43.

[99] Liu B, He Q, Jiang Z, Xu R, Hu B. Relationship between coal ash composition and ash fusion temperatures. Fuel 2013;105:293–300.

[100] Uras-Postma Ü, Carrier M, Knoetze J. Vacuum pyrolysis of agricultural wastes and adsorptive criteria description of biochars governed by the presence of oxides. J Anal Appl Pyrolysis 2014;107:123–32.

[101] Moon C, Sung Y, Ahn S, Kim T, Choi G, Kim D. Effect of blending ratio on combustion performance in blends of biomass and coals of different ranks. Exp Therm Fluid Sci 2013;47:232–40.

[102] Kastanaki E, Vamvuka D. A comparative reactivity and kinetic study on the combustion of coal-biomass char blends. Fuel 2006;85:1186–93.

[103] Kubacki ML, Ross AB, Jones JM, Williams A. Small-scale co-utilisation of coal and biomass. Fuel 2012;101:84–9.

[104] Kwong PCW, Chao CYH, Wang JH, Cheung CW, Kendall G. Co-combustion performance of coal with rice husks and bamboo. Atmos Environ 2007;41:7462–72.

[105] Schweinfurth SP. An introduction to coal quality. Virginia: 2009.

[106] Astm. Designation: D388 − 12: Standard Classification of Coals by Rank 2012;552:1–7.

[107] Zambia Development Agency. Energy Sector Profile. Lusaka: 2013.

[108] Felfli FF, Luengo CA, Suárez JA, Beatón PA. Wood briquette torrefaction. Energy Sustain Dev 2005;9:19–22.

[109] Patel B, Gami B, Bhimani H. Improved fuel characteristics of cotton stalk, prosopis and sugarcane bagasse through torrefaction. Energy Sustain Dev 2011;15:372–5.

[110] Pentananunt R, Rahman ANMM, Bhattacharya S. Upgrading of biomass by means of

torrefaction. Energy 1990;15:1175–9.

[111] Grzybek T, Pietrzak R, Wachowska H. X-ray photoelectron spectroscopy study of oxidized coals with different sulphur content. Fuel Process Technol 2002;78:1–7.

[112] Cordero T, Rodriguez-Mirasol J, Pastrana J, Rodriguez J. Improved solid fuels from co-pyrolysis of a high-sulphur content coal and different lignocellulosic wastes. Fuel 2004;83:1585–90.

[113] Jin W, Singh K, Zondlo J. Pyrolysis Kinetics of Physical Components of Wood and Wood-Polymers Using Isoconversion Method. Agriculture 2013;3:12–32.

[114] Saleh SB. Torrefaction of biomass for power production. Technical University of Denmark, 2013.

[115] Şensöz S, Demiral I, Gerçel HF. Olive bagasse (Olea europea L.) pyrolysis. Bioresour Technol 2006;97:429–36.

[116] Maiti S, Purakayastha S, Ghosh B. Thermal characterization of mustard straw and stalk in nitrogen at different heating rates. Fuel 2007;86:1513–8.

[117] Mansaray KG, Ghaly AE. Thermal degradation of rice husks in nitrogen atmosphere. Bioresour Technol 1998;65:13–20.

[118] Arias B, Pevida C, Fermoso J, Plaza MG, Rubiera F, Pis JJ. Influence of torrefaction on the grindability and reactivity of woody biomass. Fuel Process Technol 2008;89:169–75.

[119] Rousset P, Aguiar C, Labbé N, Commandré JM. Enhancing the combustible properties of bamboo by torrefaction. Bioresour Technol 2011;102:8225–31.

[120] Acharya B, Sule I, Dutta A. A review on advances of torrefaction technologies for biomass processing. Biomass Convers Biorefinery 2012;2:349–69.

[121] Chen D, Zheng Z, Fu K, Zeng Z, Wang J, Lu M. Torrefaction of biomass stalk and its effect on the yield and quality of pyrolysis products. Fuel 2015;159:27–32.

[122] Prins MJ, Ptasinski KJ, Janssen FJJG. Torrefaction of wood. Part 2. Analysis of products. J Anal Appl Pyrolysis 2006;77:35–40.

[123] Asadullah M, Adi AM, Suhada N, Malek NH, Saringat MI, Azdarpour A. Optimization of palm kernel shell torrefaction to produce energy densified bio-coal. Energy Convers Manag 2014;88:1086–93.

[124] Phanphanich M, Mani S. Impact of torrefaction on the grindability and fuel characteristics of forest biomass. Bioresour Technol 2011;102:1246–53.

[125] Lee JW, Kim YH, Lee SM, Lee HW. Optimizing the torrefaction of mixed softwood by response surface methodology for biomass upgrading to high energy density. Bioresour Technol 2012;116:471–6.

[126] Williams PT, Besler S. The influence of temperature and heating rate on the slow pyrolysis of biomass. Renew Energy 1996;7:233–50.

[127] Kumar M, Gupta RC, Sharma T. Effects of carbonisation conditions on the yield and chemical composition of Acacia and Eucalyptus wood chars. Biomass and Bioenergy 1992;3:411–7.

[128] Angın D. Effect of pyrolysis temperature and heating rate on biochar obtained from pyrolysis of safflower seed press cake. Bioresour Technol 2013;128:593–7.

[129] Bonelli PR. Slow Pyrolysis of Nutshells: Characterization of Derived Chars and of Process Kinetics. Energy Sources 2003;25:767–78.

[130] Gonzalez JF, Ramiro A, Gonzalez-Garcia CM, Ganan J, Encinar JM, Sabio E, Rubiales J. Pyrolysis of almond shells. Energy applications of fractions. Ind Eng Chem Res 2005;44:3003–12.

[131] Joubert J-E. Pyrolysis of Eucalyptus grandis. Stellenbosch, 2013.

[132] Almeida G, Brito JO, Perré P. Bioresource Technology Alterations in energy properties of

eucalyptus wood and bark subjected to torrefaction : The potential of mass loss as a synthetic indicator. Bioresour Technol 2010;101:9778–84.

[133] Chin KL, H'ng PS, Go WZ, Wong WZ, Lim TW, Maminski M, Paridah MT, Luqman A. Optimization of torrefaction conditions for high energy density solid biofuel from oil palm biomass and fast growing species available in Malaysia. Ind Crops Prod 2013;49:768–74.

[134] Grigiante M, Antolini D. Mass yield as guide parameter of the torrefaction process. An experimental study of the solid fuel properties referred to two types of biomass. Fuel 2015;153:499–509.

[135] Chen W-H, Peng J, Bi XT. A state-of-the-art review of biomass torrefaction, densification and applications. Renew Sustain Energy Rev 2015;44:847–66.

[136] Peng JH, Bi, X T Sokhansanj S, Lim CJ. Torrefaction and densification of different species of softwood residues. Fuel 2013;111:411–21.

[137] Gil MV, García R, Pevida C, Rubiera F. Grindability and combustion behavior of coal and torrefied biomass blends. Bioresour Technol 2015;191:205–12.

[138] Pach M, Zanzi R, Björnbom E. Torrefied biomass a substitue for wood and charcoal. 6th Asia-Pacific Internatioonal Symp Combust Energy Util 2002.

[139] Beis SH, Onay O, ̈Koçkar OM. Fixed-bed pyrolysis of safflower seed: Influence of pyrolysis parameters on product yields and compositions. Renew Energy 2002;26:21–32.

[140] Gheorghe C, Marculescu C, Badea A, Apostol T. Pyrolysis parameters influencing the bio-char generation from wooden biomass. Univ Politeh Bucharest Sci Bull Ser C Electr Eng 2010;72:29–38.

[141] Mandal S, Singh RK, Kumar A, Verma BC, Ngachan SV. Characteristics of Weed Biomass-derived Biochar and Their Effect on Properties of Beehive Briquettes. Indian J Hill Farming 2013;26:8–12.

[142] Guerrero M, Ruiz M, Alzueta M, Bilbao R, Millera A. Pyrolysis of eucalyptus at different heating rates: Studies of char characterization and oxidative reactivity. J Anal Appl Pyrolysis 2005;74:307–14.

[143] Ronsse F, van Hecke S, Dickinson D, Prins W. Production and characterization of slow pyrolysis biochar: Influence of feedstock type and pyrolysis conditions. GCB Bioenergy 2013;5:104–15.

Chapter 3 **Research objectives**

The main target of this dissertation is to assess the full potential of maximising the production of char from two invasive alien plants (IAPs), namely *Lantana camara* (LC) and *Mimosa pigra* (MP) by optimising process parameters of temperature, heating rate and hold time. The char should be of acceptable quality for energy applications. The main targeted application for the produced char is coal substitution in combustion application. Two thermal technologies of torrefaction and slow pyrolysis will be considered for producing char of acceptable quality (energy properties). The specific objectives based on literature review are as follows:

3.1 Objective one: To identify fuel properties for defining char quality for energy applications

Literature has shown that HHV, volatile matter and fixed carbon are important energy properties playing a key role in determining the use of char for energy applications. These properties can be considered as reliable indicators as a first approach to compare the fuel properties of biomass chars and coals. However, the characterisation of the lignocellulosic char according to these properties is not sufficient to assess the suitability of char for specific application such as co-firing with coal or individual combustion at industrial level. Due to differences in chemical compositions and physical structure, biomass chars and coals with similar HHV are likely to present differences in fuel properties. Similarly though the lignocellulosic composition of the feedstock materials is likely to influence char fuel properties, it has rarely been described. Volatiles generated from char produced from hemicelluloses, cellulose and lignin are different in nature, structure and reactivity. It is anticipated that chars produced from biomass samples with different lignocellulosic composition will react differently and also result in char with variations in quality in terms of energy properties. In

terms of char reactivity during combustion, ignition and burnout temperatures in conjunction with fuel consumption rate play a key role in determining fuel combustion performance. The combustion characteristics of char for energy applications in literature have rarely been defined either for industrial or domestic use.

3.2 Objective two: To determine the influence of thermal process parameters on char yield quality

Based on literature review, there is an opportunity to generate char from invasive alien plants (IAPs) for coal-replacement or co-firing in industry and domestically to replace charcoal produced from indigenous forests. Key to this opportunity is the need of obtaining char of a minimum acceptable quality for these applications **(objective one).**

Literature indicates that increased char quality with increasing temperature will reduce the char yield, and therefore that there is a compromise to be made between quality and yield. For instance, torrefaction gives much lower quality char in terms of energy content than slow pyrolysis, but with the benefit of significantly higher char yields. Higher char yields for torrefaction are typically in the range of 40 to 60 wt.% at 300 ˚C associated with higher gross energy yields (60-70%), with HHVs up to 27 MJ kg^{-1}, comparable with some industrial coals. Comparatively, slow pyrolysis gives lower char yields than torrefaction. Concerning slow pyrolysis, literature has further shown that the char quality in terms of HHV decreases for temperatures ≥ 600 ˚C without detailed explanations on this trend. The main influential factors related to char production during torrefaction/pyrolysis are temperature, heating rate and hold time. There is therefore need to maximise char yields, provided that the minimum acceptable char quality is still maintained. It is likely that maximising char yields will also have economic benefits.

Regarding char production, as a first approach, the main parameters of interest will be char yields and the energy content (HHV). In order to further investigate the potential of coal substitution, the combustion properties of the generated char will be assessed, as detailed in **objective four.**

3.3 Objective three: To study the influence of heat and mass transfer on char yield and properties

Literature has reported the influence of increased particle size of feedstocks on char yields, due to heat and mass transfer limitations during thermal conversion of lignocelluloses. However, most studies have been conducted in only one reactor while varying particle size, at either milligram-scale or gram-scale.

Rare studies in literature have been reported on the influence of increased particle size together with change in scale. Increasing particle size feedstock materials and moving from milligram to gram-scale process conditions of torrefaction and slow pyrolysis offers an opportunity to investigate the possible changes in char yields and the accompanying energy properties as char quality (**objective one).**

3.4 Objective four: To study combustion characteristics of chars and their potential energy applications

Based on literature, rarely have standards been defined for lignocellulosic char that could be used for co-combustion with coal. Defining the fuel standards of char requirements for co-combustion would ensure that torrefaction or slow pyrolysis processes could be adjusted to aim at producing char of acceptable quality.

3.5 Tasks for implementing thesis objectives

In order to implement or fulfil the above-stated objectives, the following tasks were carried out:

3.5.1 Task one: Characterisation of feedstock materials

Several studies have reported the lignocellulosic composition of various feedstock materials, without necessarily showing the relationship between the structural composition of the feedstocks and the process requirements of torrefaction or slow pyrolysis for producing char for energy applications. The present study contributes to the existing knowledge by studying the lignocellulosic compositions of LC and MP as a pre-requisite. Differences in lignocellulosic compositions will result in different pyrolysis mechanisms, yields and the production of chars with different energy contents **(objective one)** and combustion properties **(objective four).** In order to correlate important results with the sample composition, knowing the lignocellulosic composition of the samples is essential.

The strategy for accomplishing this task, involved the determination of the lignocellulosic composition of raw samples of LC and MP using standardised wet chemistry methods. The results of the relationships between feedstock lignocellulosic composition and thermal behaviours under torrefaction and slow pyrolysis are reported in **Chapters 5 and 6,** while the correlations with combustion behaviours are described in **Chapter 7.**

3.5.2 Task two: Optimisation of torrefaction process parameters

Due to differences in lignocellulosic compositions, differences in torrefaction mechanisms can be obtained resulting in different char yields with variations in energy contents. There is

therefore need to link lignocellulosic composition with the potential fuel properties of the char obtained through torrefaction **(objective two).**

This task was carried out in order to address the limited information in literature on the relationship between char HHV and char yield related to lignocellulosic composition under torrefaction process conditions, in order to maximise char production for energy applications.

The experimental work conducted to fulfil the above-stated **objective two** consisted in optimising torrefaction process parameters of temperature, heating rate and hold time at milligram-scale using particle size distribution (PSD) of 425 to 600 µm in a TGA reactor, in order to maximise the production of char of acceptable quality from LC and MP samples.

The influence of the parameters and the possible interactions during torrefaction conversion was studied using central composite design (CCD). The response variables were char yield and char HHV, with the latter variable analysed using a bomb calorimeter. Using this approach, optimum process conditions for maximising char yield and the accompanying energy content (HHV) were discussed. The study performed to address these tasks under torrefaction conditions is detailed in **Chapter 5.** The results of the statistical study were used to determine the conditions that were later on used to investigate the influence of heat and mass transfer.

3.5.3 Task three: Optimisation of slow pyrolysis process parameters

Due to differences in lignocellulosic compositions, differences in slow pyrolysis mechanisms can be obtained resulting in different char yields with varying energy contents. There is therefore need to link lignocellulosic composition with the desired results during slow pyrolysis **(objective two).**

Though literature has shown that feedstock lignocellulosic composition does influence char yield and the resultant energy properties like HHV and fixed carbon, rare information in literature has been reported on why lignocellulosic char HHV decreases around 600 ˚C **(objective two).** The current study seeks to add knowledge by investigating the aforementioned aspects of LC and MP samples.

The experimental work conducted to meet the requirements of the above-stated objective two, consisted in optimising slow pyrolysis process parameters of temperature, heating rate and hold time at milligram-scale using PSD of 425 to 600 µm in a TGA reactor, in order to maximise the production of char for energy applications from LC and MP samples.

To accomplish this task, the influence of the parameters and their interactions was determined using CCD. Two response variables of char yield and char HHV were considered. The detailed study performed to address these findings is contained in **Chapter 6.** The optimised slow pyrolysis process conditions were later on used to investigate the influence of heat and mass transfer.

3.5.4 Task four: Influence of heat and mass transfer from milligram to gram-scale

Increased particle size is known to influence torrefaction/pyrolysis mechanisms and char yields, therefore optimised conditions or optimum properties under optimal conditions are likely to differ depending on the scale. There exists a gap in literature on the influence of increase in particle size and sample bed-size from milligram-scale to gram-scale, especially for the energy content of the char product.

The current study hopes to add knowledge on the effects of increase of particle size of samples from milligram-scale to gram-scale **(objective three),** with the aim of using optimised conditions to produce char at larger scale.

In order to fill the knowledge gap in literature, the following tasks were conducted:

(a) To produce char at gram-scale from LC and MP based on selected process conditions from TGA using PSD of 850 to 2800 µm in a fixed bed reactor.

(b) To assess the effect of moving from milligram-scale to gram-scale on the char yield and char HHV results obtained from (a) above.

Using this approach, selected char results obtained at gram-scale were compared with those from milligram-scale in terms of char yield, fixed carbon and HHV at similar conditions in order to investigate the effects of moving from one scale to another. Any differences that arose from the obtained results were explained in terms of mass and heat transfer effects as a consequence of increased particle and sample sizes. The results are contained in **Chapters 6 and 8.** Selected chars from gram-scale experiments were later on utilised as lignocellulosic parent fuel samples for co-combustion study with coal, as a way of coal replacement outlined in **objective four.**

3.5.5 Task five: Influence of biomass composition on optimal conditions, mechanism study

Though literature has shown that lignocellulosic biomass composition does influence the yield and the composition of char obtained by thermal treatment, there still exits a knowledge gap on the relationship between feedstock properties and torrefaction and slow pyrolysis conversion mechanism behaviour. The current study seeks to understand the influence of LC and MP

lignocellulosic compositions on char yields and HHV as a function of process conditions **(objective two).**

In order to get additional information to investigate the relationship between feedstock composition and their influence on conversion mechanisms, different analytical techniques were used to characterise the volatiles released during thermal conversion. The experimental tasks were as follows:

(a) To study the composition of the volatiles released during torrefaction of LC and MP at milligram-scale using a mass spectrometer (MS) coupled on-line to the TGA. This approach focused on both condensable and incondensable volatiles with details in **Chapter 5.**

(b) To investigate the influence of exit incondensable gas compositions from LC and MP on char yield and char HHV at gram-sale under slow pyrolysis using gas chromatography (GC).

To fulfil this task, incondensable gases collected in Tedlar bags were analysed by GC. **Chapter 6** contains the details of incondensable gas analyses for both samples.

3.5.6 Task six: Combustion characteristics study

Based on literature review, information is rare on the influence of lignocellulosic biomass composition and pre-treatment temperature on combustion (and co-combustion with coal) behaviour, especially from IAP feedstocks of LC and MP **(objective four).**

In order to fill the above-stated information gap in literature, the following tasks were conducted using TGA reactor:

(a) To investigate the combustion characteristics of selected parent fuel samples, namely, torrefied lignocellulosic biomasses and pyrolyzed chars of LC and MP from gram-scale, as well as three South African coals.

(b) To investigate the combustion characteristics of blended parent fuel samples (co-combustion) of LC and MP with each of the three South African coals.

The obtained results from co-combustion would be used to predict the potential of IAP chars for practically replacing coal in specified reactors.

To fulfil these tasks, parent and blended fuels were analysed for ignition, peak and burnout temperatures, maximum combustion rate and combustion efficiency, in terms of combustion indices. The detailed study performed to fulfil these tasks is contained in **Chapter 7.**

3.5.7 Task seven: Potential use of torrefied and pyrolysed char

Based on literature, rarely have standards been defined for lignocellulosic char that could be used for co-combustion with coal. Defining the fuel standards of char requirements for co-combustion would ensure that torrefaction or slow pyrolysis processes could be adjusted to aim at producing char of acceptable quality **(objectives two and four).**

In order to address this issue, char results obtained in this study were compared for their energy properties and combustion characteristics with various fuels, namely Namibian and Zambian charcoals, and Zambian coal specifications that were replaced by three South African coal samples.

The comparative discussions and analysis of the potential applications of the chars for domestic and industrial applications are detailed in **Chapter 8.**

Chapter 4 **Materials and methods**

This chapter outlines the materials and the main equipment used for the key experimental works of the entire study. The description of the methods used to complete specific experimental tasks are given more in detail in the relevant chapters.

4.1. Materials

4.1.1 *Lantana camara* and *Mimosa pigra* samples

Two invasive alien plants (IAPs), namely *Lantana camara* (LC) and *Mimosa pigra* (MP) were harvested as mature plants from Zambia in January 2014. The wet samples were oven-dried at 75 ˚C for 6 hours to remove excessive moisture and thereafter manually cut into wood chips, before transporting them to South Africa. LC and MP were the main lignocellulosic feedstock materials for producing char at milligram and gram-scales, with detailed results in **Chapters 5-7.**

4.1.2 South African coals

In this work, three South African coal samples were obtained from North West University, to be used as benchmarks for char quality assessment. Unfortunately Zambian coal samples could not be secured or transported to South Africa, although the South African samples were of similar rank to those used in the Zambian industry. According to North West University and confirmed by characterisation at Stellenbosch University **(Chapter 7),** the composition of the South African coals in terms of fixed carbon and HHV were higher than 56 wt.% and more than 25 MJ kg^{-1}, respectively. These coals were considered as acceptable substitutes for the Zambian coal of relatively high quality, specifically for

company A and B outlined in Table 2-2, in **Chapter 2.** The three South African coal samples were used for co-combustion studies with details in **Chapter 7.**

4.1.3 Namibian and Zambian commercial charcoals

Two commercial charcoal samples, one from Namibia (Ethosha charcoal) prepared from local invasive plant materials and another Zambian charcoal prepared using the traditional earth kilning method [1,2] from miombo woodland trees [3,4], were used for comparative studies with LC and MP char for possible applications, as details in **Chapter 8.** The Zambian charcoal was obtained from Mpongwe rural district on the Copperbelt province, prepared by the traditional earth-kiln method. About 2 kg of lump charcoal was obtained and then was crushed to the required particle size for various analyses. The Namibian charcoal was obtained from local supermarkets here in Stellenbosch, packaged as barbeque charcoal. The samples were crushed to the required particle sizes for further analyses.

4.2. Equipment

4.2.1 Thermogravimetric analyser (TGA)

Thermogravimetric analysis (TGA) is an equipment that utilises a small sample of material (typically < 1 g) that is heated in a specified environment, either inert or oxidative with a controlled heating rate. Inert environments are provided by running inert gases like nitrogen or argon (baseline 5.0, Afrox), while oxidative environments exist when pure oxygen or air is introduced in the furnace. A succession of different segments, dynamic (controlled heating rate) or isothermal, can be programmed during TGA runs. The sample is heated in a furnace from a crucible at a desired rate on an electronic microbalance. As the sample is thermally decomposing, an accurate continuous record of the weight

change of the sample is measured and recorded within the TGA software (STARe). The derivative thermogravimetric (DTG) which gives the rate of change of the fuel sample on continuous basis can be plotted using the TGA software.

TGA was used to optimise process variables for maximising char production of acceptable quality utilising torrefaction **(Chapter 5)** and slow pyrolysis **(Chapter 6)** under inert conditions. For the study of combustion behaviour **(Chapter 7),** oxygen (HiQ 5.0, Afrox) was used with inert gas in order to obtain an atmosphere containing around 20% of oxygen. TGA can also provide additional information on reaction mechanisms and kinetic parameters.

It is well accepted that TGA can be used as an alternative method for proximate analysis [5]. When the TGA is operated first in an inert environment and then finally at 900 ˚C introduce oxygen for complete combustion, the measured weight of the fuel sample loss versus time on the graph, determines moisture, volatile matter, fixed carbon and the resultant ash content of the sample, as outlined in ASTM E1131 standard procedures. Proximate analysis is an important analytical technique for determining fuel quality.

The TGA model used in this work was TGA/DCS 1 Star System Mettler Toledo. The sample crucible capacities ranged from 70 to 600 µL, made from ceramic material. The heating rate goes up to 150 ˚C min^{-1}, while the maximum temperature is 1 000 ˚C. In order to protect the microbalance from produced volatiles, an argon flow of 20 mL min^{-1} is used. The main features of the TGA used in this work are shown in Figure 4-1.

Figure 4-1: Main features of TGA/DCS 1 Star System Mettler Toledo

The display window shows the operating conditions of the experiment under use, for instance, sample and reactor temperatures, sample weight, heat flow, cell gas and method gas flow rates. Samples in crucibles are placed in the rotating disc where an automated robot picks the crucibles one at a time into the furnace, and then removed at the end of each experiment. To avoid external contamination, the rotating disc is usually covered. Gaseous emissions from the hot furnace are purged out through the exit pipe where other equipment like mass spectrometer (MS) could be connected to monitor volatiles.

4.2.2 Gram-scale tubular reactor

A horizontal stainless steel tubular reactor, measuring 1 m long and 60 mm external diameter was used for gram-scale char production for LC and MP samples [6].

The stainless steel tubular reactor is inserted into an electrically heated furnace, with the first end connected to nitrogen inflow (Figure 4-2), while the exit end is connected to a steel atmospheric condenser or cold trap. The condensation of volatiles starts in the atmospheric condenser, before being subjected to further cooling through a series of four glass condensers. The four glass condensers operate at dry-ice temperature of around -55 ˚C. Each of the condensers are connected by rubber

tubing sealed enough to avoid any leakages of the volatiles. Any volatiles that exit at the end of the fourth condenser are usually analysed as permanent gases where the use of Tedlar bags for holding the gases is employed. The permanent gases are analysed in a gas chromatography for various gas compositions.

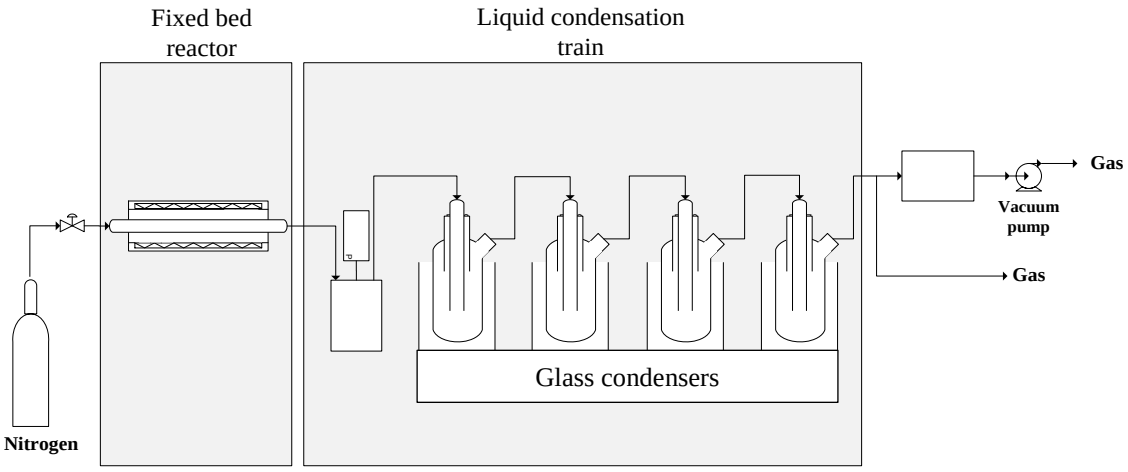

Figure 4-2: Torrefaction/slow pyrolysis experimental setup

The entire experimental setup for Torrefaction/slow pyrolysis is shown in Figure 4-2. During initial setup, the vacuum pump is connected at the exit end in order to check the system is airtight. Nitrogen provides inert conditions in the fixed bed reactor, placed and heated electrically in a furnace. The exiting volatiles first pass through a stainless steel atmospheric condenser (cold trap), before being cooled through a series of four glass condensers. At the end of the fourth condenser, the incondensable volatiles may be purged out into the exhaust system or sampled for further analysis.

In order to simplify the steps and stages of operation, of the reactor, Table 4-1 details each operational procedure.

Table 4-1: Experimental procedure for gram-scale slow pyrolysis experiments

Before the run – Assembly of unit		
Steps	Check	Notes
Weigh reactor and condenser components: - Stainless steel reactor - Steel exit reactor - Steel atmospheric condenser - Steel atmospheric connector - Glass condensers (1 x 4) - Rubber connecting tubes (1 x 4) - Glass reactor sample holder	Ensure that the reactor and condenser components are clean and dry	Weigh before and after experiment
Weigh out desired amount of sample and place into glass reactor sample holder	8 g per experimental run	Ensure that sample is even spread in the glass sample holder
Place the glass reactor sample holder in the centre of the Stainless steel reactor tube	Use baffle to move glass sample holder to the correct position in the Stainless steel reactor tube	Ensure that the sample holder has been placed in the centre of the reactor
Insert the Stainless steel reactor tube into furnace	Ensure the sample holder is centred in the middle of the furnace	Ensure that the sample does not spill during the insertion of the Stainless steel reactor into the furnace
Secure the end caps	Slide the metal flanges onto the Stainless steel reactor tube followed by the Teflon seals and end caps	Tighten the bolts coupling to the end caps and flanges in a star shape being careful not to over tighten
Assemble the steel atmospheric condenser	Place the rubber seal between the condenser and top plate and bolt together in a star pattern.	Ensure that the rubber seal is in correct position for effective sealing
Attach steel atmospheric connecting pipe to steel condenser and Stainless steel reactor tube	Tighten the link between the steel condenser and reactor	Ensure that the reactor contents still remain in position during the tightening
Assemble the 4 glass condensers	Seal the tops with petroleum jelly between the glass component	Ensure that condensers arranged in waterfall formation
Connect all condensers using the rubber pipes	Look out for small fragments of rubber that might be cut-out and fall away during the process of fastening the screws	Gently fasten screw connections
Add cooling medium to glass condensers	Iced water for first two glass condensers Dry ice at -55 ˚C for last two glass condensers	Ensure that there is enough dry ice available for further additions when necessary
Check for leaks	Attach vacuum pump to last glass condenser	Run the vacuum pump at a set vacuum pressure and ensure that the value of the desire vacuum pressure is maintained for at least 5 min

Table 4-1. Continued…

During experimental runs		
Steps	Check	Notes
Set the heating program and exit pipe temperature on the control panel	Insert a memory stick for saving of data during the process	Ensure that the memory stick has been identified by the electronic system and that there is enough memory capacity for the storing of the data
Start N_2 flow	0.5 $L.min^{-1}$	Purge the reactor and determine the exit flow rate before switching on the furnace
Switch on the furnace	Ensure that the reactor is well position, as it might have shifted during the fastening of the screws located at both ends	Ensure that the maximum temperature, heating rate and hold time are correctly set, before switching on the furnace
Monitor process during experiment		Check for the temperature rise up to the maximum temperature
After experimental runs		
Steps	Check	Notes
Switch off furnace	Switch off the furnace at the end of the specified hold time	Maintain N_2 flow rate
Allow the reactor contents to cool down to < 60 ˚C		Ensure that the reactor and sample temperatures are both < 60 ˚C to avoid possible combustion of the char
Measure N_2 flow rate at the end of the experiment	0.5 $L.min^{-1}$	This is very important for gas sampling as it ensures that the flow rate is the same from start up to the end
Stop N_2 flow		
Disassemble and weigh sections: - Stainless steel reactor - Steel exit reactor - Steel atmospheric condenser - Steel atmospheric connector - Glass condensers (1 x 4) - Rubber connecting tubes (1 x 4) - Glass reactor sample holder		Ensure accurate weighing of each component after cooling and drying, especially glass condensers

4.2.3 Bulk density cylinder

Bulk density in this study was adapted from the Food and Agriculture Organisation (FAO) report, on the quality control of charcoal and by-products [7]. The standard method uses a 100 ml calibrated cylinder that is filled with the solid sample and then tapped until the marked position is reached. Due

to limited char samples obtained from the fixed bed steel reactor (section 4.2.2), the 100 ml calibrated cylinder was replaced with a calibrated 10 ml cylinder, as outlined below. Preliminary tests for bulk density determination for raw samples of LC and MP were conducted in both 100 ml and 10 ml graduated cylinder in order to check on accuracy, and the results showed similarities.

The raw or char sample was poured into a 10 ml calibrated cylinder. After each addition, the cylinder with its contents was tapped gently on a wooden bench until the volume was constant. When the 10 ml calibration mark was reached, the cylinder content were weighed accurately on an electronic balance. The weight of the sample multiplied by 100 gives the bulk density per litre, as expressed in kg m^{-3}. When available, the procedure could be facilitated by using a specifically designed shaking machine. Triplicate results were obtained for each sample.

4.2.4 Bomb calorimeter

A bomb calorimeter measures the energy content of fuel samples (liquid or solid) in a vessel with constant mass, volume and pressure in an isothermal environment. The vessel, referred to as “bomb” is filled with pure oxygen to ensure complete combustion of the fuel, after an ignition is introduced. The temperature rise is proportional to the energy released from the fuel sample, which will yield the specific energy if the weight of the sample is known. The gross calorific value or higher heating value (HHV) obtained is then related to the calibration and an HHV is obtained. The equipment is usually calibrated with a benzoic acid tablet. Solid fuel samples are usually placed in metallic crucibles, while liquid samples may be enclosed in capsule or directly placed into the crucible.

The bomb calorimeter was used to determine the HHVs of the raw samples of LC and MP, as well as all the fuels used in **Chapters 5-7**. Though several correlations may be used to determine HHV from

elemental [8] and proximate [9,10] analyses, bomb calorimetry is generally considered to be more accurate and reliable.

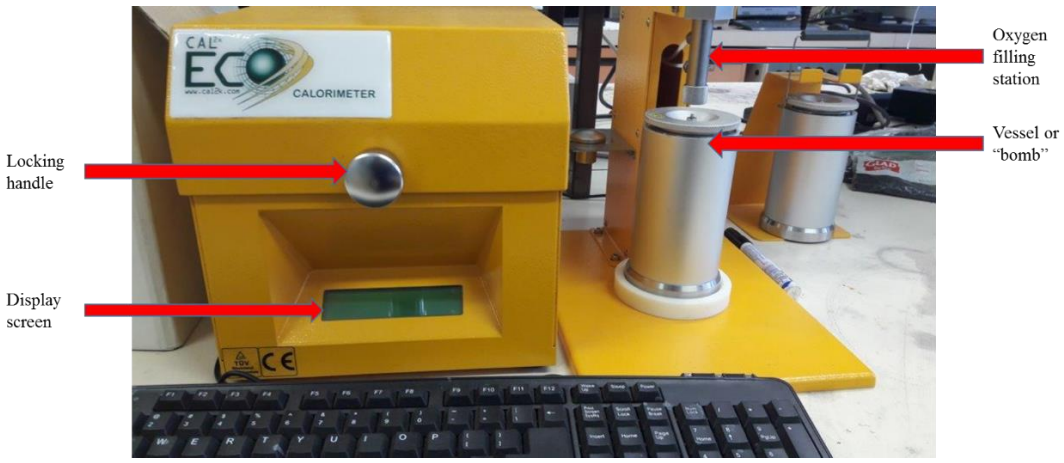

Figure 4-3: Main features of Cal2k ECO Bomb Calorimeter (2013)

The bomb calorimeter model (Cal2k ECO, 2013) used in this work with its main features, is shown in Figure 4-3. The oxygen filling station with pressure gauges (not shown) is directly connected to an oxygen cylinder. The vessel or bomb is filled with oxygen after the sample preparations are done. The main calorimeter compartment is opened using a locking handle, where the bomb is slowly lowered and closed so that the experiment can start. The display window shows the manually entered sample mass (grams) and the final calorific value or higher heating value (HHV; MJ kg^{-1}). The standardised method is outlined in accordance with ASTM method D5865-11a [11].

A sample mass in grams is weighed from an analytical balance and placed into a metallic crucible, with a firing-cotton attached to the sample, whilst tied to the firing (igniting) circuit. The minimum sample allowed is 0.2 grams, while the maximum sample is 1.999 grams. The firing circuit acts as the main cover of the bomb. The calorimeter vessel has a capacity of 0.2 litres of oxygen by volume, taking about 30 to 60 seconds to be filled with 99.5% of pure oxygen from a cylinder using a filling station. Each vessel has a unique number so that the calorimeter can identify which vessel is being

used. The gauge pressure required for reactive samples like lignocellulosic char is 1, 500 kPa (15 bars), while 3, 000 kPa (30 bars) is for less reactive samples like coal. The mass of the sample is manually entered into the ECO calorimeter via the PC keyboard prior to HHV determination. For firing, a length of pure cotton thread (CAL2K-4-FC) is tied to the firing wire with its "tail" touching the sample. The oxygen-full vessel is then lowered into the main calorimeter compartment and the lid closed with a securing locking handle. The calorimeter commences a displayed screen count-down for 10 minutes to equilibrate the temperature inside the vessel. After 10 minutes, the firing circuit introduces an electric spark to ignite the sample through the standard firing cotton attached to the sample. Temperature rise due to the burnt sample inside the vessel is accurately measured and the HHV calculated by the instrument after 10 minutes. The entire cycle takes 20 minutes, where at the end of each cycle, with corrections internally applied, the corrected HHV is displayed on the screen in MJ kg^{-1}. In case of any problems due to unburnt sample, a message of "misfire" is displayed, which would require starting the procedure again.

4.3. References

[1] Hibajene SH, Kalumiana OS. Manual for charcoal production in earth kilns in Zambia. Lusaka: 1994.

[2] Chidumayo EN. Estimating fuelwood production and yield in regrowth dry miombo woodland in Zambia. For Ecol Manage 1988;24:59–66.

[3] Chidumayo EN. Forest degradation and recovery in a miombo woodland landscape in Zambia: 22 years of observations on permanent sample plots. For Ecol Manage 2013;291:154–61.

[4] Chidumayo EN, Gumbo DJ. The environmental impacts of charcoal production in tropical ecosystems of the world: A synthesis. Energy Sustain Dev 2013;17:86–94.

[5] Naron DR, Collard F, Tyhoda L, Görgens JF. Characterisation of lignins from different sources by appropriate analytical methods : Introducing thermogravimetric analysis-thermal desorption-gas chromatography – mass spectroscopy. Ind Crop Prod 2017;101:61–74.

[6] Carrier M, Hugo T, Gorgens J, Knoetze H. Comparison of slow and vacuum pyrolysis of sugar cane bagasse. J Anal Appl Pyrolysis 2011;90:18–26.

[7] Domac J. Trossero M. Industrial Charcoal Production. vol. 3101. Zagreb: 2008.

[8] Sheng C, Azevedo JLT. Estimating the higher heating value of biomass fuels from basic analysis data. Biomass and Bioenergy 2005;28:499–507.

[9] Parikh J, Channiwala SA, Ghosal GK. A correlation for calculating HHV from proximate analysis of solid fuels. Fuel 2005;84:487–94.

[10] Nhuchhen DR, Abdul Salam P. Estimation of higher heating value of biomass from proximate analysis: A new approach. Fuel 2012;99:55–63.

[11] ASTM. Standard Test Method for Gross Calorific Value of Coal and Coke. Pennsylvania.: 2014.

Chapter 5 Torrefaction of invasive alien plants: Influence of heating rate and other conversion parameters on mass yield and higher heating value

Published in Bioresource Technology 209 (2016) 90–99

Title: "Torrefaction of invasive alien plants: Influence of heating rate and other conversion parameters on mass yield and higher heating value."

Authors: Jhonnah Mundike, François-Xavier Collard and Johann F. Görgens

Objective of dissertation in this chapter

This chapter addresses **specific objectives one and two,** which focus on the identification of fuel properties for defining of char quality **(objective one)**, by characterisation of feedstock materials of LC and MP by wet chemistry, and then optimise torrefaction temperature, heating rate and hold time at milligram-scale for the production of torrefied biomass **(objective two).** During torrefaction, study the composition of the volatiles released from LC and MP at milligram-scale, in order to analyse the conversion mechanisms using a mass spectrometer (MS) coupled on-line to the TGA **(objective two).**

Candidate declaration

In chapter 5 page numbers 65 to 96 of this dissertation, the type and scope of my contribution were as follows:

Nature of contribution	Contribution (%)
Planning of experiments	70
Executing experiments	100
Interpretation of results	60
Writing the chapter	100

The listed co-authors have contributed to chapter 5 page numbers 65 to 96 of this dissertation.

Name	e-mail address	Type of contribution	Contribution (%)
François-Xavier Collard	fcollard@sun.ac.za	Experimental planning	30
		Reviewing of chapter	30
Johann F. Görgens	jgorgens@sun.ac.za	Interpretation of results to correlate with literature	10
		Reviewing of chapter	10

Signature of candidate:……..

Date:……

Declaration by co-authors

The undersigned hereby confirm that

- the declaration above accurately reflects the type and extent of the contributions of the candidates and co-authors to chapter 5 page numbers 65 to 96 in the dissertation,
- no other authors contributed to chapter 5 page numbers 65 to 96 in the dissertation besides those specified above , and
- potential conflicts of interest have been revealed to all interested parties and that necessary arrangements have been made to use the material in to chapter 5 page numbers 65 to 96 of this dissertation.

Institutional affiliation	Date	Signature

Abstract

With the aim of controlling their proliferation, two invasive alien plants, *Lantana camara* (LC) and *Mimosa pigra* (MP), both widespread in Africa, were considered for torrefaction for renewable energy applications. Using thermogravimetric analysis, the influence of heating rate (HR: 2.18–19.82 ˚C min^{-1}) together with variable temperature and hold time on char yield and HHV (in a bomb calorimeter) were determined. Statistically significant effects of HR on HHV with optima at 10.5 ˚C min^{-1} for LC and 20 ˚C min^{-1} for MP were obtained. Increases of HHV up to 0.8 MJ kg^{-1} or energy yield greater than 10%, together with a 3-fold reduction in torrefaction conversion time could be achieved by optimisation of HR. Analysis of the torrefaction volatiles by TG–MS showed that not only hemicelluloses, but also lignin conversion, could influence the optimum HR value.

Keywords

Torrefaction, heating rate, higher heating value, temperature, invasive alien plants

5.1 Introduction

Globally, the easy and free movement of people within and across continents has led to the proliferation of non-indigenous or invasive alien plants (IAPs) in many places. These IAPs may have been intentionally or unintentionally introduced to various regions. Some of the widely reported impacts resulting from IAPs are minimised biodiversity in affected areas, harbouring of insect pests in some selected places, bush and grazing pasture encroachment and reduced access to water points [1,2]. This paper deals with the valorisation through torrefaction of two IAP biomasses prevalent in Zambia and other parts of tropical Africa, i.e. *Mimosa pigra* (MP) and *Lantana camara* (LC). It is hoped that through torrefaction of IAP biomasses, the control and management of these plants will be promoted, as they will be harvested as raw materials for commercial products.

In Zambia, MP is mainly found in Lochinvar National Park along the Kafue Flood Plains [3], while LC is a prevalent weed in Mosi-O-Tunya (Victoria Falls) National Park, as well as general bush encroachment countrywide. In trying to control and manage IAPs worldwide, 3 control and management strategies have mainly been applied; biological control, which uses living organisms or biocontrol agents; chemical control, which utilises chemical herbicides and mechanical control, employing physical means [2,4]. Despite the economic and ecological impacts resulting from IAPs, the management strategies for these weeds have recorded minimal success in their use as control measures [1,5].

Recently, the opportunity of converting IAP biomass by thermochemical conversion as means of value-addition to mechanically harvested biomass has gained interest [1,6]. In particular the utilisation of MP in Thailand [7] and LC in India [8] have been reported for energy applications. This bioenergy application opportunity will therefore promote the use of IAP biomass for the production of biofuels, thereby minimising deforestation of indigenous trees. This work is focused on the conversion of IAPs into torrefied biomass.

Compared with other thermochemical processes, torrefaction operates at relatively low temperatures 200-300 ˚C and is often conducted in inert environments [9,10]. Torrefaction has attracted various research works as a viable process for char production. Some of the notable advantages of torrefaction are that it reduces moisture content [11,12], lowers the ratios of H/C and O/C [13,14], and thereby increasing the fixed carbon content in the torrefied char [15,16], which ultimately results in higher calorific values, comparable to coal [11,13]. Furthermore, torrefied biomass has a longer storage time than original biomass as it becomes hydrophobic [15,17,18], while also exhibiting improved grindability [9,19], where particle size reduction is applicable.

Several studies have shown that during torrefaction, temperature is the main determining factor for torrefied biomass yield as well as its energy content. In case of torrefaction temperature, the higher the temperature, the more oxygenated groups become unstable and are converted into volatiles, resulting in lower char yield and increased char HHV. In case of torrefied biomass at 250 ˚C, char yields usually range from 75 to 90%, with a range of char HHV increase of 1-3 MJ kg^{-1}, while at 300 ˚C, char yields from 40 to 60% with corresponding char HHV increase of 3-7 MJ kg^{-1} are obtainable [14,16,20]. In general, longer residence time during torrefaction allows more time for the production of oxygenated volatiles, resulting in lower char yield and elevated HHV. For instance using corn stover, increasing hold time from 10 to 30 min at 250 ˚C, char yields decrease of 1.3 wt.% and HHV increase of 0.1 MJ kg^{-1} were observed, while prolonging the same hold time at 300 ˚C, a 4.1 wt.% reduction in char yields and 0.6 MJ kg^{-1} HHV increase were obtained [16]. From these results it appears that process parameters should not be studied independently and this highlights the need to use statistical methods taking the interactions between parameters into account.

Most works on biomass torrefaction have used fixed heating rate usually between 2 and 20 ˚C min^{-1} [21–23]. The influence of heating rate has therefore been rarely reported [24]. The slow pyrolysis of pine wood in a batch reactor by Williams and Besler, [25] showed that at 300 ˚C (a pyrolysis temperature applicable to torrefaction), heating rate could influence mass yields. A 13% change in char yield was obtained using heating rates of 5 and 80 ˚C min^{-1}, with the highest char yield recorded from the higher heating rate, though the char HHV was not determined.

In the present work, the torrefaction of two IAPs (LC and MP) biomasses for the production of char for energy applications is presented. A comprehensive process parameter assessment of multiple heating rates compared with variable temperature and hold time as well as their interactions on the desired char is reported. A central composite design was used to statistically assess the influence of process variables on char yields and char HHV. Thanks to very accurate monitoring of torrefaction

conversion at milligram scale with a thermogravimetric analyser and HHV determination with a bomb calorimeter, the influence of heating rate, temperature and hold time on the char yield and HHV could be determined.

5.2 Materials and methods

5.2.1 Feedstock preparation

Stems and branches of LC and MP plant materials were harvested in Zambia. LC samples were obtained from Mosi-O-Tunya National Park, near the Victoria Falls in Livingstone of the southern province and in Kitwe, up north on the Copperbelt province. The age of the LC plants was not established, although they were mature, some with a height above 2 m. MP samples were obtained from Lochinvar National Park along the Kafue Flood Plains. The age of the MP plants was about 5 years, based on the last harvesting exercise that had been conducted as a control measure in 2008. Both biomass samples were harvested in mid-January 2014. The samples were oven-dried at 75 ˚C for 6 hours and processed into wood chips before transporting them to South Africa. Upon arrival in South Africa, the samples were ground in a Retsch (SM 100) mill in preparation for further particle size reduction using various sieves. Thereafter, the sample materials were finally sieved using a Retsch shaker (AS 200) to a particle size distribution (PSD) of 425-600 μm. Before use, the biomass samples were stored in air-tight plastic bags to prevent external interferences.

5.2.2 Analytical methods

The raw biomasses were characterised for lignocellulosic composition as outlined in Technical Association for Pulp and Paper Industries (TAPPI) methods, from sample preparation to the various chemical analyses. Acid-insoluble lignin was determined in accordance to TAPPI Method T 222 *om-*

11, while hemicellulose was determined as outlined in TAPPI Method T 223 *cm-10*. Cellulose was determined by difference. Proximate analyses were performed according to ASTM standard E1131, using thermogravimetric analysis TGA/DCS 1 Star System Mettler Toledo. The HHV measurement for raw biomasses and chars was performed according to ASTM standard D5865-11a, using a bomb calorimeter, Cal2k Eco Calorimeter (model 2013), which was calibrated using benzoic acid (Cal2K).

5.2.3 Design of experiments (DoE)

The influence of torrefaction process parameters on mass yields and char HHV was studied using central composite design (CCD), using a statistical tool, Statistica version 12 software. CCD is a statistical method suitable for assessing the influence of process variables and their interactions on the desired product distribution. CCD is a useful tool for optimisation of process parameters [26]. Three independent variables were considered, being maximum temperature, hold time (HT) and heating rate (HR). The choice of values for the DoE ranged from the low, central and high temperature (220, 250, 280 ˚C), while the HT had (25, 52.5, 80 min), with a HR of (6, 11, 16 ˚C min^{-1}), respectively. The DoE resulted into 16 experiments, including two centre-points, which are detailed in the Appendices A-1 and A-2. The resultant operating ranges were 197.1-302.9 ˚C for temperature, 4.0-101.0 min for HT and 2.2-19.8 ˚C min^{-1} for HR. The range of HR falls within those mainly used for torrefaction [12,14,10]. The response variables were char yield (Ychar, wt.%) and HHV, (MJ kg^{-1}). The generated experimental data was used in the statistical tool to assess an analysis of variance (ANOVA) in order to determine the optimal values of temperature, HT and HR to maximise the Ychar and its energy content. Duplicate results for Ychar and HHV of the torrefied samples were subjected to ANOVA using a 95% confidence limit for each condition. The influence of torrefaction process parameters on response variables was determined individually. A p-value < 0.05 from the ANOVA table was considered to be statistically significant.

5.2.4 Torrefaction process

LC and MP raw biomass samples of PSD 425-600 µm were used during torrefaction in the TGA. Argon, at a flow rate of 70 ml min^{-1} was used as a method process gas. 600 µL sample crucibles containing 200-350 mg raw biomass were used in the TGA. A start-up temperature of 30 ˚C initiated the torrefaction process at a specified HR until the required torrefaction temperature was reached, where the sample materials were held at a specific HT, depending on the experimental conditions outlined in section 4.2.3. The torrefied samples were only removed from the TGA reactor after cooling to <100 ˚C in order to avoid any possibilities of combustion of the desired char.

The mass yield of the product was determined from the generated data of the TGA. From TGA and the derivative thermogravimetric (DTG) curves it appears that moisture was removed between 30-180 ˚C, while torrefaction chemical reactions only started at higher temperatures (at 180 ˚C, DTG ≈ 0%/min). The sample mass at 180 ˚C was considered as dry mass and the yield results were expressed on dry basis.

5.2.5 Analysis of torrefaction volatiles using TGA-MS

In order to study the composition of the volatiles released during torrefaction of LC and MP biomasses, Mettler Toledo TGA/DCS 1 thermogravimetric analyser (TGA) was coupled to a Pfeiffer Vacuum ThermoStar™ GSD320 T3 quadrupole mass spectrometer (MS). The conversion conditions in TGA were the same as detailed in section 4.2.4 except that the sample mass was reduced to 60 ± 3 mg. Volatiles produced in TGA were transferred using a pre-heated capillary tube at 190 ˚C to minimise possible condensation of vapours. The electron ionization voltage of the MS was set at 70 eV. The TGA reactor was purged until argon concentration reached 99.5%. Based on studies on torrefaction volatiles [14,27,28] and the database of National Institute for Standards and Technology

(NIST) the monitored fragmentation ions were *m/z* 18, 28, 29, 31, 32, 43 and 44. Triplicate samples were prepared for reproducibility. The mass loss of the sample between 30 and 180 ˚C is essentially due to the release of moisture and resulted in the formation of a peak in the curve corresponding to the evolution of ion *m/z* 18. By comparing the mass loss (obtained from TGA) and the surface area under the curve corresponding to the ion *m/z* 18 between 30 and 180 ˚C, the MS curves were normalised. Comparisons of volatiles production during torrefaction conversion (T > 200 ˚C) were made based on ion current intensity and area under the curve. The average relative standard deviation (RSD) on surface area determination was 12.7%.

5.3 Results and discussion

5.3.1 Lignocellulosic characterisation

The composition of LC and MP raw biomasses is shown in Table 5-1. Both feedstock materials as indicated in Table 5-1 had almost the same amount of cellulose (≈48%), while LC contained more hemicelluloses (28.9%) than MP (22.0%). MP had more lignin (28.9%) compared to LC (20.6%). explaining its higher fixed carbon content (19.43%) compared to LC (18.50%). The raw biomasses had comparable energy contents, measured as HHV (17.98 MJ kg^{-1} for LC and 17.67 MJ kg^{-1} for MP). The lignocellulosic compositions of both raw biomasses are consistent with those reported in literature [7,8].

5.3.2 Torrefaction

The char yields (Ychar, dry wt.%) and higher heating values (HHV, MJ kg^{-1}) obtained from replicate tests are detailed in Appendices A-1 and A-2. The average Ychar values were obtained with an average standard deviation of (± 0.10 wt.%) for LC and (± 0.07 wt.%) for MP, while the average

standard deviation for char HHV for both samples was (± 0.10 MJ kg^{-1}). The use of CCD coupled with analytical results with small standard deviations enhanced the detection of statistically significant effects.

In the summarised results of the statistical analysis in Table 5-2 several p-values, extracted from ANOVA tables, highlighted the significant influence (p-values < 0.05) of the factors on Ychar and HHV for both samples. Temperature and HT were found to have a significant effect on both Ychar and HHV for all linear (L) factors. Though HR did not present any significant effects on Ychar, it was found to influence the HHV linear factor for MP and quadratic (Q) factor for LC. Linear interactions between temperature and HR (1L by 3L) as well as HT and HR (2L by 3L) have not been included in Table 5-2, due to their statistical insignificance (p-values > 0.05). The adequacy of the models (LC and MP) from Statistica can be confirmed from the values for R-squared (R^2) and adjusted R-square (R^2 adj) being >0.95.

The simplified general model equation from Statistica software is thus: $y = \beta_0 + \beta_1 x_1 + \beta_2 x_2 + \beta_3 x_3 + \beta_{11} x_1^2 + \beta_{22} x_2^2 + \beta_{33} x_3^2 + \beta_{12} x_1 x_2$

Where: $y = response\ variable;\ \beta_{0-3} = model\ coefficients\ from\ statistical\ analysis;\ x_1 = temperature; x_2 = HT;\ x_3 = HR$

5.3.2.1 Ychar and HHV for torrefied samples

The influence of temperature, HT and HR on Ychar and char HHV for both biomass samples is presented in the following sections.

5.3.2.1.1 Influence of temperature on Ychar

Temperature played a major role in influencing Ychar for both samples with statistical significance (p-values <1 x 10^{-6}). As expected, a higher degree of conversion and lower Ychar were observed with increasing torrefaction temperature for both biomasses, as indicated by the negative linear factor coefficient associated to temperature in Table 5-2 (- 16.10 for LC and - 12.72 for MP) and reported previous [14,16]. The influence of temperature on Ychar is illustrated in Figure 5-1a for a HT of 52.5 min and a HR of 11 ˚C min^{-1}. While during low temperature torrefaction at 220 ˚C there was minimal conversion, with Ychar >95 wt.%, the conversion became more significant at 250 ˚C, with similar Ychar for both biomasses of 80.03 wt.% for LC and 82.64 wt.% for MP. As the temperature increased to 302.9 ˚C the conversion intensified and Ychar drastically reduced almost by half, especially for LC. The difference in the degree of conversion (Ychar 43.38 wt.% for LC and 52.14 wt.% for MP) can be explained by the higher hemicelluloses content in LC (Table 5-1), the biomass component that is known to be the less stable under torrefaction [14,17].

5.3.2.1.2 Influence of temperature on char HHV

Based on Table 5-2, torrefaction temperature significantly influenced the HHV of char products for both biomasses, with p-values < 1 x 10^{-6} for the linear factors. Both samples showed an increase in char HHV in response to an increase in temperature, as confirmed by the positive linear coefficients in Table 5-2 (+ 2.27 for LC and + 1.50 for MP) and reported in literature [12,10]. In Figure 5-1b the influence of temperature on char HHV is illustrated for the same conditions (HT of 52.5 min and HR of 11 ˚C min^{-1}). Both samples at the lowest temperature produced char with slightly higher energy content (>18 MJ kg^{-1}) than the initial biomass. As the temperature increased more deoxygenation was promoted resulting in reduced Ychar (Figure 5-1a), ultimately producing char with an increased HHV (Figure 5-1b). While the conversion at 250 ˚C improved the fuel properties of both biomasses (+ 2.10 MJ kg^{-1} for LC and + 1.49 MJ kg^{-1} for MP compared to 197.1 ˚C), a more substantial HHV increase

was observed between 250 and 280 ˚C (+ 6.19 MJ kg^{-1} for LC and + 4.62 MJ kg^{-1} for MP), which is consistent with the important mass loss observed on the same temperature range (Figure 5-1a).

5.3.2.1.3 Influence of hold time (HT) on Ychar

For both biomasses, HT significantly influenced Ychar, with p-values <1 x 10^{-6} for the linear factors (Table 5-2). The linear factor coefficients (- 4.41 for LC, and - 3.29 for MP), are in agreement with the fact that longer HT ultimately reduced the Ychar values [18,9]. This trend was particularly pronounced under severe torrefaction as illustrated in Figure 5-2a, which shows Ychar results at 280 ˚C with a HR of 16 ˚C min^{-1} (similar results are obtained with a HR of 6 ˚C min^{-1}). LC Ychar reduced by 20.5% from a HT of 25 min to 80 min compared with 9.3% for MP under similar torrefaction conditions. A catalytic effect due to the difference in inorganic content and composition, or more probably due to the volatiles produced [29,30], in particular the carboxylic acids during hemicelluloses conversion, could explain that HT had a greater effect on reducing Ychar for LC biomas3s than MP during the isothermal conditions.

5.3.2.1.4 Influence of hold time (HT) on char HHV

In case of the influence of HT on char HHV, both samples recorded statistically significant p-values, which were <1 x 10^{-6} for LC and <2.1 x 10^{-5} for MP, with positive effects from the linear coefficient factors (+ 0.62 for LC and + 0.34 for MP), indicating that HHV increased with prolonged HT [16,21]. For tests with same temperature and HR, an increased HHV were always recorded for longer HT. During severe torrefaction conditions at 280 ˚C, LC recorded an increase in HHV of 11.5% from a HT of 25 min to 80 min, while MP HHV increased by 1.6% under similar torrefaction conditions as illustrated in Figure 5-2b. This result is consistent with the respective degree of conversion of the two biomasses (Figure 5-2a).

5.3.2.1.5 Influence of heating rate (HR) on Ychar

The Ychar results for both biomasses were not statistically influenced by HR, as indicated by the p-values (>0.05) in Table 5-2. However, it is worth noting that both char samples recorded positive coefficients for the linear HR factors (+ 0.27 for LC and + 0.16 for MP), which would indicate a possible increase in Ychar with increasing HR. Interestingly, a careful analysis of the Ychar (Appendices A-1 and A-2) shows that throughout torrefaction, for identical temperature and HT, the torrefied samples consistently followed a trend where elevated HRs promoted increased Ychar results. The decreased Ychar associated with lower HR could be due to longer conversion time or differences in torrefaction mechanisms as detailed in section 5.3.2.2.

5.3.2.1.6 Influence of heating rate (HR) on char HHV

Although HR had minimal effects on Ychar, its influence on char HHV was statistically significant for both samples. For MP a significant p-value (0.01) was obtained for the linear HR factor only, with an associated positive coefficient (+ 0.17), indicating that increasing HR increased HHV. This trend is illustrated in Figure 5-3a (MP model) for a temperature of 250 ˚C. In order to study the extent of this trend, additional experimental works were conducted for HR of 25 and 30 ˚C min^{-1} as illustrated in Appendix A-3. From these tests it appeared that an optimum HR is observed around 20 ˚C min^{-1} (20.62 MJ kg^{-1} according to the statistical model and 20.76 MJ kg^{-1} obtained from the experimental test at 19.82 ˚C min^{-1}), after which the MP char energy values begin to decrease. This was confirmed by torrefaction at a HR of 25 ˚C min^{-1}, which recorded HHV (20.34 MJ kg^{-1}), while 20.27 MJ kg^{-1} was obtained from a HR of 30 ˚C min^{-1}. In case of LC, only the quadratic HR factor was significant with a p-value (2.3 x 10^{-3}), accompanied with a negative coefficient (- 0.20), an indication of an optimum HR as it can be observed in Figure 5-3b for a temperature of 250 ˚C. For the example of a HT of 52.5 min (Appendix A-3) the optimum was obtained at 10.5 ˚C min^{-1}. At the optimum HR, HHV of 20.96 MJ kg^{-1} was predicted from the model (while 20.94 MJ kg^{-1} was obtained for the test

at 11 ˚C min^{-1}) compared with 20.42 MJ kg^{-1} obtained at the lowest range of HR (2.2 ˚C min^{-1}), while at the highest range of HR (19.8 ˚C min^{-1}), HHV of 19.88 MJ kg^{-1} was recorded.

5.3.2.2 Volatile evolution profiles during torrefaction

In order to gain an insight into the influence of torrefaction on char energy content, the evolution profiles of some key volatiles was analysed by coupling TGA with a MS analyser. For a more complete picture of volatile evolution profiles during torrefaction the results for the most severe conditions (280 ˚C) are reported.

5.3.2.2.1 Comparison of LC and MP torrefaction

According to several works studying the individual conversion of biomass constituents [14,28,30], in the torrefaction range most of the mass loss takes place due to the thermal conversion of the hemicelluloses, while up to 20% of the initial lignin content is converted to volatiles. Cellulose is rather stable below 300 ˚C with a slow mass loss mostly due to some dehydration reaction [31]. As LC and MP present similar cellulose content (≈48%), the conversion of cellulose is likely to generate similar amount of H_2O. As a consequence, differences in volatile production during torrefaction between the two biomasses are expected to be essentially related to the higher hemicelluloses content of LC and increased lignin content of MP.

The derivative thermogravimetric (DTG) curve and evolution profiles of some key ions obtained with a HR of 16 ˚C min^{-1} are detailed in Figures 5-4a and b. While the DTG curve obtained from LC, composed of a peak at 274 ˚C and a shoulder around 240 ˚C, is characteristic of hemicelluloses conversion, any shoulder is more difficult to detect on MP DTG curve. For both samples, the maximum mass loss rate was observed just before the sample temperature reached 280 ˚C (at 978 s

and 274 ˚C for LC and at 1013 s and 275 ˚C for MP). Compared to MP, the higher DTG peak obtained for LC is consistent with its higher hemicelluloses content and degree of conversion.

During torrefaction, volatiles reported to be produced with significant yields are H_2O, CO_2, CO, methanol, acetol, hydroxyacetaldehyde (HAA) and acetic acid [28,30]. Based on NIST library and torrefaction yield [28], the fragmentation ions *m/z* 18, 44 and 28 can be used as indicator of H_2O, CO_2, CO production respectively. Their evolution profiles are presented in Figures 5-4a-c. Other monitored ions were *m/z* 29 (obtained from methanol, HAA), *m/z* 31 (acetol, methanol, HAA), *m/z* 32 (methanol, HAA) and *m/z* 43 (acetic acid, acetol). The evolution profiles of these ions during the main conversion stage (220-280 ˚C) are represented in Figures 5-5a-c. It can be observed that the curves corresponding to H_2O and CO_2 production present a shape similar to the DTG curve, while CO formation starts later. Comparing the intensities of the monitored ions between 200 and 280 ˚C, higher intensities were obtained for LC (except for H_2O), which is consistent with its higher degree of conversion. With regards to H_2O production, higher intensity was recorded for MP during the main mass loss step around 1000 s. However, during the isothermal step at 280 ˚C, LC H_2O production became superior. When comparing H_2O release between 200 ˚C and the end of the experiment by calculating the surface area under the curve, similar H_2O production was obtained for a HT of 25 min ($18.4 \pm 0.6 \times 10^{-6}$) for LC and ($17.8 \pm 0.7 \times 10^{-6}$) for MP and higher for LC at 80 min ($26.5 \pm 1.9 \times 10^{-6}$) versus ($22.8 \pm 0.4 \times 10^{-6}$) for MP. It is worth noting that for the ions *m/z* 31, 32 and to a lower extent *m/z* 29, a peak/shoulder was observed at 233 ˚C for LC and 245 ˚C for MP with similar intensities for both samples, indicating at least 2 different steps of production. Based on the relative intensities of ions *m/z* 31 and 32 (in comparison with NIST library), the first step of production is rather due to methanol formation (and not HAA which is rather produced during the second step). The production of methanol at such temperature has already been reported, due to fragmentation of the methoxyl group of the 4-O-methyl-α-D-glucuronic acid in hemicelluloses, but also by the breakage of the bond C_β-C_γ in lignin alkyl chain [30]. Based on the relatively high intensity observed for *m/z* 31 and 32

during the first step of mass loss of MP, the biomass with the higher lignin content, it can be deduced that a significant amount of methanol was produced from lignin and that along with hemicelluloses, it is highly probable that lignin conversion also contributed to the first step of mass loss.

5.3.2.2.2 Influence of HR (2-20 ˚C min^{-1}) on volatile production

As detailed in section 5.3.2.1.5, it was observed when comparing experiments implemented with same temperature and HT that tests with lower HR always gave lower Ychar. This trend could be due to longer conversion time in case of slow HR, but also due to differences in conversion mechanism. In the case of pyrolysis conversion (T > 300 ˚C), it is well accepted that elevated HR give higher volatiles production while low HR promote Ychar [7,25,30]. This trend is particularly due to the characteristics of cellulose conversion. Compared to Ychar obtained from the conversion of individual constituents at 100 ˚C min^{-1}, [32] found that the use of a HR of 2 ˚C min^{-1} led to char increase significantly higher for cellulose (+ 206%) than for xylan (+ 46%) and lignin (+ 15%). With regards to polysaccharides conversion, elevated HR is known to promote depolymerisation reaction (breakage of the glycosidic bond) while low HR result in more dehydration reactions, higher reticulation of the matrix and thus higher Ychar [30]. As most of hemicelluloses conversion happens before 280 ˚C, a similar trend is expected for hemicelluloses, especially under severe torrefaction. Concerning lignin conversion, various types of linkages are involved on a wide temperature range and the influence of HR, in particular during torrefaction, is scarcely documented [24].

Another result commonly true for torrefaction and pyrolysis, is that when the degree of conversion increases, the char HHV increases simultaneously [22,33] (as observed for a temperature increase for instance in Figure 5-1). However, in this work it was observed that HHV was statistically influenced by the HR with an optimum at 10.5 ˚C min^{-1} for LC and around 20 ˚C min^{-1} for MP. This result means that a higher degree of conversion does not systematically mean a higher HHV. For instance, when

comparing chars obtained from MP conversion at 250 ˚C and a HT of 52.5 min, HR of 19.8 ˚C min^{-1} led to a slightly higher char yield (82.76% vs 82.30%) and a significantly higher HHV (20.76 MJ kg^{-1} vs 20.04 MJ kg^{-1}) than 2.18 ˚C min^{-1}.

In order to better understand the influence of HR on char HHV, the volatiles produced by MP torrefaction at a temperature of 280 ˚C and a HT of 25 min were compared for HR of 16 and 6 ˚C min^{-1} (char HHV of 21.80 MJ kg^{-1} and 21.11 MJ kg^{-1} respectively) as illustrated in Figures 5-4 and 5-5. As the original trend regarding the influence of HR on HHV clearly appears for torrefaction temperature from 250 ˚C, a particular attention should be given to differences in mechanism during the first step of conversion (around 240 ˚C). For both experiments, the higher production rate of H_2O, CO_2 and CO was observed simultaneously to that of the DTG peak (Figures 5-4b and c). Regarding quantitative analysis of MS results, as intensities obtained from experiments with different HR are hardly comparable, surface area under the curve was used. While results were overlapping for CO and CO_2, a significant difference was obtained for H_2O production ($19.7 \pm 1.1 \times 10^{-6}$) for HR6 and ($17.8 \pm 0.7 \times 10^{-6}$) for HR16. The higher H_2O production was consistent with the expected higher degree of polysaccharide dehydration for lower HR.

From the curves illustrating the evolution profiles of ions *m/z* 31 and 32 (Figures 5-5b and c), a particular difference in volatile formation can be observed. While for a HR of 6 ˚C min^{-1} these ions are mostly detected during the main mass loss, for a HR of 16 ˚C min^{-1} an important production was also observed during the first step of conversion (240 ˚C). This result means that a reaction associated with methanol formation at 240 ˚C (and promoted for a HR of 16 ˚C min^{-1}) could be related to a mechanism leading to enhanced deoxygenation, resulting in an increased char HHV. Increased HHV could have also have been as a result of decarboxylation reactions during the conversion mechanism.

The existence of an optimum can certainly be considered as an indicator of different trends, that the various reactions improving the HHV are differently influenced by the HR. As the optimum was obtained for a higher HR for MP (sample with the higher lignin content) than for LC (20 ˚C min^{-1} and 10.5 ˚C min^{-1} respectively), an explanation could be that for lignin torrefaction, HHV was promoted by an increase in HR. It is worth reminding that these observations concern the range of HR considered in this work (≤ 20 ˚C min^{-1}). A study of the influence of the HR during the individual torrefaction of the biomass constituents could help to understand the original result described in this dissertation.

5.3.2.2.3 Torrefied IAPs for energy application and benefits of HR optimisation

Using standard coal classification based on American Standard for Testing of Materials (ASTM) D 388, where fixed carbon content or HHV can be used as a ranking factor, the torrefied char samples were compared with coal for their HHV. Throughout torrefaction, temperature was the most influential factor for both biomasses. At 220 ˚C, most of the obtained torrefied chars recorded a HHV <19.5 MJ kg^{-1}, comparable to lignite A coal. At 250 ˚C, both biomasses produced char that can be classified as sub-bituminous *C* coal (19.31-22.09 MJ kg^{-1}). Drawing a parallel with slow pyrolysis, it could be assumed that during torrefaction reduced HR produce chars with increased yields and HHV values. This study evidenced that HHV evolution showed a different trend with the identification of an optimum HR. In case of LC at 250 ˚C and with a HT of 52.5 min, the optimum HR was observed at 10.5 ˚C min^{-1} and recorded a char HHV of 20.96 MJ kg^{-1}. Decreasing the HR up to 2 ˚C min^{-1} reduced the HHV to 20.40 MJ kg^{-1}, while 20.20 MJ kg^{-1} was obtained at 20 ˚C min^{-1}. In case of MP at 250 ˚C and HT of 52.5 min, the optimum condition was observed for a higher HR close to 20 ˚C min^{-1} and resulted in a HHV of 20.62 MJ kg^{-1}, a value 3.9% higher than what is obtained for a HR of 7.5 ˚C min^{-1} (19.85 MJ kg^{-1}).

At 280 ˚C, depending on the HT, LC char HHV was comparable to sub-bituminous *B* (22.09-24.42) MJ kg^{-1}) or *A* (24.42-26.74 MJ kg^{-1}) coal, while MP char was equivalent to sub-bituminous *C* or *B* coal. At the highest torrefaction temperature, MP char was classified under sub-bituminous *A* coal, while LC char was categorised as high volatile bituminous *C* coal (26.74-30.23 MJ kg^{-1}), due to its important conversion during the isothermal step at maximum temperature. Under severe torrefaction, similarly to what was observed at 250 ˚C, for similar HT, the optimisation of HR can result in energy gain up to 0.8 MJ kg^{-1}.

Another example illustrating the benefit of HR optimisation can be seen in Figure 5-6, where the conversion time and gross energy yield (EnY) of different processes are compared. EnY is the ratio of the preserved energy after torrefaction to that of the energy contained in the raw biomass [11]. From the experimental results obtained for MP at 280 ˚C, it appeared that similar HHV were recorded for MP4 (21.96 MJ kg^{-1}) and MP7 (21.84 MJ kg^{-1}), while the test MP7 was significantly shorter due to higher HR and shorter HT, and gave substantially higher Ychar (Appendix A-2). As a consequence with a conversion time divided by 3, MP7 had an EnY of 89.9% compared to 81.5% for MP4. An even more substantial difference can be found from the extraction of the predicted results for the optimised HR (Model OPT with a HT of 25 min, HHV of 22.32 MJ kg^{-1}) and an unfavourable HR (Model low, 7.5 ˚C min^{-1} with a HT of 80 min, HHV of 22.19 MJ kg^{-1}). As illustrated in Figure 5-6 the optimisation of the HR can result in increase in EnY higher than 10% with a process time divided by a factor 3. The input energy to the torrefaction process is therefore considerably reduced, while producing a similar quality char with better EnY.

5.4 Conclusion

This work investigated the influence of HR during the torrefaction of two IAP biomasses on char yield and HHV. It demonstrated that HR statistically influenced the char HHV together with temperature and HT. While under pyrolysis conditions (T > 300 ˚C), low HR are known to promote char yield and HHV, optimum torrefaction HR were found between 10 and 20 ˚C min^{-1}. An optimisation of HR can result in HHV increase up to 0.8 MJ kg^{-1} or to the production of similar char quality with increased energy yield by 10% together with a process time divided by a factor 3.

Acknowledgements

The authors wish to thank the staff at Mount Makulu Research Station under the Ministry of Agriculture and Livestock in Chilanga Zambia and the Directorate of Plant Health Division of the Ministry of Agriculture, Forestry and Fisheries, in South Africa for providing guidance and obtaining of the phytosanitary certificate for *Lantana camara* and *Mimosa pigra* samples. The phytosanitary certificate facilitated for the smooth transportation of both biomass sample materials from Zambia to South Africa.

5.5 References

[1] Liao R, Gao B, Fang J. Invasive plants as feedstock for biochar and bioenergy production. Bioresour Technol 2013;140:439–42.

[2] Vardien W, Richardson DM, Foxcroft LC, Thompson GD, Wilson JRU, Le Roux J. Invasion dynamics of Lantana camara L. (sensu lato) in South Africa. South African J Bot 2012;81:81–94.

[3] Shanungu GK. Management of the invasive Mimosa pigra L. in Lochinvar National Park, Zambia. Biodiversity 2009;10:56–60.

[4] Zalucki MP, Day MD, Playford J. Will biological control of Lantana camara ever succeed? Patterns, processes & prospects. Biol Control 2007;42:251–61.

[5] McConnachie MM, Cowling RM, van Wilgen BW, McConnachie DA. Evaluating the cost-effectiveness of invasive alien plant clearing: A case study from South Africa. Biol Conserv 2012;155:128–35.

[6] De Jongh WA, Carrier M, Knoetze JHH. Vacuum pyrolysis of intruder plant biomasses. J Anal Appl Pyrolysis 2011;92:184–93.

[7] Wongsiriamnuay T, Tippayawong N. Non-isothermal pyrolysis characteristics of giant sensitive plants using thermogravimetric analysis. Bioresour Technol 2010;101:5638–44.

[8] Kumar R, Chandrashekar N. Study on chemical, elemental and combustion characteristics of Lantana camara wood charcoal. J Indian Acad Wood Sci 2013;10:134–9.

[9] Arias B, Pevida C, Fermoso J, Plaza MG, Rubiera F, Pis JJ. Influence of torrefaction on the grindability and reactivity of woody biomass. Fuel Process Technol 2008;89:169–75.

[10] Pimchuai A, Dutta A, Basu P. Torrefaction of agriculture residue to enhance combustible properties. Energy and Fuels 2010;24:4638–45.

[11] Kim YH, Lee SM, Lee HW, Lee JW. Physical and chemical characteristics of products from the torrefaction of yellow poplar (Liriodendron tulipifera). Bioresour Technol 2012;116:120–5.

[12] Rousset P, Aguiar C, Labbé N, Commandré JM. Enhancing the combustible properties of bamboo by torrefaction. Bioresour Technol 2011;102:8225–31.

[13] Lee JW, Kim YH, Lee SM, Lee HW. Optimizing the torrefaction of mixed softwood by response surface methodology for biomass upgrading to high energy density. Bioresour Technol 2012;116:471–6.

[14] Prins MJ, Ptasinski KJ, Janssen FJJG. Torrefaction of wood. Part 2. Analysis of products. J Anal Appl Pyrolysis 2006;77:35–40.

[15] Felfli FF, Luengo CA, Suárez JA, Beatón PA. Wood briquette torrefaction. Energy Sustain Dev 2005;9:19–22.

[16] Medic D, Darr M, Shah A, Potter B, Zimmerman J. Effects of torrefaction process parameters on biomass feedstock upgrading. Fuel 2012;91:147–54.

[17] Li H, Liu X, Legros R, Bi XT, Lim CJ, Sokhansanj S. Torrefaction of sawdust in a fluidized bed reactor. Bioresour Technol 2012;103:453–8.

[18] Pach M, Zanzi R, Björnbom E. Torrefied biomass a substitue for wood and charcoal. 6th Asia-Pacific Internatioonal Symp Combust Energy Util 2002.

[19] Bridgeman TG, Jones JM, Williams A, Waldron DJ. An investigation of the grindability of two torrefied energy crops. Fuel 2010;89:3911–8.

[20] Neves D, Thunman H, Matos A, Tarelho L, Gómez-Barea A. Characterization and prediction of biomass pyrolysis products. Prog Energy Combust Sci 2011;37:611–30.

[21] Almeida G, Brito JO, Perré P. Bioresource Technology Alterations in energy properties of eucalyptus wood and bark subjected to torrefaction : The potential of mass loss as a synthetic

indicator. Bioresour Technol 2010;101:9778–84.

[22] Asadullah M, Adi AM, Suhada N, Malek NH, Saringat MI, Azdarpour A. Optimization of palm kernel shell torrefaction to produce energy densified bio-coal. Energy Convers Manag 2014;88:1086–93.

[23] Chin KL, H'ng PS, Go WZ, Wong WZ, Lim TW, Maminski M, Paridah MT, Luqman A. Optimization of torrefaction conditions for high energy density solid biofuel from oil palm biomass and fast growing species available in Malaysia. Ind Crops Prod 2013;49:768–74.

[24] Chen W-H, Peng J, Bi XT. A state-of-the-art review of biomass torrefaction, densification and applications. Renew Sustain Energy Rev 2015;44:847–66.

[25] Williams PT, Besler S. The influence of temperature and heating rate on the slow pyrolysis of biomass. Renew Energy 1996;7:233–50.

[26] Bandaru VVR, Somalanka SR, Mendu DR, Madicherla NR, Chityala A. Optimization of fermentation conditions for the production of ethanol from sago starch by co-immobilized amyloglucosidase and cells of Zymomonas mobilis using response surface methodology. Enzyme Microb Technol 2006;38:209–14.

[27] Melkior T, Jacob S, Gerbaud G, Hediger S, Le Pape L, Bonnefois L, Bardet M. NMR analysis of the transformation of wood constituents by torrefaction. Fuel 2012;92:271–80.

[28] Lê Thành K, Commandré J-M, Valette J, Volle G, Meyer M. Detailed identification and quantification of the condensable species released during torrefaction of lignocellulosic biomasses. Fuel Process Technol 2015:17–9.

[29] Mamleev V, Bourbigot S, Le Bras M, Yvon J. The facts and hypotheses relating to the phenomenological model of cellulose pyrolysis. Interdependence of the steps. J Anal Appl Pyrolysis 2009;84:1–17.

[30] Collard FX, Blin J. A review on pyrolysis of biomass constituents: Mechanisms and

composition of the products obtained from the conversion of cellulose, hemicelluloses and lignin. Renew Sustain Energy Rev 2014;38:594–608.

[31] Scheirs J, Camino G, Tumiatti W. Overview of water evolution during the thermal degradation of cellulose. Eur Polym J 2001;37:933–42.

[32] Elyounssi K, Collard FX, Mateke JAN, Blin J. Improvement of charcoal yield by two-step pyrolysis on eucalyptus wood: A thermogravimetric study. Fuel 2012;96:161–7.

[33] Chen WH, Cheng WY, Lu KM, Huang YP. An evaluation on improvement of pulverized biomass property for solid fuel through torrefaction. Appl Energy 2011;88:3636–44.

Table 5-1: Composition of raw biomasses used in this study.

Analysis		*Lantana camara*	*Mimosa pigra*
Proximate (%, wet)			
	Moisture	6.27 ± 0.24	7.37 ± 0.01
	Volatile matter	73.30 ± 0.11	71.41 ± 0.46
	Fixed carbon	18.50 ± 0.26	19.43 ± 0.31
	Ash	1.93 ± 0.07	1.79 ± 0.13
Lignocellulosic (%, dry)			
	Extractives	2.3 ± 0.5	1.6 ± 0.1
	Hemicellulose	28.9 ± 1.0	22.0 ± 0.8
	Cellulose[a]	48.2 ± 1.5	47.5 ± 0.3
	Lignin	20.6 ± 3.1	28.9 ± 0.1
Energy (MJ kg^{-1})			
	HHV	17.98 ± 0.03	17.67 ± 0.11

[a] Determined by difference

Table 5-2: Statistical results with p-values for Ychar (%) and HHV (MJ kg^{-1}) for LC and MP chars and their effects.

Variables	Factor	Coeff. (LC Ychar)	LC Ychar (p-value)	Coeff. (MP Ychar)	MP Ychar (p-value)	Coeff. (LC HHV)	LC HHV (p-value)	Coeff. (MP HHV)	MP HHV (p-value)
β_0	Mean/Intercept	79.89	<1 x 10^{-6}	82.66	<1 x 10^{-6}	20.96	<1 x 10^{-6}	19.91	<1 x 10^{-6}
β_1	Temp (˚C) (L)	-16.10	<1 x 10^{-6}	-12.72	<1 x 10^{-6}	2.27	<1 x 10^{-6}	1.50	<1 x 10^{-6}
β_{11}	Temp (˚C) (Q)	-3.60	<1 x 10^{-6}	-2.41	<1 x 10^{-6}	0.71	<1 x 10^{-6}	0.47	<1 x 10^{-6}
β_2	HT (min) (L)	-4.41	<1 x 10^{-6}	-3.29	<1 x 10^{-6}	0.62	<1 x 10^{-6}	0.34	2.20 x 10^{-5}
β_{22}	HT (min) (Q)	0.89	2 x 10^{-2}	1.48	<1 x 10^{-6}	-0.24	5.0 x 10^{-4}	0.01	0.91
β_3	HR (˚C min^{-1}) (L)	0.27	0.37	0.16	0.39	-0.06	0.29	0.17	0.01
β_{33}	HR (˚C min^{-1}) (Q)	-0.32	0.36	0.01	0.98	-0.20	2.40 x 10^{-3}	0.12	0.11
$\beta_1\beta_2$	1L by 2L	-2.63	<1 x 10^{-6}	-0.94	1.1 x 10^{-3}	0.62	<1 x 10^{-6}	0.08	0.33

Coeff. : Coefficients; L: linear function, Q: quadratic function, 1L by 2L: linear interaction functions between temperature and hold time, LC: *Lantana camara*, MP: *Mimosa pigra*, HHV: higher heating value, HT: hold time, HR: heating rate, $\beta_{0\text{-}3}$ = coefficients

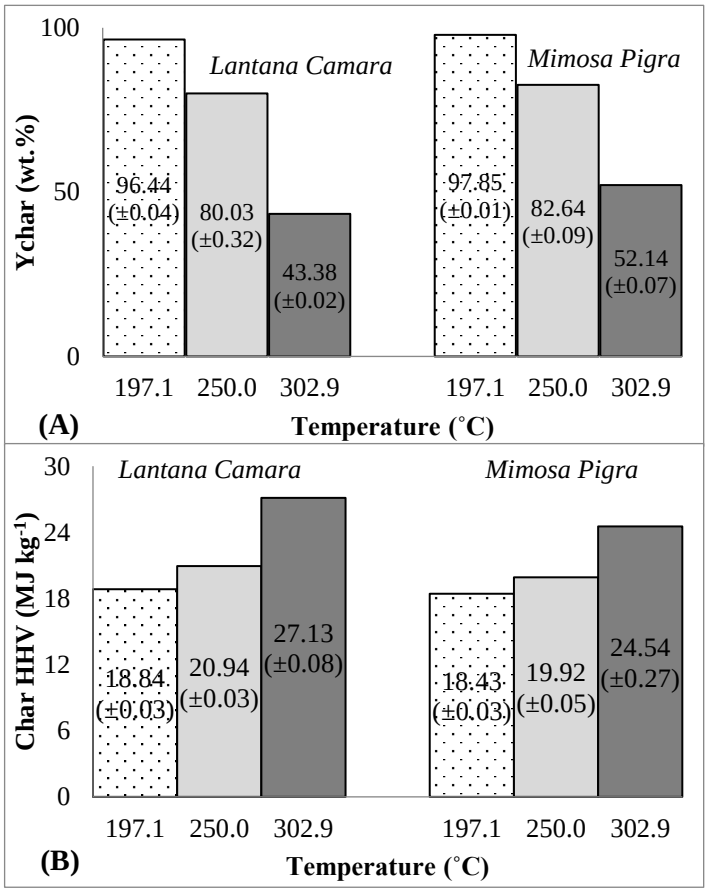

Figure 5-1: Influence of temperature on *Lantana camara* and *Mimosa pigra* (a) Ychar (b) char HHV at hold time of 52.5 min using a constant heating rate of (11 ˚C min^{-1}).

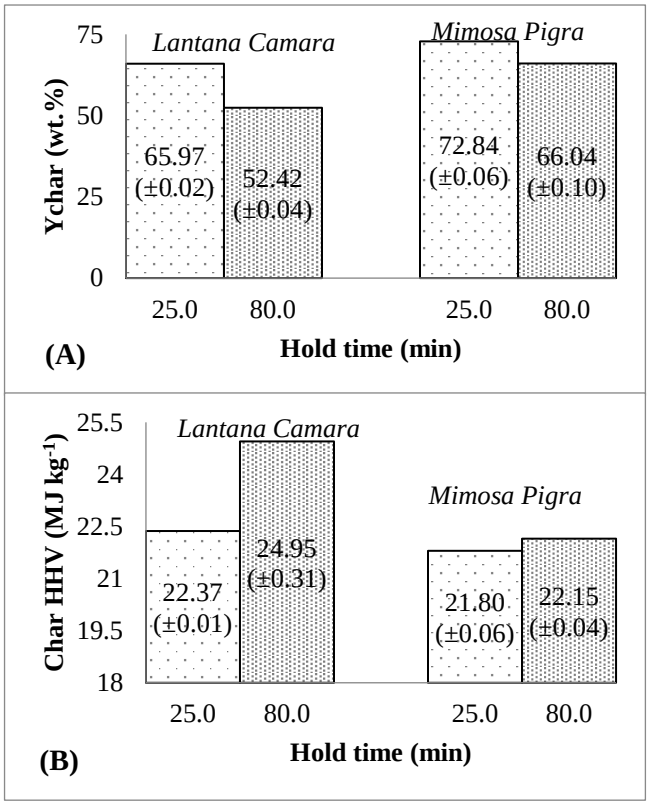

Figure 5-2: Influence of temperature on *Lantana camara* and *Mimosa pigra* (a) Ychar (b) char HHV at 280 ˚C using a constant heating rate of (16 ˚C min^{-1}).

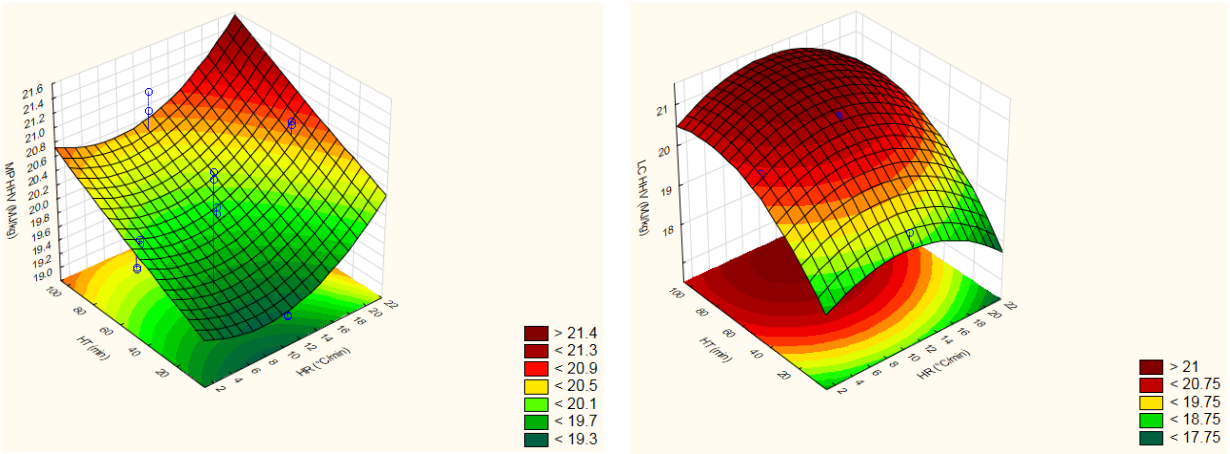

Figure 5-3: Influence of heating rate (HR) on (a) *Mimosa pigra* (MP) showing rise in HHV as the HR increases (b) *Lantana camara* (LC) char HHV, showing optimum conditions using Statistica surface plots at 250 ˚C.

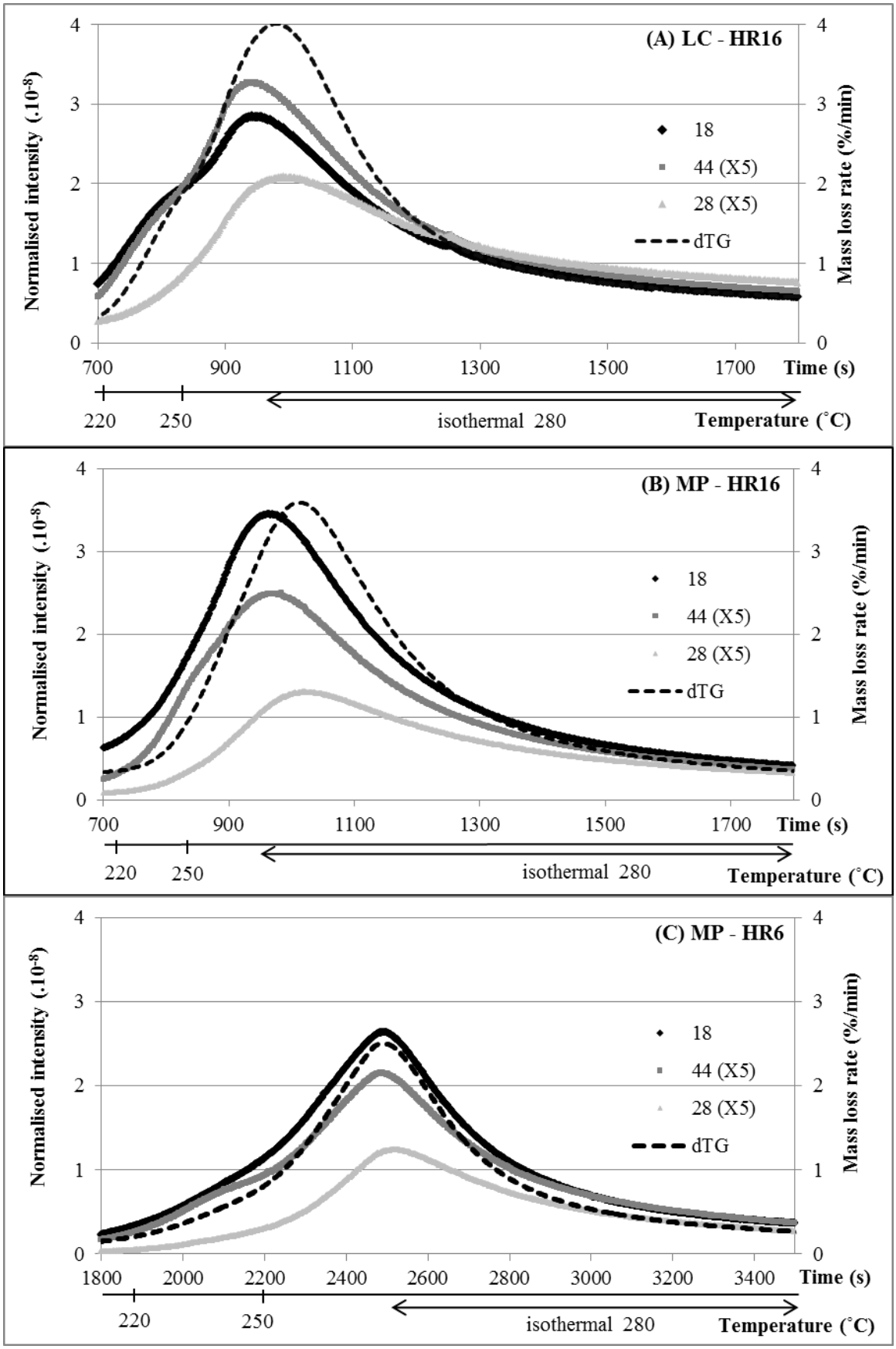

Figure 5-4: Evolution of fragmentation ions *m/z* 18 (H_2O), 44 (CO_2 and 28 (CO) analysed by MS, and of mass loss rate (DTG) during torrefaction of *Lantana camara* (LC) and *Mimosa pigra* (MP).

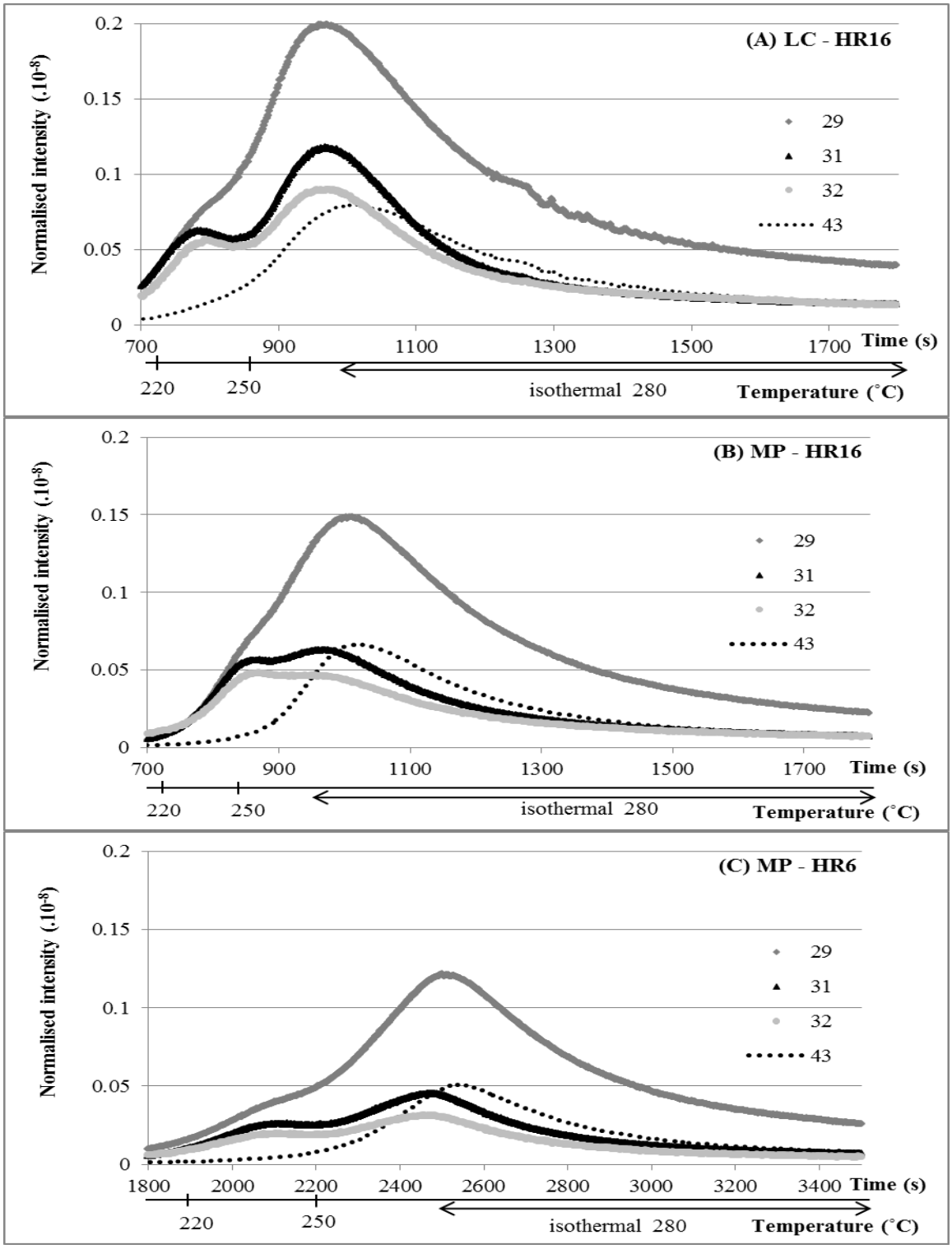

Figure 5-5: Evolution of fragmentation ions *m/z* 29, 31, 32 and 43 analysed by MS during torrefaction of *Lantana camara* (LC) and *Mimosa pigra* (MP) with a heating rate of 6 (HR6) or 16 (HR16) and a maximum temperature of 280 ˚C.

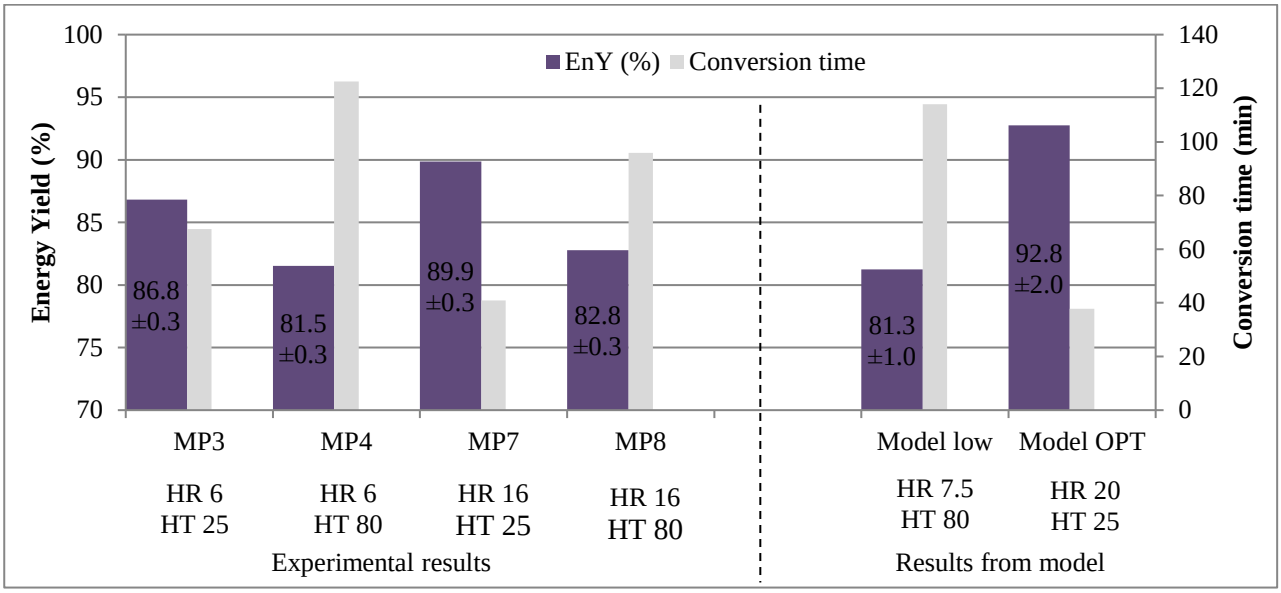

Figure 5-6: Energy yield (EnY, %) and conversion time during torrefaction of *Mimosa pigra* at 280 ˚C for different heating rates (HR, ˚C min^{-1}) and hold times (HT, min).

Chapter 6 **Pyrolysis of *Lantana camara* and *Mimosa pigra*: Influences of temperature, other process parameters and incondensable gas evolution on char yield and higher heating value**

Published in Bioresource Technology 243 (2017) 284-293

Title: "Pyrolysis of *Lantana camara* and *Mimosa pigra*: Influences of temperature, other process parameters and incondensable gas evolution on char yield and higher heating value."

Authors: Jhonnah Mundike, François-Xavier Collard and Johann F. Görgens

Department of Process Engineering, University of Stellenbosch, Private Bag X1, Matieland 7602, South Africa

Objective of dissertation in this chapter

This chapter addresses **specific objectives one, two, and three,** which focus on the production of char through optimisation of process parameters using slow pyrolysis at milligram-scale **(objective two)**. Based on optimised conditions from milligram-scale, produce char at gram-scale and assess the effect of increased particle and bed sizes on char yield and HHV **(objective three).** Thereafter, collect exit incondensable gases in Tedlar bags for analysis in a gas chromatography in order to assess the relationship of gas evolution with char yield and energy properties in terms of HHV **(objective one).**

Candidate declaration

In chapter 6 page numbers 97 to 130 of this dissertation, the type and scope of my contribution were as follows:

Nature of contribution	Contribution (%)
Planning of experiments	70
Executing experiments	100
Interpretation of results	60
Writing the chapter	100

The listed co-authors have contributed to chapter 6 page numbers 97 to 130 of this dissertation.

Name	e-mail address	Type of contribution	Contribution (%)
François-Xavier Collard	fcollard@sun.ac.za	Experimental planning	30
		Reviewing of chapter	30
Johann F. Görgens	jgorgens@sun.ac.za	Interpretation of results to correlate with literature	10
		Reviewing of chapter	10

Signature of candidate:……..

Date:……

Declaration by co-authors

The undersigned hereby confirm that

- the declaration above accurately reflects the type and extent of the contributions of the candidates and co-authors to chapter 6 page numbers 97 to 130 in the dissertation,
- no other authors contributed to chapter 6 page numbers 97 to 130 in the dissertation besides those specified above , and
- potential conflicts of interest have been revealed to all interested parties and that necessary arrangements have been made to use the material in to chapter 6 page numbers 97 to 130 of this dissertation.

Institutional affiliation	Date	Signature

Abstract

Pyrolysis of invasive non-indigenous plants, *Lantana camara* (LC) and *Mimosa pigra* (MP) was conducted at milligram-scale for optimisation of temperature, heating rate and hold time on char yield and higher heating value (HHV). The impact of scaling-up to gram-scale was also studied, with chromatography used to correlate gas composition with HHV evolution. Statistically significant effects of temperature on char yield and HHV were obtained, while heating rate and hold time effects were insignificant. Milligram-scale maximised HHVs were 30.03 MJ kg^{-1} (525 ˚C) and 31.01 MJ kg^{-1} (580 ˚C) for LC and MP, respectively. Higher char yields and HHVs for MP were attributed to increased lignin content. Scaling-up promoted secondary char formation thereby increasing HHVs, 30.82 MJ kg^{-1} for LC and 31.61 MJ kg^{-1} for MP. Incondensable gas analysis showed that temperature increase beyond preferred values caused dehydrogenation that decreased HHV. Similarly, CO evolution profile explained differences in optimal HHV temperatures.

Keywords

Slow pyrolysis, temperature, higher heating value, sample size, incondensable gas

6.1 Introduction

Lignocellulose generally has a higher heating value (HHV) that is lower than that of fossil fuels such as coal, although its direct application as a fuel in both domestic and industrial applications has been practiced for some time. The low HHV of lignocelluloses (< 20 MJ kg^{-1}) is mainly due to higher contents of moisture and oxygen, compared to fossil fuels [1,2]. The moisture and oxygen contents of lignocellulose can be reduced through various thermal technologies that yield valuable end products such as char (also called charcoal), which has increased energy densities (calorific or heating values) and a more homogeneous composition [1]. Thermochemical conversion technologies like torrefaction and slow pyrolysis have the potential to produce char from lignocellulose with properties

that could compete favourably with coal in the market for energy applications [3]. Different qualities of char can be obtained from pyrolysis of lignocellulose due to variations in type and origin of the feedstock materials [4,5], as well as the process conditions applied. In particular, the proportions of cellulose, hemicelluloses, lignin and inorganics in lignocelluloses are known to influence char yield and energy content. Furthermore, reactor temperature, heating rate and conversion time can significantly modify the yield and fuel properties of the pyrolysis end products [6,7]. Because of these combined effects, it is important to optimise the pyrolysis conversion conditions for each lignocellulosic feedstock utilised, to obtain the desired quality of the char product for its intended application.

It is generally accepted that temperature is the most significant factor influencing char yield during slow pyrolysis, with a reduced mass yield as the temperature rises. Most studies on slow pyrolysis utilise temperatures ranging from 300-600 ˚C [8–10]. For instance, during pyrolysis of *Lantana camara*, [11], obtained a 39 wt.% yield of char when pyrolyzed at 300 ˚C; the char yield reduced to 27 wt.% at 600 ˚C. Xiong et al. [12], reported slow pyrolysis mass yields of 37 and 27 wt.% at 400 and 600 ˚C, respectively, for bamboo sawdust. Similarly, Angin [13] used a heating rate of 10 ˚C min^{-1} to obtain 34 and 26 wt.% after pyrolyzing safflower seed cake at 400 and 600 ˚C, respectively. The majority of mass loss during slow pyrolysis of lignocelluloses occurs between 300-450 ˚C, with limited decreases in char yields when further increasing process temperature beyond 600 ˚C [11,12,14]. For example, an increase in pyrolysis temperature from 600 to 700 ˚C resulted in a decrease of less than 1 wt.% in mass yield of char [9]. Concerning char HHV evolution, [11], recorded char HHVs for *Lantana camara* of 27.8 and 31.7 MJ kg^{-1} at 300 and 600 ˚C, respectively. At 400 and 600 ˚C, Xiong et al. [12] recorded HHV results of 28 and 32 MJ kg^{-1} for bamboo sawdust, respectively. Literature has reported similar increase in HHV results of various lignocellulosic chars within temperatures of 300 to 600 ˚C [13–15]. However, some studies have reported decreases in

HHVs for conversion temperatures higher than 500 ˚C, some estimating an optimum temperature in the range of 500-600 ˚C [11,12,14,15]. Hypotheses to explain these decreases in HHV have not been reported. Some works have shown that most of the condensable volatiles are produced between 200 and 450 ˚C, with associated increases in char HHVs due to significant deoxygenation. Such deoxygenation is observed through the production of oxygenated organic compounds, H_2O and permanent gases such as CO_2 and CO. Increasing pyrolysis temperatures above 500 ˚C will increase the fraction of permanent gases present in the volatiles product; together with CO and CO_2 other gas species like CH_4 and H_2 are produced in significant yields [9,16,17]. However, the impact of the evolution of incondensable gases on char HHV has been investigated minimally.

Hold time during slow pyrolysis is the time under which lignocellulosic sample is held isothermally at the final temperature in the reactor, after which the reactor contents are then cooled down. Concerning hold time, various works have reported “baking” or holding lignocellulosic samples at pyrolysis temperature for 30 min [7,12,18–20]. Generally, prolonged hold time reduces the mass yield as the HHV increases [19,21]. HHV of pyrolyzed cherry sawdust increased by 0.6 MJ kg^{-1} as hold time increased from 15 to 30 min at 450 ˚C [19]. However, as conversion temperature increases, the effect of hold time tends to decrease. For instance, an increase of less than 0.1 MJ kg^{-1} in the HHV, as hold time was increased from 10 to 60 min at 600 ˚C, was observed for both green waste and wood [21].

Slow pyrolysis usually operates at atmospheric pressure with relatively slow heating rates (≤ 20 ˚C min^{-1}), which are known to promote char yield, contrary to fast pyrolysis [9,10,15,22]. In a previous study under torrefaction conditions [23], it was evidenced that for heating rates below 20 ˚C min^{-1}, heating rate optimisation could result in significant improvements in the gross energy conversion efficiency. Heating rate variation could also influence the properties of the char produced during slow

pyrolysis, by influencing pyrolysis mechanisms and changing the amount of time spent at various temperature points during heat-up of the sample. Various trends in the relationship between heating rate and the char HHV have been described [13,15], although the resulting effect is typically lower than 1 MJ kg^{-1}. For instance, at 500 ˚C a decrease in the heating rate from 20 to 5 ˚C min^{-1}, increased the mass yields of almond shell residues by 4.2 wt.%, while char HHV increased by 0.6 MJ kg^{-1} [15].

Several works using lignocellulosic biomass have studied the influence of pyrolysis temperature [11,12,14,17], heating rate [8,13,15,24] and hold time [19,21] on char HHV, mostly using a single particle size range and a single reactor. The use of thermogravimetric analysis (TGA) at milligram-scale is a common technique for studying lignocellulose pyrolysis mechanisms/trends. TGA allows assessment of the thermal stability of a sample and identifying the steps of conversion associated to the main mass losses. However, due to limited sample size in TGA reactor, and the use of small particle size, the influence of heat and mass transfer on char yield cannot be determined. It has been reported that due to longer residence time of the volatiles within the particle and the particle bed, secondary reactions are likely to increase the char yield during scale-up [25,26]. While the effect of particle size was often reported for fast pyrolysis [27,28], it is less documented for slow pyrolysis [25,26]. Aguiar et al. [26] studied the pyrolysis of orange peel and reported char yields of 24.6 wt.% with a corresponding HHV of 28.3 MJ kg^{-1}, at 600 ˚C for particle sizes < 300 µm. At the same temperature for particle size > 800 µm, they obtained char yields of 25.6 wt.% with HHV of 29.1 MJ kg^{-1}. The influence of scale-up by increasing the size of the reactor and the sample mass is rarely described.

Of late, lignocellulosic biomass from alien (non-indigenous) and invasive plant species (IAPs) has gained interest in solid bioenergy applications [10,23]. The use of IAP lignocelluloses for energy applications is one way of avoiding deforestation of indigenous trees, often associated with charcoal production in Africa [29]. In this work, raw lignocellulosic samples of *Lantana camara* (LC) and

Mimosa pigra (MP), IAPs from Zambia, were pyrolyzed in a TGA with the resultant char HHV determined in a bomb calorimeter. The influences of temperature, heating rate and hold time on the mass yield and char HHV were assessed using a statistical technique. In order to study the effect of scale-up from milligram-scale to gram-scale, some TGA experiments were reproduced at gram-scale and the energy content of the char products were compared. Evolution of gas formation during gram-scale experiments were analysed by gas chromatography, to assess the influence of incondensable gas composition on char HHV.

6.2 Materials and methods

6.2.1 Feedstock preparations

Mature and flowering plants of LC and MP were harvested from Zambia. MP samples were collected along the Kafue River Flood Plains of Lochinvar National Park, while LC plants were mainly obtained from around the Victoria Falls in the Mosi-O-Tunya National Park in Livingstone. In order to remove excessive moisture for purposes of transportation, the samples were oven-dried at 75 ˚C for 6 hours and processed into wood chips before transporting them to South Africa. Both feedstock were exported to South Africa from Zambia, after meeting the invasive plant material requirements of both countries. The samples were milled using a Retsch (SM 100) mill and sieved in a Retsch shaker (AS 200). For pyrolysis experiments, particle size distribution (PSD) between 425-600 µm was used at milligram-scale (TGA), while 850-2800 µm was used at gram-scale (bed-scale reactor).

6.2.2 Analytical methods

The raw lignocellulosic biomasses were characterised in terms of composition and energy content (Table 6-1). Lignocellulosic composition was determined in accordance to the Technical Association for Pulp and Paper Industries (TAPPI) standards. Hemicellulose was determined as outlined in TAPPI

Method T 223 *cm-10*, while TAPPI Method T 222 *om-11* was used to determine acid-insoluble lignin. Cellulose content was determined by difference. Proximate analysis was performed in accordance to ASTM standard E1131, using thermogravimetric analysis TGA/DCS 1 Star System Mettler Toledo. The char HHV analysis was conducted in a bomb calorimeter, model 2013 (Cal2k Eco Calorimeter), calibrated with benzoic acid (Cal2K). The HHV determination was based on ASTM standard D5865-11a.

6.2.3 Milligram-scale (TGA) pyrolysis study

At milligram-scale, the pyrolysis experimental studies were conducted in the same thermogravimetric analyser as used for proximate analysis, and the results assessed using a statistical method as detailed in sections 6.2.3.1 and 6.2.3.2.

6.2.3.1 Design of experiments

The influence of process variables of temperature, heating rate and hold time during conversion at milligram-scale on mass yields and char HHV was studied using central composite design (CCD), Statistica software version 12. The design of experiments (DoE) range of chosen values for the lower, middle and upper temperatures were 330, 440 and 550 ˚C, with holding times of 15, 30 and 45 min, while the heating rates were 4, 8 and 12 ˚C min^{-1}, respectively. As detailed in Tables 6-2 and 6-3, the resultant DoE temperatures ranged from 255.0-625.0 ˚C, while heating rate varied from 1.3-14.7 ˚C min^{-1}, with a hold time range of 4.8-55.2 min. The two studied response variables were char yield (Ychar; wt. %) and char HHV (MJ kg^{-1}), with two replicates for each process condition. An assessment of analysis of variance (ANOVA) was performed to evaluate the influence of temperature, heating rate and hold time on Ychar and char HHV. When a p-value was < 0.05, (95% confidence limit) the related factor was considered statistically significant. In order to confirm optimum

temperatures, additional tests were conducted for both samples. For LC, additional temperatures of 485, 500, 525 and 575 ˚C were tested with a hold time of 15 min and a heating rate of 12 ˚C min^{-1}. In case of MP, the additional temperatures were 525, 580, 595, with an extension beyond the upper DoE range up to 700 ˚C, using a hold time of 15 min and a heating rate of 15 ˚C min^{-1}. For each lignocellulose, the heating rate was selected based on preliminary tests (see section 6.3.2.3 and Appendix B-1).

6.2.3.2 Milligram-scale (TGA) char preparation

As earlier indicated (section 6.2.1), PSD from 425-600 µm for LC and MP feedstocks were used for char generation in the TGA reactor in this study. Argon gas, at a flow rate of 70 ml min^{-1} was used with ceramic sample crucibles of 600 µL, filled with about 200 mg for LC and 300 mg for MP of the raw sample. The first segment of char evolution involved the removal of moisture from samples in the TGA reactor from 30 to 110 ˚C at a specified heating rate and thereafter, samples were isothermally held for 5 min to ensure complete removal of excess moisture. Then the samples were pyrolyzed to the final temperature at the indicated heating rate (according to experimental conditions detailed in Tables 6-2 and 6-3), ending with an isothermal treatment at a specified hold time and final cooling of the desired solid product. The resultant char was only removed from the reactor as the temperature reached < 60 ˚C to avoid any possibilities of combustion. The char samples were stored in airtight containers for further analyses.

6.2.4 Gram-scale char preparation

A horizontal tubular stainless steel reactor, 1 m long, 60 mm outside diameter, was used for pyrolyzing LC and MP samples with a PSD from 850 to 2800 µm (section 6.2.1). Two platinum thermocouples were placed from one end of the reactor with their tip-ends at the middle of the reactor.

The top thermocouple, close to the reactor wall, was used to control the heating by measurement of the reactor temperature, while the one close to the reactor centre was used to measure the sample temperature. The sample temperature was used for reporting all the results, to take into account variations between sample and reactor temperatures (± 2-15 ˚C). A quartz sample holder with raw feedstock materials (8 g ± 0.3 g) was placed in the middle of the reactor. The inert environment inside the reactor was maintained by a continuous flow of N_2 at an exit rate of 0.5 L min^{-1} up to the end of each experimental run. The other exit end of the reactor was connected to the exhaust line to release condensable vapours and incondensable gases.

After collection of the condensable volatiles using a series of 4 condensers, the first one held at ambient conditions, with the rest at - 55 ˚C (dry ice), the permanent or incondensable gases were sampled into 1L Tedlar bags and analysed just after collection in a gas chromatography (CompactGC 4.0). The instrument was calibrated to determine the concentrations of N_2, CO, CO_2, CH_4, H_2, C_2H_6 and C_2H_4. Mixtures containing known concentrations of the different gases (Afrox) were used for gas chromatography calibration.

Gram-scale experiments for LC were carried out at pyrolysis temperatures between 440 and 625 ˚C with a heating rate of 12 ˚C min^{-1}, while the conversion conditions for MP were between 440 and 700 ˚C, at a heating rate of 15 ˚C min^{-1}. For both samples, hold time at the final temperature was 15 min. At the end of each experiment, after the sample temperature had reached < 60 ˚C, the glass sample holder was removed from the disassembled reactor setup and allowed to cool down to ambient conditions. The char samples were then weighed and stored in airtight containers for further analysis.

6.3 Results and discussions

After detailing lignocellulosic compositions, the following sections outline the results for the influences of temperature, heating rate and hold time on Ychar and char HHV during the pyrolysis of both samples at milligram-scale. Thereafter the effect of scale-up to gram-scale is discussed.

6.3.1 Characterisation of raw lignocellulosic biomasses

The compositions of LC and MP raw samples are shown in Table 6-1. The major difference in terms of lignocellulosic composition between the samples is that MP is richer in lignin (28.9 wt.%) compared with 20.6 wt.% for LC. In case of proximate analysis, MP has slightly more fixed carbon (20.4 wt.%) than LC (19.3 wt.%), while both raw samples have similar HHVs (≈ 18 MJ kg^{-1}).

6.3.2 Optimisation of char properties at milligram-scale

The Ychar (dry, wt.%) and higher heating value (HHV, MJ kg^{-1}), obtained from milligram-scale pyrolysis in replicates are detailed in Tables 6-2 and 6-3. The average Ychar values were obtained with an average standard deviation of (± 0.04 wt.%) for LC and (± 0.08 wt.%) for MP, while the average standard deviations for char HHV were (± 0.08 and ± 0.11 MJ kg^{-1}) for LC and MP, respectively. Such relatively small standard deviations highlight the ability of TGA for reproducing similar conversion conditions thus resulting in char products with similar properties. Table 6-4 shows summarised details of statistical analysis from ANOVA tables with several p-values highlighting significant influences (p-values < 0.05) of the factors on Ychar and char HHV for both samples. Based on linear factors, temperature was found to have significantly influenced both Ychar and char HHV. Though heating rate and hold time were not detected to have statistically influenced Ychar and char HHV, some quadratic (Q) p-values for heating rate were relatively small (≈ 0.10), showing that heating rate could have influenced char HHV for both samples.

6.3.2.1 Influence of temperature, heating rate and hold time on Ychar

From Table 6-4 it can be seen that pyrolysis temperature for both samples, with p-values of 1 x 10^{-6} for the linear (L) factor, was found to have a pronounced effect on Ychar, while no significant effect was detected for the heating rate, hold time and the interactions (data not shown) between the variables. The negative linear factor coefficients on Ychar of -9.87 and -10.59, for LC and MP respectively (refer to Effect in Table 6-4), confirmed a reduction in Ychar as the temperature increased. In case of heating rate and hold time, the linear factor coefficients for both were less than – 0.8, an indication that compared to temperature both parameters minimally impacted on Ychar. Figure 6-1 illustrates the influence of temperature on Ychar from 330 to 625 ˚C for the example of hold time ≤ 30 min. It can be seen that an increase in temperature systematically resulted in a reduction in char yield, with a more pronounced effect on the lower range of studied temperatures. The conversion (volatilization) of both samples was higher than 54 wt.% at 330 ˚C and then 71 wt.% at 625 ˚C.

Comparing pyrolysis at 330 and 440 ˚C, there was a conversion representing around 10 wt.% for both LC and MP, attributed mostly to some further cellulose depolymerisation. For results between 440 and 550 ˚C, the conversion differences dropped to around 3 and 4 wt.% for LC and MP, respectively. From 550 to 625 ˚C, conversion differences still appear to be more pronounced for MP than for LC but were observed to be < 3wt.% for both samples. The trend that more conversion was still taking place at higher temperatures (T > 440 ˚C) for MP in comparison with LC was seen as a consequence of the higher lignin content in MP. Indeed, lignin degradation is known to occur on a wide range of temperature with significant mass loss up to 600 ˚C [16]. As illustrated in Figure 6-1, at similar conditions throughout the studied temperature range, MP consistently recorded higher Ychar results than LC, which was also interpreted as a consequence of the difference in the content of lignin, the constituent known to give higher char yields [5].

Although statistical analysis showed that both heating rate and hold time minimally impacted on Ychar results (Table 6-4), some trends could be observed from the analysis of Table 6-2 and Table 6-3. In case of hold time, it was observed that at lower temperatures (330 ˚C) larger differences in Ychar were obtained than at higher temperatures (550 ˚C). For instance, increased Ychar reductions at 330 ˚C (up to 3.2 wt.% for MP and 2.1 wt.% for LC) were obtained compared with those at 550 ˚C (up to 0.9 wt.% for MP and 0.2 wt.% for LC), as hold time was prolonged from 15 to 45 min. In case of heating rate, the trend showed that lower heating rates promoted increased Ychar results throughout the studied range. For the example of hold time of 15 min, Ychar differences of 1.6 wt.% for MP and 1.2 wt.% for LC were obtained at 330 ˚C compared with 1.0 wt.% for MP and 0.9 wt.% for LC at 550 ˚C, as heating rate was reduced from 12 to 4 ˚C min^{-1}.

6.3.2.2 Influence of temperature, heating rate and hold time on char HHV

Table 6-4 also shows the p-values and the corresponding factor effects on char HHV for both samples, obtained from summarised ANOVA tables. Temperature significantly influenced char HHV results, with p-values < 1 x 10^{-6} for the linear factors for both samples. According to the positive linear effects in Table 6-4 (+ 2.34 for MP and + 1.76 for LC), the char HHV tended to increase with the rise in pyrolysis temperature as usually reported. This evolution is seen as a consequence of lignocellulosic deoxygenation, which mostly occurs between 250 and 500 ˚C [16]. However, in case of the quadratic factors, the effects are negative for both char samples (- 0.95 for MP and – 1. 31 for LC), an indication that there is a possibility of an optimum temperature for each sample. Figure 6-2 further illustrates the influence of temperature on char HHV for both samples, for the example of hold times > 15 min. The HHV results at 330 ˚C for both samples were less than 28 MJ kg^{-1}. The energy content of the char prepared at 440 ˚C increased to values in the range 28.5-29.4 MJ kg^{-1}. As the temperature increased to 550 ˚C, increased HHV results were obtained, especially for MP (up to 31.1 MJ kg^{-1}), while for LC the change was less pronounced (up to 29.9 MJ kg^{-1}). Interestingly, for both sample

chars, the HHVs at 625 ˚C were found to be significantly lower than for some at 550 ˚C (Figure 6-2), a confirmation of the existence of an optimum, as earlier indicated (based on ANOVA results from Table 6-4). Literature has reported a similar trend of char HHV reduction for temperatures > 600 ˚C [11,12].

At 330 and 440˚C, with other conditions unchanged, most of LC char HHV results were higher than MP values (for the two exceptions, results were not statistically different). As LC was richer in polysaccharides, especially hemicelluloses, the increased HHV was seen as a result of deoxygenation occurring at lower temperature than for MP. This hypothesis is consistent with the fact that compared to MP, LC Ychar were consistently lower (section 6.3.2.1). However, at temperatures above 550 ˚C, the char HHV trend was reversed where MP recorded increased results of HHV than LC. MP and LC samples contained similar amount of inorganics (refer to ash in Table 6-1). Following removal of most of the oxygen in the char, MP gave more char due to higher lignin content, resulting in higher organic/inorganic ratio, consistent with an increased HHV. Proximate analysis of the char products confirmed this assumption. In the case of char prepared at 625 ˚C for instance, char organic content corresponded to 94.3 wt.% (79.5 wt.% fixed carbon) for MP and 92.8 wt.% (76.8 wt.% fixed carbon) for LC.

Variations of heating rate and hold time (both not statistically influencing char HHV) at each temperature for both samples resulted in energy differences of < 0.9 MJ kg^{-1}. However, the quadratic p-values for heating rate in Table 6-4 were close to 0.1 for both char HHV, showing that this factor could have an impact on the HHV. Similarly, other works investigating the influence of heating rate have reported HHV changes lower than 0.8 MJ kg^{-1} [8,13,15]. In our case, the stronger influence from temperature, with smaller p-values (< 1 x 10^{-4}) could have been overriding the influence from heating rate. As for hold time, for conversion at 330 ˚C both samples showed that longer hold times decreased Ychar as HHV increased. Interestingly, while the same trend was observed for MP at 550 ˚C, the

opposite trend was noticed for LC (increasing hold time still decreased Ychar but also decreased HHV), showing that for LC, further conversion at T > 550 ˚C, negatively affected HHV. Just like Ychar (section 6.3.2.1), the influence from the interactions between the studied variables on char HHV was not statistically detected for both samples (results not shown).

6.3.2.3 HHV optimisation

Temperature was found to be the main factor influencing char HHV (section 6.3.2.2). Several temperatures were tested at milligram-scale for both samples as earlier indicated in section 6.2.3.1, until an optimum for each was found. Additional pyrolysis experiments were implemented, using a heating rate of 12 ˚C $min^{-1}$for LC and 15 ˚C min^{-1} for MP (based on preliminary tests with variable heating rates and then confirmed at optimum temperature, see Appendix B-1), while holding the samples isothermally for 15 min. Since hold time had minimal influence on char HHV at higher temperatures, 15 min, the shortest hold time was chosen for both samples. Figure 6-3a shows the detailed results of temperature optimisation for LC char HHV, whose results progressively increased from 440 up to 525 ˚C. At 525 and 550 ˚C, a peak plateau optimum was obtained with overlapping HHVs of 30.03 ± 0.10 and 29.91 ± 0.15 MJ kg^{-1}, respectively. In order to save input energy, a lower optimum temperature at 525 ˚C was selected. The HHV results at higher temperatures > 550 ˚C were significantly lower than the peak plateau optima values. For instance, a further increase in temperature up to 575 ˚C, yielded char with lower HHV of 29.29 ± 0.08 MJ kg^{-1}. In case of MP char HHV temperature optimisation, Figure 6-3b shows that the samples were pyrolyzed at temperatures between 525 up to 700 ˚C. A peak HHV result of 31.01 ± 0.06 MJ kg^{-1} was obtained at 580 ˚C, while a further increase in temperature from 595 up to 700 ˚C, produced chars with lower HHVs. For example, at 700 ˚C, a lower char HHV of 29.78 ± 0.03 MJ kg^{-1} was obtained. The optimum temperature for LC was lower (525 ˚C) than that of MP (580 ˚C), probably due to the later lignocellulose being richer in lignin as earlier indicated. As for MP, it seemed that significant

deoxygenation could have been taking place up to 580 ˚C, as lignin conversion is known to occur over a wide range of temperatures. Indeed, lignin is composed of highly stable oxygenated groups in the form of phenols. As phenol deoxygenation is suspected to occur at temperatures higher than 500 ˚C [16], significant deoxygenation still occurred for MP between 500 and 580 ˚C. This hypothesis is discussed in section 6.3.4.

As earlier indicated, based on the quadratic p-values in Table 6-4, heating rate could have an impact on char HHV; therefore, a heating rate assessment was conducted at HHV optimal temperatures for both samples. Significant differences in HHV results were obtained but variations were found to be lower than 1 MJ kg^{-1} as indicated in Appendix B-1. There was no optimisation study conducted as no clear trend could be detected. Heating rates of 12 ˚C min^{-1} for LC and 15 ˚C min^{-1} for MP, recorded the highest results of HHV, thereby confirming the relevance of their selection for the temperature optimisation study.

6.3.3 Scaling-up from milligram to gram-scale

The feedstock materials used at milligram and gram scales were milled from the same batch of raw lignocellulosic biomasses and sieved through the same set of standard sieves, resulting into different fractions of the same batch, thereby making it suitable to assess the effect of lignocellulosic biomass particle size and bed size on product distribution [28]. The study on the effect of scale-up on Ychar (wt.%) and char HHV (MJ kg^{-1}) was from milligram-scale with PSD of 425-600 µm to gram-scale with PSD of 850-2800 µm.

6.3.3.1 Effect of scale-up on Ychar

During TGA char preparation, the sample and reactor temperatures were almost the same (± 2 ˚C), while at gram-scale, sample and reactor temperature differences were in the range ± 2-15 ˚C. Therefore, the values used for comparison and shown in Table 6-5 (in brackets) under gram-scale are those for the thermocouple closer to the sample (section 6.2.4.). The replicated Ychar results (wt.%) at milligram and gram scales for both samples are shown in Table 6-5. The Ychar results at gram-scale were systematically higher than the results obtained from milligram-scale at similar operating conditions. The increase in Ychar at gram-scale can be attributed to the mass transfer limitation inside the lignocellulosic particle matrix, resulting in trapped volatiles, more likely to be converted into secondary char [16,25]. During milligram-scale, volatiles from the TGA reactor were almost immediately purged out due to the small size of the well-ventilated reactor environment. The increased sample mass at gram-scale ultimately increased the sample bed size, which could have further promoted and favoured secondary char formation reactions. From the results (Table 6-5), it can be observed that, as a result of scaling-up, Ychar increased by less than 1.0 wt.% at 300 ˚C for both samples. Secondary char formation is due to the recombination of some volatile compounds, for instance phenols, which are mostly produced from the depolymerisation of lignocellulosic constituents [16]. At 300 ˚C cellulose and lignin are only partially converted, explaining the minimal percent change in Ychar when comparing both scales. However, as the temperature increased to 440 ˚C, more volatiles likely to recombine were generated [16] (Ychar < 35 wt.% at milligram-scale), resulting in an increase of 2.9 and 3.5 wt.% of Ychar due to scale-up for LC and MP, respectively. At similar temperatures, the Ychar increase was always higher for MP than for LC. The formation of more secondary char for MP was consistent with the higher content of lignin in the raw sample. Indeed, lignin conversion is the main source of phenols, which are suspected to be the main source of secondary char through recombination [5].

6.3.3.2 Effect of scale-up on char HHV

The effect of scale-up on char HHV could best be explained by comparing energy values at milligram and gram scales at similar temperature conditions, as shown in Table 6-5. On a comparative basis, LC char energy contents at both scales at 300 ˚C, had char HHV of 27.1 ± 0.1 MJ kg^{-1}, an indication that partial conversion had little impact on the char energy properties (section 6.3.3.1). For T ≤ 525 ˚C, differences in HHV results between milligram- and gram-scale values were not more than 1 MJ kg^{-1}. In case of T > 525 ˚C, char HHV results at gram-scale became significantly higher than those from milligram-scale. From proximate analysis, it appeared that at such temperatures the additional organic material obtained at gram-scale (secondary char) contributed to an increase in the fixed carbon content of the char, in agreement with increased HHV results. For instance, for the char prepared at 625 ˚C, fixed carbon content at gram-scale was 80.6 wt.% versus 76.8 wt.% at milligram-scale. The results evidenced that the optimal temperature at gram-scale was > 570 ˚C and the highest result of HHV was obtained at 614 ˚C, with a value of 30.82 MJ kg^{-1} significantly higher than the optimum HHV of 30.03 MJ kg^{-1} obtained at milligram-scale. As the temperature was further increased from 614 to 635 ˚C, the HHV decreased by 0.78 MJ kg^{-1}. Under the temperature condition giving the maximum results of HHV (525 ˚C at milligram-scale and 614 ˚C at gram-scale) for LC, similar char yields of 28.5 ± 0.3 wt.% were produced. Consequently, higher energy yield, of 49.3% at gram-scale compared with 47.3% at milligram-scale were obtained from similar char yields.

In case of MP char HHV, at 300 ˚C, both scales recorded similar char energy content of 24.4 ± 0.2 MJ kg^{-1}. For T > 580 ˚C, increased results of HHVs at gram-scale than milligram-scale were obtained with HHV differences of up to 1.8 MJ kg^{-1} at 698 ˚C (optimal HHV temperature for MP at gram-scale). Similarly, fixed carbon content in MP char samples at gram-scale were higher than those from milligram-scale, in agreement with increased HHV results. For instance, for the char prepared at 625 ˚C, the fixed carbon content at gram-scale was 84.0 wt.% versus 79.5 wt.% at milligram-scale. A further increase of temperature to 749 ˚C at gram-scale yielded a char HHV of 29.81 MJ kg^{-1}, a result

significantly lower than the value at optimal HHV temperature. The HHV results for MP char showed that optimal temperature at gram-scale was greater than 625 ˚C, with the highest result of HHV at 698 ˚C (31.61 MJ kg^{-1}), a value significantly higher than the milligram-scale maximum HHV of 31.01 MJ kg^{-1}. Similar MP char yields of 29.7 ± 0.3 wt.% were obtained from different temperatures giving the highest results of HHV (580 ˚C at milligram-scale and 698 ˚C at gram-scale). Despite the similarity in char yields, the gross energy yield results were 51.7 and 53.5% for milligram and gram-scale, respectively, showing that similar char yield and increased HHV will result in increased energy conversion. The energy yield for MP (53.5%) was higher than LC (49.3%) due to increased lignin in the former lignocellulosic sample. TGA gave an insightful first approach, but scale-up was necessary later on in order to estimate energy conversion results.

6.3.4 Evolution of permanent gases during pyrolysis

In order to assess the impact of the evolution of incondensable gases on char HHV, key permanent gases released during pyrolysis at gram-scale were analysed with gas chromatography. The pyrolysis conditions with the accompanying gas analysis method were conducted as outlined in section 6.2.4. The considered incondensable gases were CO_2, CO, CH_4, H_2, C_2H_6, and C_2H_4. Figure 6-4a and b show the gas evolution profiles during pyrolysis up to the final temperature for each sample. The mass loss profiles (obtained from TGA under the same conditions) were included in Figure 6-4a and b, for comparison purposes. Among the considered gases, CO_2 and CO were the earliest to be detected, with significant concentrations above 0.1% around 220 ˚C and relatively high concentrations during the main conversion stage between 300 and 400 ˚C. Since more polysaccharides yield more CO_2 and CO during pyrolysis [16], LC, richer in hemicelluloses, recorded higher concentrations of CO_2 and CO than MP, especially during the hemicelluloses conversion around 300 ˚C [9,17]. In case of CH_4 and C_2 hydrocarbons (data not shown), similar evolution profiles were observed. Appreciable amounts (> 0.1%) of CH_4 were detected from temperature of 400 ˚C,

with maximum concentrations at 580 ˚C for LC and 600 ˚C for MP. H_2 concentrations higher than 1% were only obtained from temperatures higher than 450 ˚C. Recombination reactions of benzene rings in the char mainly contributed to the release of CH_4 and H_2. As reported in literature [9,17], further increase in temperature consistently resulted in increased production of H_2.

At gram-scale, the pyrolysis conditions to obtain the optimal HHV were found to be at temperatures higher than 570 ˚C. As it can be seen in Figure 6-4, the mass loss of the sample is minimal at such temperatures and major fractions of the released volatiles are permanent gases produced from rearrangement reactions [16]. While the formations of CO_2 and CO resulted in a more deoxygenated char, the release of hydrocarbons composed of C-C and C-H bonds probably negatively affected the char HHV. Between 600 and 650 ˚C (Figure 6-4b), the concentrations of the different gases dropped, except for H_2 whose concentration kept increasing until the end of the experiment (700 ˚C). Through the linkage of some C-H bonds, dehydrogenation reactions certainly contributed to the decrease of char HHV at higher temperatures and thus to the existence of an optimal temperature.

Gas evolution profile was consistent with literature for both samples. Differences in deoxygenation at T > 400 ˚C could be related to the different optimal temperatures. For LC, further temperature increase consistently resulted in decrease in CO_2 and CO productions with concentrations lower than 1% at 500 ˚C dropping down to 0.4% at 600 ˚C. Comparatively, CO concentration remained relatively high for MP with concentrations around 1.8% at 500 ˚C and still higher than 1.5% at 600 ˚C.

The increased concentration of CO from MP is probably coming from the fragmentation of phenol rings from lignin, as most of the other oxygenated groups are usually converted at T < 500 ˚C. Phenols in lignin are more stable than other oxygenated groups. Literature has shown that CO mainly released from lignin pyrolysis can extend up to 600 ˚C [16]. Significant deoxygenation still occurring at

relatively high temperature was seen as the main reason for the increased optimal HHV temperature for MP, the raw lignocellulosic sample with the higher lignin content.

6.4 Conclusion

The influence of pyrolysis temperature, heating rate and hold time on char yield and HHV were investigated using LC and MP samples, together with the effect of scaling-up (milligram to gram-scale). Temperature was the most influential and optimal temperatures depended on lignocellulosic composition. Scaling-up favoured secondary char formation, ultimately increasing optimal HHV from 30.03 to 30.82 MJ kg^{-1} for LC and 31.01 to 31.61 MJ kg^{-1} for MP. Increased lignin gave higher char yields and HHVs above 550 ˚C, with significant deoxygenation needed to reach optimal HHV. At higher temperatures, HHV decrease was correlated to dehydrogenation.

Acknowledgements

The authors acknowledge the financial support from the Process Engineering Department of Stellenbosch University in South Africa and the Copperbelt University in Kitwe, Zambia.

6.5 References

[1] Garcia R, Pizarro C, Lavin AG, Bueno JL. Characterization of Spanish biomass wastes for energy use. Bioresour Technol 2012;103:249–58.

[2] Medic D, Darr M, Shah A, Potter B, Zimmerman J. Effects of torrefaction process parameters on biomass feedstock upgrading. Fuel 2012;91:147–54.

[3] Lee JW, Kim YH, Lee SM, Lee HW. Optimizing the torrefaction of mixed softwood by response surface methodology for biomass upgrading to high energy density. Bioresour Technol 2012;116:471–6.

[4] Basu P. Biomass Gasification, Pyrolysis and Torrefaction: Practical Design and Theory. second ed. London: Academic Press; 2013.

[5] Hosoya T, Kawamoto H, Saka S. Role of methoxyl group in char formation from lignin-related compounds. J Anal Appl Pyrolysis 2009;84:79–83.

[6] Assis MR, Brancheriau L, Napoli A, Trugilho PF. Factors affecting the mechanics of carbonized wood: literature review. Wood Sci Technol 2016;50:1–18.

[7] Beis SH, Onay, O.˙Koçkar OM. Fixed-bed pyrolysis of safflower seed: Influence of pyrolysis parameters on product yields and compositions. Renew Energy 2002;26:21–32.

[8] Carrier M, Hugo T, Gorgens J, Knoetze H. Comparison of slow and vacuum pyrolysis of sugar cane bagasse. J Anal Appl Pyrolysis 2011;90:18–26.

[9] Lee Y, Eum P-R-BRB, Ryu C, Park Y-KK, Jung J-HH, Hyun S. Characteristics of biochar produced from slow pyrolysis of Geodae-Uksae 1. Bioresour Technol 2013;130:345–50.

[10] Liao R, Gao B, Fang J. Invasive plants as feedstock for biochar and bioenergy production. Bioresour Technol 2013;140:439–42.

[11] Kumar R, Chandrashekar N. Study on chemical, elemental and combustion characteristics of Lantana camara wood charcoal. J Indian Acad Wood Sci 2013;10:134–9.

[12] Xiong S, Zhang S, Wu Q, Guo X, Dong A, Chen C. Investigation on cotton stalk and bamboo sawdust carbonization for barbecue charcoal preparation. Bioresour Technol 2014;152:86–92.

[13] Angın D. Effect of pyrolysis temperature and heating rate on biochar obtained from pyrolysis of safflower seed press cake. Bioresour Technol 2013;128:593–7.

[14] Bonelli PR. Slow Pyrolysis of Nutshells: Characterization of Derived Chars and of Process Kinetics. Energy Sources 2003;25:767–78.

[15] Gonzalez JF, Ramiro A, Gonzalez-Garcia CM, Ganan J, Encinar JM, Sabio E, Rubiales J. Pyrolysis of almond shells. Energy applications of fractions. Ind Eng Chem Res 2005;44:3003–12.

[16] Collard FX, Blin J. A review on pyrolysis of biomass constituents: Mechanisms and composition of the products obtained from the conversion of cellulose, hemicelluloses and lignin. Renew Sustain Energy Rev 2014;38:594–608.

[17] Uçar S, Karagöz S. The slow pyrolysis of pomegranate seeds: The effect of temperature on the product yields and bio-oil properties. J Anal Appl Pyrolysis 2009;84:151–6.

[18] Apaydin-Varol E, Pütün E, Pütün AE. Slow pyrolysis of pistachio shell. Fuel 2007;86:1892–9.

[19] Gheorghe C, Marculescu C, Badea A, Apostol T. Pyrolysis parameters influencing the bio-char generation from wooden biomass. Univ Politeh Bucharest Sci Bull Ser C Electr Eng 2010;72:29–38.

[20] Mandal S, Singh RK, Kumar A, Verma BC, Ngachan SV. Characteristics of Weed Biomass-derived Biochar and Their Effect on Properties of Beehive Briquettes. Indian J Hill Farming 2013;26:8–12.

[21] Ronsse F, van Hecke S, Dickinson D, Prins W. Production and characterization of slow pyrolysis biochar: Influence of feedstock type and pyrolysis conditions. GCB Bioenergy 2013;5:104–15.

[22] Noumi ES, Blin J, Rousset P. Optimization of Quality of Charcoal for Steelmaking using Statistical Analysis Approach. 5th Int Conf Eng Waste Biomass Valoris 2014:1–14.

[23] Mundike J, Collard F-X, Görgens JF. Torrefaction of Invasive Alien Plants: Influence of heating rate and other conversion parameters on mass yield and higher heating value. Bioresour Technol 2016;209:90–9.

[24] Manyà JJ, Ruiz J, Arauzo J. Some peculiarities of conventional pyrolysis of several agricultural residues in a packed bed reactor. Ind Eng Chem Res 2007;46:9061–70.

[25] Haykiri-Acma H. The role of particle size in the non-isothermal pyrolysis of hazelnut shell. J Anal Appl Pyrolysis 2006;75:211–6.

[26] Aguiar L, Marquez-Montesinos F, Gonzalo A, Sanchez JL, Aruzo J. Influence of temperature and particle size on the fixed bed pyrolysis of orange peel residues. J Anal Appl Pyrolysis 2008;83:124–30.

[27] Demirbas A. Effects of temperature and particle size on bio-char yield from pyrolysis of agricultural residues. J Anal Appl Pyrolysis 2004;72:243–8.

[28] Shen J, Wang X-S, Garcia-Perez M, Mourant D, Rhodes MJ, Li C-Z. Effects of particle size on the fast pyrolysis of oil mallee woody biomass. Fuel 2009;88:1810–7.

[29] Chidumayo EN, Gumbo DJ. The environmental impacts of charcoal production in tropical ecosystems of the world: A synthesis. Energy Sustain Dev 2013;17:86–94.

Table 6-1: Composition of raw samples of *Lantana camara* and *Mimosa pigra*.

Analysis	*Lantana camara*	*Mimosa pigra*
Lignocellulosic (wt.%)[db]		
Extractives	2.3	1.6
Cellulose*	48.2	47.5
Hemicelluloses	28.9	22.0
Lignin	20.6	28.9
Proximate (wt.%)[db]		
Volatile matter	78.5	77.4
Fixed carbon	19.3	20.4
Ash	2.2	2.2
Inorganics (wt.%)[db]		
Ca	1.1	1.4
Fe	0.1	0.1
K	0.4	0.4
Mg	0.2	0.3
Na	< 0.1	0.1
Energy (MJ kg^{-1})		
Higher heating value	17.98	17.67

* Determined by difference; db: dry basis.

Table 6-2: Average (Av) and standard deviation (SD) for pyrolysis of *Lantana camara* (LC) Ychar (wt.%) and higher heating value (HHV, MJ kg^{-1}) at each temperature, hold time (HT) and heating rate (HR).

Sample	Temperature (˚C)	HT (min)	HR (˚C min^{-1})	LC Ychar (Av)	SD (±)	HHV (Av)	SD (±)
LC15	255.0	30.0	8.0	79.71	0.01	20.00	0.11
LC1	330.0	15.0	4.0	40.87	0.03	27.00	0.09
LC2	330.0	15.0	12.0	39.72	0.06	27.65	0.13
LC3	330.0	45.0	4.0	38.82	0.04	27.21	0.08
LC4	330.0	45.0	12.0	37.91	0.11	27.85	0.05
LC11	440.0	4.8	8.0	31.70	0.06	28.78	0.08
LC13	440.0	30.0	1.3	31.46	0.01	29.37	0.06
LC9.1	440.0	30.0	8.0	30.43	0.04	28.97	0.04
LC9.2	440.0	30.0	8.0	30.42	0.01	28.86	0.08
LC14	440.0	30.0	14.7	29.77	0.06	29.32	0.11
LC12	440.0	55.2	8.0	30.10	0.08	29.18	0.08
LC5	550.0	15.0	4.0	28.35	0.04	29.63	0.01
LC6	550.0	15.0	12.0	27.49	0.04	29.91	0.15
LC7	550.0	45.0	4.0	28.17	0.01	29.17	0.03
LC8	550.0	45.0	12.0	27.28	0.02	29.61	0.12
LC10	625.0	30.0	8.0	26.94	0.01	29.19	0.06
				Av. SD	0.04	Av. SD	0.08

Table 6-3: Average (Av) and standard deviation (SD) for pyrolysis of *Mimosa pigra* (MP) Ychar (wt.%) and higher heating value (HHV, MJ kg^{-1}) at each temperature, hold time (HT) and heating rate (HR).

Sample	Temperature (˚C)	HT (min)	HR (˚C min^{-1})	MP Ychar (Av)	SD (±)	HHV (Av)	SD (±)
MP15	255.0	30.0	8.0	81.24	0.13	20.29	0.21
MP1	330.0	15.0	4.0	45.78	0.02	26.41	0.13
MP2	330.0	15.0	12.0	44.20	0.09	26.30	0.12
MP3	330.0	45.0	4.0	42.54	0.04	27.06	0.08
MP4	330.0	45.0	12.0	41.69	0.16	27.17	0.13
MP11	440.0	4.8	8.0	34.53	0.01	28.79	0.06
MP13	440.0	30.0	1.3	33.82	0.06	29.14	0.05
MP9.1	440.0	30.0	8.0	33.04	0.16	28.74	0.13
MP9.2	440.0	30.0	8.0	32.99	0.06	28.49	0.06
MP14	440.0	30.0	14.7	32.55	0.13	28.51	0.17
MP12	440.0	55.2	8.0	32.54	0.03	28.51	0.12
MP5	550.0	15.0	4.0	30.48	0.11	30.57	0.06
MP6	550.0	15.0	12.0	29.50	0.18	29.89	0.12
MP7	550.0	45.0	4.0	29.62	0.01	31.08	0.04
MP8	550.0	45.0	12.0	29.10	0.04	31.09	0.06
MP10	625.0	30.0	8.0	28.24	0.09	29.93	0.17
				Av. SD	0.08	Av. SD	0.11

Table 6-4: Summary of ANOVA results for *Lantana camara* and *Mimosa pigra* Ychar and char HHV.

Factor	*Lantana camara* (Ychar; wt.%)		*Mimosa pigra* (Ychar; wt.%)	
	p-value	Effect	p-value	Effect
Mean/Intercept	1×10^{-6}	+30.92	1×10^{-6}	+33.42
Temperature (L)	1×10^{-6}	-9.87	1×10^{-6}	-10.59
Temperature (Q)	7.7×10^{-5}	+6.89	2.3×10^{-5}	+6.67
Heating rate (L)	0.68	-0.49	0.67	-0.44
Heating rate (Q)	0.43	-1.13	0.46	-0.94
Hold time (L)	0.67	-0.51	0.47	-0.76
Hold time (Q)	0.47	-1.04	0.52	-0.82
	Lantana camara (HHV; MJ kg^{-1})		*Mimosa pigra* (HHV; MJ kg^{-1})	
	p-value	Effect	p-value	Effect
Mean/Intercept	1×10^{-6}	+28.82	1×10^{-6}	+28.50
Temperature (L)	1×10^{-6}	+1.76	1×10^{-6}	+2.34
Temperature (Q)	1.2×10^{-4}	-1.31	1.2×10^{-4}	-0.95
Heating rate (L)	0.50	+0.14	0.46	-0.13
Heating rate (Q)	0.15	+0.37	0.09	+0.36
Hold time (L)	0.91	+0.02	0.24	+0.20
Hold time (Q)	0.33	+0.24	0.16	+0.30

L: linear function, Q: quadratic function.

Table 6-5: Effect of scale-up on Ychar (wt.%) and char higher heating value (HHV, MJ kg^{-1}) from milligram-scale (particle size 425-600 µm) to gram-scale (particle size 850-2800 µm).

	Lantana camara (Ychar; wt.%)		*Lantana camara* char HHV (MJ kg^{-1})	
Temperature (˚C)	Milligram-scale	Gram-scale	Milligram-scale	Gram-scale
300 (300)	43.38 ± 0.02	43.97 ± 0.32	27.13 ± 0.08	27.01 ± 0.12
440 (442)	30.40 ± 0.02	33.25 ± 0.28	28.92 ± 0.06	28.76 ± 0.01
525 (522)	28.32 ± 0.07	31.45 ± 0.05	30.03 ± 0.10	29.07 ± 0.14
575 (570)	27.13 ± 0.12	29.92 ± 0.03	29.29 ± 0.08	30.11 ± 0.12
625 (614)	26.94 ± 0.01	28.76 ± 0.21	29.19 ± 0.06	30.82 ± 0.09
- (635)	-	28.72 ± 0.06	-	30.04 ± 0.08
	Mimosa pigra (Ychar; wt.%)		*Mimosa pigra* char HHV (MJ kg^{-1})	
Temperature (˚C)	Milligram-scale	Gram-scale	Milligram-scale	Gram-scale
300 (300)	52.14 ± 0.07	52.64 ± 0.32	24.54 ± 0.27	24.37 ± 0.10
440 (440)	33.10 ± 0.02	36.62 ± 0.21	28.62 ± 0.01	27.51 ± 0.20
525 (517)	30.40 ± 0.20	34.12 ± 0.20	29.83 ± 0.01	30.27 ± 0.15
580 (578)	29.44 ± 0.06	33.85 ± 0.15	31.01 ± 0.06	30.74 ± 0.08
625 (619)	28.24 ± 0.09	31.06 ± 0.08	29.93 ± 0.17	31.39 ± 0.13
700 (698)	25.73 ± 0.18	29.93 ± 0.03	29.78 ± 0.03	31.61 ± 0.04
- (749)	-	28.85 ± 0.13	-	29.81 ± 0.19

Note: All values in brackets are for gram-scale sample temperature (˚C).

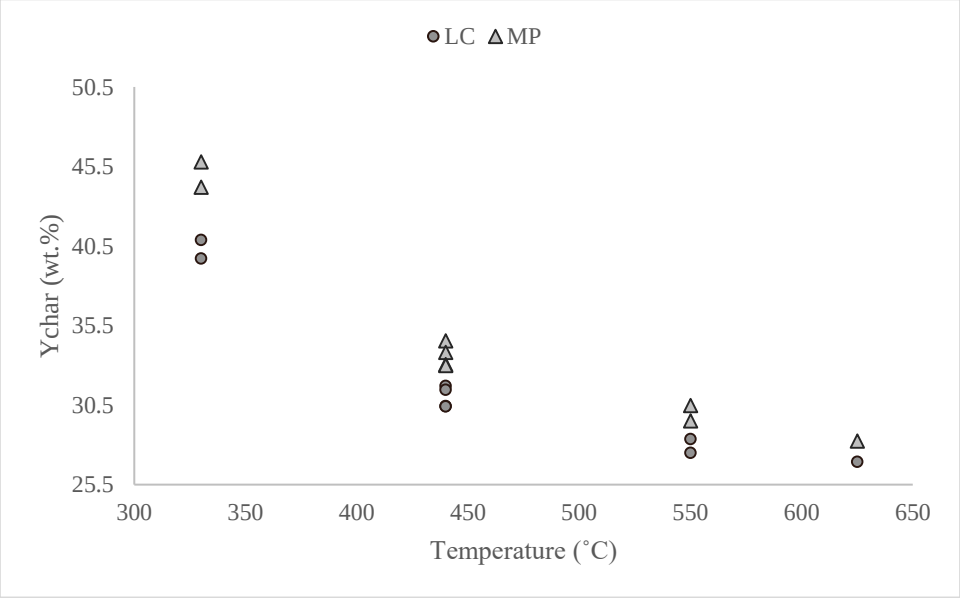

Figure 6-1: Influence of temperature on Ychar (wt.%) for *Lantana camara* (LC) and *Mimosa pigra* (MP) at milligram-scale. Tests with hold times from 5 to 30 min were used.

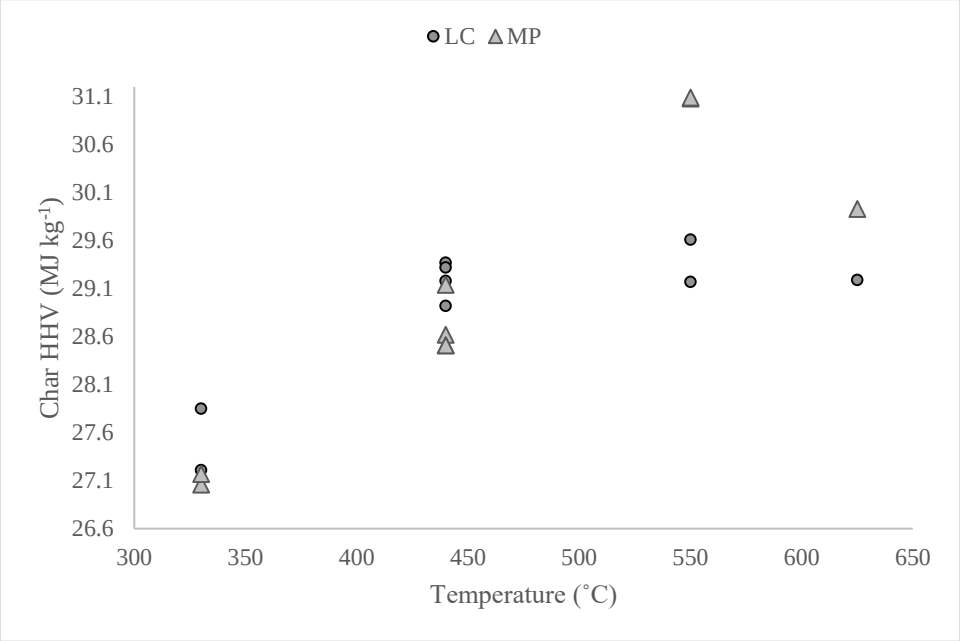

Figure 6-2: Influence of temperature on char higher heating value (HHV; MJ kg^{-1}) for *Lantana camara* (LC) and *Mimosa pigra* (MP) at milligram-scale. Tests with hold times greater than 15 min were used.

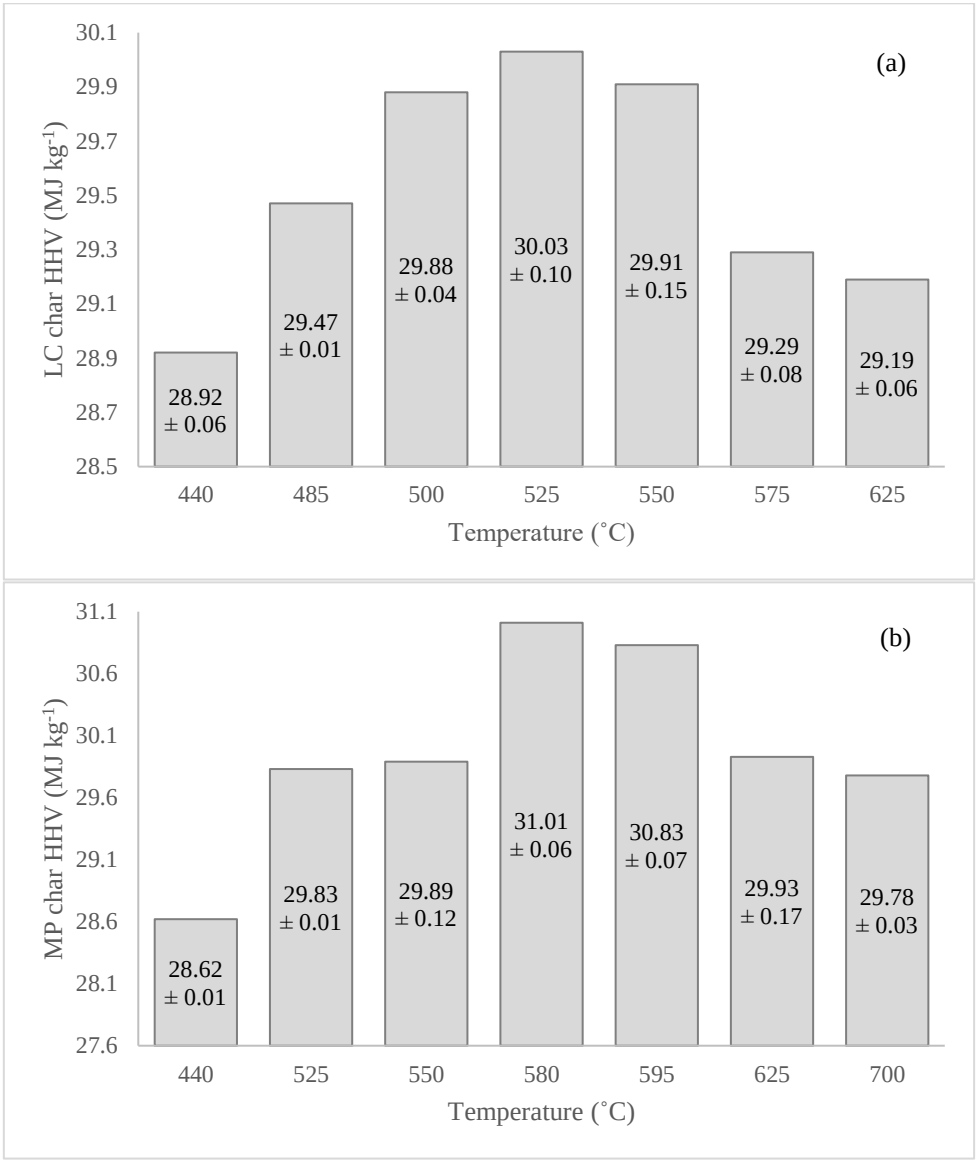

Figure 6-3: (a) *Lantana camara* (LC) char higher heating value (HHV; MJ kg^{-1}) temperature optimisation from 485 to 575 ˚C, using a constant heating rate of 12 ˚C min^{-1} and a hold time of 15 min (b) *Mimosa pigra* (MP) char higher heating value (HHV; MJ kg^{-1}) temperature optimisation from 525 to 700 ˚C, using a constant heating rate of 15 ˚C min^{-1} and a hold time of 15 min. For comparison purposes, results from the design of experiments (440 and 625 ˚C) with a hold time of 30 min were included.

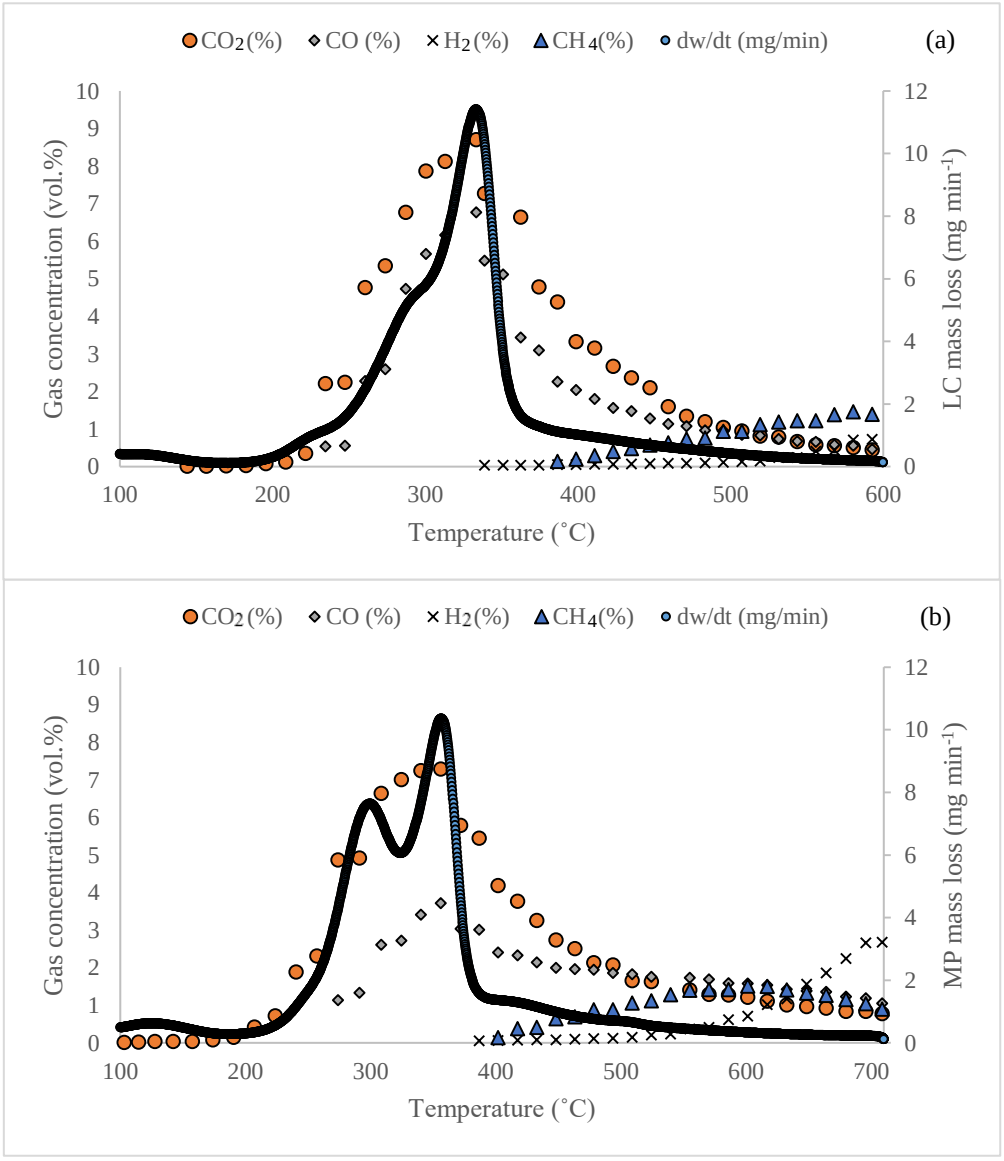

Figure 6-4: Concentration of incondensable gases and the sample temperature during pyrolysis of (a) *Lantana camara* (LC) and (b) *Mimosa pigra* (MP).

Chapter 7 **Co-combustion characteristics of coal with Invasive Alien Plant chars prepared by torrefaction or slow pyrolysis**

Submitted to Fuel

Title: "Co-combustion characteristics of coal with Invasive Alien Plant chars prepared by torrefaction or slow pyrolysis"

Authors: Jhonnah Mundike, François-Xavier Collard and Johann F. Görgens

Objective of dissertation in this chapter

This chapter addresses specific **objective four**, to investigate the combustion behaviours of individual parent fuels of torrefied and pyrolysed chars of *Lantana camara* (LC) and *Mimosa pigra* (MP), and three coals. Thereafter, the study considered the combustion behaviours of blended LC and MP chars with each of the three coals (co-combustion).

Candidate declaration

In chapter 7 page numbers 131 to 160 of this dissertation, the type and scope of my contribution were as follows:

Nature of contribution	Contribution (%)
Planning of experiments	70
Executing experiments	100
Interpretation of results	60
Writing the chapter	100

The listed co-authors have contributed to chapter 7, page numbers 131 to 160 of this dissertation.

Name	e-mail address	Type of contribution	Contribution (%)
François-Xavier Collard	fcollard@sun.ac.za	Experimental planning	30
		Reviewing of chapter	30
Johann F. Görgens	jgorgens@sun.ac.za	Interpretation of results to correlate with literature	10
		Reviewing of chapter	10

Signature of candidate:……..

Date:……

Declaration by co-authors

The undersigned hereby confirm that

- the declaration above accurately reflects the type and extent of the contributions of the candidates and co-authors to chapter 7, page numbers 131 to 160 in the dissertation,
- no other authors contributed to chapter 7, page numbers 131 to 160 in the dissertation besides those specified above, and
- potential conflicts of interest have been revealed to all interested parties and that necessary arrangements have been made to use the material in to chapter 7, page numbers 131 to 160 of this dissertation.

Institutional affiliation	Date	Signature

Abstract

Lignocellulosic samples of *Lantana camara* (LC) and *Mimosa pigra* (MP) were pre-treated by torrefaction (300 ˚C) or pyrolysis (> 500 ˚C) in order to study their potential use as coal substitutes. Combustion of the resultant chars, three coals and some blends was investigated by thermogravimetric analysis (10 ˚C min^{-1}). The effects of biomass composition, pre-treatment temperature of char and blending ratios, on combustibility parameters of ignition and burnout temperatures, and the combustion indices were determined. The addition of reactive char in the fuel mixture consistently resulted in reduction of ignition temperature, while lowered burnout temperatures of the blends indicated interactions between char and coal during co-combustion. Blends up to 15% showed similar combustion characteristics as those of the parent coals, with co-combustion occurring within the coal combustion zone. Most of the lowest combustion indices were obtained at 30% blends, mainly due to combustion occurring on a wide temperature range, while for blends ≥ 60%, co-combustion took place in the char combustion zone, with better co-combustion efficiencies, by up to 75% for 60% blend and 244% for 90% blend when compared to parent coal. Comparatively, pyrolysed char blends recorded higher combustion indices than torrefied sample blends. The results also showed that lignocellulosic composition of the precursor influenced the combustion mechanisms.

Keywords

Char, coal, co-combustion, burnout temperature, reactivity, combustion index.

7.1 Introduction

Combustion is a process whereby a fuel undergoes complete oxidation, mainly to generate heat energy [1]. The fuel could be a gas, liquid or solid, in the presence of oxygen, with a source of heat that initiates the combustion process. Lignocellulosic biomass has at a domestic scale been used as a fuel by mankind, either directly burned as firewood or indirectly used as charcoal [2]. At a commercial

level, coal for a long time now, has dominated the energy sector as the main source of heat energy in various industrial processes, despite its environmental impacts [3,4]. Of late, the demand for use of cleaner fuels has generated interest with the hope of substituting fossil fuels and minimising their environmental impacts [5–7]. Co-combustion of coal and lignocellulosic biomass has recently been studied due to its environmental benefits [8–11]. The environmental benefits of co-utilisation of lignocellulosic biomass and coal in energy applications are in the form of minimised pollutant emissions [8–10] and reduced greenhouse gas emissions in terms of CO_2 [12]. Co-firing of lignocellulosic biomass with coal has the ability to improve burning properties of coal [13–16]. Some of the expected improvements in the burning characteristics of coal when co-combusted with lignocellulose are lowered ignition, peak and burnout temperatures [11,17,18], as well as reduced duration of combustion process time [11]. The potential of lowering combustibility temperatures through co-combustion can therefore be enhanced by adding more reactive biomass fuel to less reactive coal [18]. However, for use in current reactors designed for coal combustion, the proportions of reactive biomass should be limited, otherwise the combustion behaviour of the fuel is likely to be modified to such extent that a new dedicated reactor should be designed.

Several works on co-combustion studies reported in literature used blended raw lignocelluloses with various coals [13,16,19,20]. The most utilised lignocelluloses in co-combustion studies with various coals are various agricultural wastes [18] and wood [19,21]. In recent times, the use of invasive alien plants, in particular wood from *Lantana camara* (LC) and *Mimosa pigra* (MP), as feedstock materials for solid bioenergy applications has generated interest [22–24]. The use of these invasive plants in co-combustion works would reduce the emissions of greenhouse gases and pollutant emissions [8,9,12], while providing a means of management and control of these invasive weeds [24]. Though LC and MP have been considered for their possible use in bioenergy applications [22,23], both studies did not consider co-combustion.

In comparison with coal fuel properties, lignocellulosic biomass has higher oxygen content (40-50 wt.%), volatile matter content (> 75 wt.%) and decreased higher heating value (HHV), ranging from 16 to 20 MJ kg^{-1} [25]. Some studies have considered the potential of a thermal pre-treatment of biomass, in order to get fuel properties closer to those of coal [24,26] and use increased proportions of biomass.

Thermochemical conversion technologies like torrefaction and slow pyrolysis are the common means for converting lignocellulose into a char product with increased energy density, suitable for use in energy demanding processes [27,28]. The desired char can be a possible substitute for coal in various industrial energy applications [5–7]. In order to investigate the potential use of an alternative substitute for coal in industrial energy processes, for partial or complete substitution, there is need to study the combustion characteristics or thermal behaviour of alternative solid fuels, in this case the desired lignocellulosic-derived char.

A commonly used technique for studying the thermal behaviour of fuels in oxidative environments is a thermogravimetric analyser (TGA) [22,29–32]. A burning profile or combustion characteristic of a fuel is a measure of the oxidation behaviour of a given fuel sample when burnt in oxygen rich environments under a specific heating rate [22,33]. From a plot of the rate of weight loss against temperature (DTG) while burning a fuel sample under oxidising atmosphere, an ignition temperature corresponds to the point at which the burning profile undergoes a rapid rise [33,34]. The temperature where the rate of weight loss due to combustion is highest is called a peak temperature [33]. During the combustion process, the temperature on the thermograms at which there is no further significant weight loss is called burnout temperature [35]. Though thermal pre-treatment results in fuel properties closer to those of coals, lignocellulosic-derived char generally still has lower ignition, peak and burnout temperatures compared to coal [31]. In case of char produced from torrefaction or slow pyrolysis of lignocellulosic biomass, its reactivity is directly influenced by pre-treatment process conditions [28], with temperature being the most influential factor [30]. The ignition temperature,

which is related to the volatile matter release, typically increases with increasing pre-treatment temperature. Generally, the fuel (char) consumption rate at peak temperature increases with increasing pre-treatment temperature [18].

A few studies have considered blending various types of chars with coal for co-combustion [18,21]. Sahu et al. [18] utilised low temperature biomass chars (300 and 450 ˚C) to blend with a coal characterised by a relatively high ash content (47.5 wt.%) at various blending ratios. Their study confirmed that the presence of char lowered the activation energy and improved the combustion reactivity. The use of char blending ratios less than 50% was recommended as they were found to have better performance. Kastanaki and Vamvuka [21] used high temperature chars (850 ˚C) prepared from four different types of biomass for blending with hard coal and lignite. Peak temperatures were observed in the range of 378 to 511 ˚C for the biomass chars, at 434 ˚C for lignite and at 592 ˚C for hard coal. Due to combustion in a more similar region, it was found that the effect of interactions when blending with biomass char was more pronounced on lignite than on hard coal. Further investigations are needed in order to better understand the influence of biomass composition, pre-treatment temperature and coal composition on the performance of the blends.

This current work investigated the combustion behaviour of parent fuels, namely, low temperature (torrefied at 300 ˚C) and high temperature chars (> 500 ˚C) of LC and MP, two biomass samples with different lignocellulosic composition. For blending with biomass chars, three South African coals classified as high volatile *C* bituminous coal or sub-bituminous *A* coal, in accordance with ASTM D388 standards, were used among the parent fuels. Thereafter, the low and high temperature biomass chars were blended with each one of the three coals using blending ratios of 5 to 90 wt.% (biomass char content). In addition to the study of combustion characteristic temperatures of the parent fuels and their blends, the comprehensive performances, through the use of combustion indices [13,17,29] for the various blends were assessed.

7.2 Materials and methods

7.2.1 Materials

The two invasive alien plants, *Lantana Camara* (LC) and *Mimosa Pigra* (MP) used in this work were sourced from Zambia. LC was mainly harvested from Livingstone near the Mosi-O-Tunya (Victoria Falls) and up north in Kitwe. MP was obtained from the Kafue River Flood Plains in Lochinvar National Park.

The lignocellulosic compositions showed that compared to MP, LC was richer in hemicelluloses (22.0 and 28.9 wt.%, respectively), MP contained more lignin (28.9 and 20.6 wt.%, respectively), as both samples had similar cellulose contents (47.5 and 48.2 wt.%, respectively [24]. Raw samples of particle size distribution (PSD) ranging from 850 to 2800 μm were used for char production using a bed-scale horizontal steel reactor (1 m long, 60 mm outside diameter). The detailed experimental procedure using the bed-scale steel reactor for char production was fully described in our previous work [36]. The final treatment temperatures for char production were 300 and 522 ˚C for LC, and 300 and 578 ˚C for MP. The difference in slow pyrolysis temperature was due to the fact that MP required a higher temperature to reach the optimum HHV [36].

Three coal samples (Inyanda, Tshikondeni and Phalanndwa) from South Africa were used for blending with LC and MP chars. Before blending the coal and the lignocellulosic chars, the fuels were pulverised to about 212 μm. Thereafter, the char to coal blends were mixed in different ratios from 5, 15, 30, 60 and 90 wt.%, based on biomass char content. The blended samples were manually homogenised by further crushing the mixed samples in a pestle and mortar in order to obtain a final PSD in the range of 75 to 150 μm as previously suggested for TGA study [18]. The homogenised blends were finally used for combustion characteristic determinations. Proximate analysis for all the parent fuels was conducted according to ASTM standard E1131, using thermogravimetric analysis TGA/ DCS 1 Star System Mettler Toledo. The HHVs for the parent fuels were conducted in a bomb

calorimeter, model 2013 (Cal2k Eco Calorimeter), calibrated with benzoic acid (Cal2K), based on ASTM standard D5865-11a.

7.2.2 Study of combustion behaviour in TGA

The combustion behaviour of the fuels was determined using a thermogravimetric analyser TGA/DCS 1 Star System Mettler Toledo. A sample weighing 5 mg ± 0.3 mg was placed in a 600 µL ceramic crucible by evenly spreading the sample on the bottom surface of the crucible to ensure that oxygen had unlimited contact with fuel materials during combustion. The combustion analyses were carried out using 5 ml min^{-1} of oxygen (baseline 5.0, Afrox) and 20 ml min^{-1} of inert gas (argon baseline 5.0 Afrox), at a heating rate of 10 ˚C min^{-1}, from 30 ˚C up to 800 ˚C, beyond which no mass loss was detectable. The fuel sample mass loss and its first derivative as a function of temperature (derivative thermogravimetric, DTG) were obtained from the TGA data analysis software (STARe). The thermograms were further analysed in order to determine the combustion parameters of ignition (T_{ig}, ˚C), peak (T_{pk};˚C), and burnout (T_{bo};˚C) temperatures. T_{ig} and T_{bo}, are temperatures where fuel combustion rate reaches 1 wt.% min^{-1} for the first time and begins to diminish to less than 1 wt.% min^{-1}, respectively. T_{pk} is the temperature at which maximum fuel combustion rate is achieved. Additionally, the maximum combustion rate (DTG_{max}) and mean or average combustion rate (DTG_{mean}) (wt.% min^{-1}), and the combustion index (C_i) were also evaluated. DTG_{mean} was determined between T_{ig} and T_{bo}. The C_i is a measure of comprehensive combustion performance of the fuel being studied and can be determined by equation 1 [17,29]:

$$\frac{DTG_{max} \cdot DTG_{mean}}{T_{ig}^2 \cdot T_{bo}} \quad \text{.....(1)}$$

7.3 Results and discussion

7.3.1 Proximate analyses and energy contents of parent fuels

Table 7-1 shows the measured proximate analysis and HHV results of the four parent lignocellulosic chars and three coal samples before blending. The raw biomass samples had similar HHV (18.0 MJ kg^{-1} for LC and 17.7 MJ kg^{-1} for MP). Following torrefaction at 300 ˚C, LC richer in hemicelluloses as earlier stated (section 7.2.1) was significantly converted (char yield of 43.4 wt.%), resulting in an HHV of 27.0 MJ kg^{-1}, almost equivalent to that of Phalanndwa coal (27.3 MJ kg^{-1}), and even higher than that of Inyanda coal (26.5 MJ kg^{-1}). MP torrefied at 300 ˚C was characterised by a lower degree of conversion (char yield of 52.1 wt.%) and an HHV of 24.4 MJ kg^{-1}, mainly due to increased lignin, which is less reactive during torrefaction [24]. Additionally, through torrefaction at 300 ˚C, LC produced a char with more fixed carbon content of 53.7% compared with 45.9% obtained from MP at similar conversion conditions. During pyrolysis conversion (T > 500 ˚C), MP required higher temperatures to reach optimum HHV than LC, as the former biomass was richer in lignin [36]. LC522 char HHV was slightly lower (29.1 MJ kg^{-1}) than that for Tshikondeni, the coal with the highest energy content, while the energy content for MP578 was higher (30.7 MJ kg^{-1}). Both chars had volatile matter around 15%, lower than that of the 3 coals (> 20%). Among the 3 coals, Tshikondeni recorded the highest energy content due to increased fixed carbon of 62.4% and the lowest ash content of 14.8%. Inyanda coal HHV was 26.5 MJ kg^{-1}, the lowest result, mainly due to increased ash content of 17.5%.

7.3.2 Combustion behaviour of parent fuels

7.3.2.1 Combustibility profiles (DTG) of parent fuels

The combustion profiles of the parent lignocellulosic fuels (LC300, LC522, MP300 and MP578) and the 3 coals (Inyanda, Tshikondeni and Phalanndwa) are shown in Figure 7-1. The key parameters used to compare solid fuel combustibility and their reactivities, such as ignition temperature (T_{ig}), peak temperature (T_{pk}) and burnout temperature (T_{bo}) were computed from the derivative thermogravimetric (DTG) results. A weight gain was observed for all parent fuel samples, especially for Tshikondeni coal around 300 ˚C, before the commencement of the main combustion process. Similar net weight gains were reported in literature and were interpreted as a consequence of oxygen chemisorption [13,17].

The combustion profiles of the coals compared to lignocellulosic chars showed that coal ignition required higher temperatures (> 363 ˚C), while lignocellulosic chars had T_{ig} values < 353 ˚C, mainly due to the differences in chemical composition between coal and lignocellulosic char. For lignocellulosic samples torrefied at 300 ˚C, LC300 had the lowest T_{ig} of 262 ˚C, while MP recorded a T_{ig} of 273 ˚C. Similar results of T_{ig} range were obtained in literature for char samples pre-treated at 300 ˚C [18]. Despite an increased volatile matter content of 50.9% for MP300, compared with 41.8% for LC300, the former biomass fuel had a higher T_{ig}. This result was again interpreted as a consequence of the higher content of stable lignin in MP. The volatiles were released at a higher temperature than for LC, resulting in a higher T_{ig}. In the case of pyrolysis, LC522 had a lower T_{ig} (323 ˚C) than MP578 (354 ˚C), which was consistent with the lower pre-treatment temperatures.

In case of the T_{ig} results for the 3 coals, the higher the volatile matter, the lower the T_{ig}, with Phalanndwa coal recording the lowest T_{ig} of 362 ˚C, followed by Tshikondeni (378 ˚C) and Inyanda (395 ˚C). In comparison with the coals used for this study, the lower T_{ig} values for the four

lignocellulosic chars, even for pre-treatment temperature as high as 578 ˚C (MP578), were consistent with results previously reported in literature [18,21], for coals of sub-bituminous or higher quality.

Regarding the main combustion process [11], the major peaks for torrefied chars were observed at T_{pk} of 415 ˚C for LC300 and 450 ˚C for MP300. The T_{pk} for LC522 was at 421 ˚C, very close to that of LC300, while the T_{pk} for MP578 was at 467 ˚C. Despite the differences in pre-treatment temperatures, MP300 had a higher T_{pk} (450 ˚C) compared with LC522 (421 ˚C). For biomass chars, it seemed T_{pk} depended more on biomass composition than on pre-treatment temperature, where higher T_{pk} values were obtained from the lignin rich sample (in this case MP). For each biomass, the peak corresponding to the main combustion step became narrower and higher in intensity with increase in pre-treatment temperature, with the highest peak profile being that of MP578. As for the three coal samples, DTG curves gradually rose from 350 to 400 ˚C (mainly combustion of volatile matter), followed by a more pronounced rise from 400 up to 600 ˚C (combustion of fixed carbon). Compared with LC522 and MP578, the DTG curves were relatively broader with a T_{pk} between 500 and 530 ˚C. Literature has reported similar DTG curves for coal [21].

As for the coal DTG_{max} results, Inyanda and Tshikondeni recorded 8.3 and 8.4 % min^{-1}, respectively, compared with Phalanndwa with 6.8 % min^{-1}. These results were similar as those obtained for torrefied biomass and lower than for the pyrolysed biomass. Amongst the coals, Phalanndwa had an intermediate HHV, while Inyanda and Tshikondeni had the lower and upper HHVs, respectively (Table 7-1). However, the two coals showing similar combustion behaviours were Inyanda and Tshikondeni. The combustion behaviour for coal was more correlated to the composition in terms of proximate analysis, with lower T_{ig} due to higher volatile matter content and lower DTG_{max} as well as lower fixed carbon for Phalanndwa.

Similarly to T_{pk}, the burnout temperature (T_{bo}) was more influenced by the biomass composition than by the pre-treatment temperature. The T_{bo} for LC300 and LC522 were 470 and 477 ˚C, respectively. The T_{bo} for MP300 was 496 ˚C, while that for MP578 was 500 ˚C. In case of the 3 coals, T_{bo} was

observed at higher temperatures, from 577 ˚C for both Inyanda and Phalanndwa, and up to 584 ˚C for Tshikondeni.

7.3.2.2 Combustion performance of parent fuels

The combustion indices (C_i), which are a measure of fuel combustion efficiency [13], are shown in Table 1 for each fuel. Better performing fuels have higher values of C_i. For the torrefied chars, LC300 with C_i of 1.1 x 10^{-6} showed a better performance than MP300 with a C_i of 7.3 x 10^{-7}. LC522 recorded the highest C_i of 1.2 x 10^{-6}, among the lignocellulosic chars, while MP578 had a C_i of 1.1 x 10^{-6}. For each type of pre-treatment (torrefaction or slow pyrolysis), LC and MP char samples presented similar DTG profiles, but shifted at lower temperature for LC. Consequently, higher C_i was mostly due to lower T_{ig} and T_{bo}, thus highlighting that the combustion performance was dependent on biomass type, with LC fuel chars performing better than MP.

In case of the coals, though Inyanda and Tshikondeni ranked differently, their combustion curves were similar (Figure 7-1) and both had C_i values of 3.8 x 10^{-7}, higher than for Phalanndwa (3.2 x 10^{-7}). In comparison with these two coals, the DTG curve for Phalanndwa was characterised by a more progressive profile with slightly higher intensity at early stage due to higher volatile matter content, and much lower intensity at DTG_{max} due to lower fixed carbon content. Comparatively, lignocellulosic chars, whether torrefied or pyrolysed had higher values of C_i than the coals.

7.3.3 Co-combustion behaviour of lignocellulosic biomass chars and coal blends

This section presents the co-combustion behaviour of lignocellulosic biomass char samples (LC and MP), blended with 3 coals, using blending ratios of 5, 15, 30, 60 and 90 wt.% (biomass content). Based on the DTG curves in Figure 7-1, Inyanda and Tshikondeni showed similar combustion

behaviours. As similar DTG profiles were also observed for co-combustion, the DTG curves related to co-combustion of Tshikondeni coal with LC and MP chars can be found in Supplementary Material.

7.3.3.1 Co-combustion behaviour of Inyanda coal blends and their performances

Figure 7-2a and b shows the combustion characteristics of LC with Inyanda coal for pre-treatment temperatures of 300 and 522 ˚C, respectively. As expected, increasing the content of reactive biomass char resulted in lower ignition temperatures (T_{ig}). For LC300, the T_{ig} was lowered by 19, 47 and 99 ˚C at 5, 15 and 30% blends, respectively, with up to T_{ig} reduction of 126 ˚C for 90% blend. At 5 and 15% blends for LC300 with Inyanda coal, the DTG curves were similar to that of the parent coal, while for both blends, combustion indices (C_i) were 3.5 x 10^{-7} and 3.4 x 10^{-7}, respectively. At 30% blend, the peak corresponding to coal combustion was difficult to identify and the burnout temperature (T_{bo}) was significantly lowered, a sign that char combustion enhanced the reactivity of Inyanda coal. However, as the combustion occurred progressively with a relatively low DTG_{max}, the C_i was found to decrease to 3.1 x 10^{-7} in comparison with blends with a lower biomass char content. At 60% and 90% blends, the main peak of the DTG curve corresponded to the combustion of the char and the T_{bo} was significantly reduced (from 577 ˚C for Inyanda coal to 493 ˚C for the 90% blend). The C_i values for 60 and 90% blends increased to 3.9 x 10^{-7} and 7.7 x 10^{-7}, respectively (Figure 7-2c), due to the increased amounts of reactive char in the fuel mixture.

As for LC522 blends with Inyanda coal, the T_{ig} was lowered by 20, 28 and 36 ˚C at 5, 15 and 30% blends, respectively, while a T_{ig} reduction of up to 69 ˚C was obtained at 90% blend. The evolution was generally less pronounced than that for LC300. Indeed, higher biomass pre-treatment temperature resulted in volatiles being released at higher temperature. In Figure 7-2b, the 5 and 15% blends had

DTG curves similar to that of the parent coal. The C_i value at 5% blend was slightly higher (3.9 x 10^{-7}) than that of the parent coal (3.8 x 10^{-7}). Then, a C_i decrease towards 30% blend (2.9 x 10^{-7}) was observed. Indeed, the DTG profile corresponding to coal combustion at 30% blend (Fig. 2b) was characterized by a progressive co-combustion and a relatively low DTG_{max}. For blends with increased char content, the conversion mostly occurred in the char combustion region and the T_{bo} significantly decreased (from 577 ˚C for the parent coal to 485 ˚C for the 90% blend). At 60% blend, the C_i value increased significantly to 5.9 x 10^{-7} (Figure 7-2d), with a further C_i increase of up to 1.1 x 10^{-6} at 90% blend.

Figure 7-3a and b shows the combustion characteristics of MP blends with Inyanda coal for pre-treatment temperatures of 300 and 578 ˚C. The T_{ig} values were generally lowered with an increase in biomass char content in the blends, an indication of early release of volatiles. The T_{ig} blends of MP300 with Inyanda coal decreased by 44, 38 and 91 ˚C for 5, 15 and 30% blends, respectively, with a further reduction of up to 117 ˚C, for the 90% blend. For MP300 char blends at 5 to 15%, the DTG curves were similar to that of the parent coal, resulting into constant C_i values of 3.4 x 10^{-7} for both blends (Figure 7-3c). As for the 30% blend, the C_i was also 3.4 x 10^{-7}, as the reduced intensity of the main combustion peak was balanced by the lower T_{ig}. For the different MP300 blends from 5 to 30%, minimal reduction in T_{bo} was observed (3 ˚C for both 5 and 15% blends and 6 ˚C for the 30% blend). It is only for blends from 60% upwards that T_{bo} was significantly lowered, resulting in T_{bo} of 577 ˚C for the parent coal being lowered to 518 ˚C for the 90% blend with MP300. Ultimately, C_i values increased with an increase in biomass char content in the blends (Figure 7-3c).

The T_{ig} for MP578 with Inyanda coal, were lowered by 7, 16 and 25 ˚C for 5, 15 and 30% blends, respectively (less than MP300 at similar blending ratios with the same coal). The DTG curves for 5 and 15% blends showed similarities with that of the parent coal (Figure 7-3b). The C_i values for the blends showed a reduction towards 30%; 3.7 x10^{-7} for 5%, 3.5 x 10^{-7} for 15% and 3.0 x 10^{-7} for 30%. At 30% blend, the DTG curve was characterized by a lower intensity of the coal peak, while no

significant effect on T_{bo} was observed. As for the blends from 60% upwards, the DTG curves were composed of a main peak corresponding to the char combustion, which was found to influence the coal reactivity. At 90% blend, the T_{bo} decreased to 511 ˚C, a temperature even lower than the observed T_{pk} for pure Inyanda coal (526 ˚C), resulting in a significant increase of the C_i value, up to 9.2 x 10^{-7} for the 90% blend.

7.3.3.2 Co-combustion behaviour of Phalanndwa coal blends and their performances

The results of LC char pre-treated at 300 and 522 ˚C, blended with Phalanndwa coal are shown in Figure 7-4a and b. Co-combustion for LC300 blends commenced earlier than that of the parent coal as evidenced by the lowering of T_{ig} by 16, 23, 56 ˚C for 5, 15 and 30% blends, respectively. The DTG curves for 5 and 15% blends resembled that of the parent coal, while the DTG curve for the 30% blend had the most diminished peaks. In Figure 7-4c, the combustion indices of the blends were reducing towards 30% blending ratio, resulting into C_i values of 3.1 x 10^{-7} for 5% and 3.0 x 10^{-7} for 15%, while that for 30% was the lowest at 2.8 x 10^{-7}. The influence of char on coal in the blends, minimally lowered the T_{bo} for 5 and 15% blends, while at 30% blend, there was a T_{bo} difference of 10 ˚C. The DTG curves for 60 and 90% blends closely resembled that of the parent biomass char with T_{bo} differences of up to 101 ˚C with a corresponding C_i of 9.2 x 10^{-7} for the 90% blend.

As for the DTG curves for LC522 blends with Phalanndwa coal, their T_{ig} for 5 and 15% were minimally lowered by 3 and 9 ˚C, respectively. At 30%, a T_{ig} reduction of 14 ˚C was obtained, with diminished peak intensity of the DTG curve (Figure 7-4b). The C_i values for blends between 5 and 30% were in the range of 2.8 x 10^{-7} to 3.2 x 10^{-7}. As more char was added to the fuel mixture, T_{bo} decreased from 577 ˚C for the parent coal to 486 ˚C for the 90% blend, resulting into progressively increased C_i values (Figure 7-4d).

Figure 7-5a and b shows the DTG curves for the blends of Phalanndwa coal with MP pre-treated at 300 and 578 ˚C. The 5 and 15% DTG curves for MP300 blends with the coal, both resembled that of the parent coal, with T_{ig} values reduced by 10 and 29 ˚C, respectively. At 30% blend, T_{ig} was reduced by 60 ˚C, while DTG curve was characterized by relatively low peak intensity. The C_i values of 3.1 x 10^{-7} for 5% and 3.0 x 10^{-7} for 15% were obtained (Figure 7-5c), while at 30% blend the lowest C_i value of 2.9 x 10^{-7} was recorded. Again, increasing the char content resulted in more pronounced decrease of T_{ig} and T_{bo} and significant C_i increase. T_{ig} for the parent coal reduced from 363 ˚C to 276 ˚C, while T_{bo} was lowered from 577 ˚C to 513 ˚C, with a corresponding C_i value of 5.8 x 10^{-7} for the 90% blend.

In case of blends of MP578 with Phalanndwa coal, insignificant T_{ig} reductions (< 3 ˚C) were obtained up to 30% blends. The C_i values for 5 and 15 % were 3.0 x 10^{-7} and 3.1 x 10^{-7}, respectively. Contrary to what was observed with the other char/coal mixtures, the DTG curve of the 30% blend was characterized by an increased peak intensity, in comparison with the lower blends, resulting in a significant increase in the C_i value (3.7 x 10^{-7}). The peak was located at 478 ˚C, close to T_{pk} for MP578 (467 ˚C). It appeared that the simultaneous volatile production from Phalanndwa coal, the coal with the highest volatile matter content, was responsible of the relatively high peak intensity. In this particular case, the influence of interactions on combustion performance is unsure. Indeed, compared to the parent coal, T_{bo} decrease observed for the 30% blend was only of 8 ˚C. As for the other mixtures, further increase in char content in the blends, further reduced the $T_{bo,}$ from 577 ˚C for the parent coal to 514 ˚C and increased the C_i value to 9.0 x 10^{-7} for the 90% blend.

7.3.3.3 Comprehensive co-combustion performances of the blends

In order to assess the combustion performances of the various blends of the parent lignocellulosic chars with each one of the 3 coals, the C_i values for the various blends were determined as earlier

indicated in sections 7.3.3.1 to 7.3.3.2. A summary of the results is detailed in this section with particular attention to the observed trends in the influence of pre-treatment temperature and lignocellulosic composition on the fuel mixtures during co-combustion. For all the fuel mixtures, it was observed that increasing the proportion of char resulted in lower T_{ig}. This trend was due to the release of volatiles at lower temperature for chars, as observed for the parent fuels (Figure 7-1). Due to lower pre-treatment temperature, torrefied samples released volatiles at lower temperatures than pyrolysed samples. As a consequence, for the same biomass type at the same blending ratio, torrefied blends had more pronounced T_{ig} reductions than those from pyrolysed char blends. The T_{ig} decreases were in the range of 87 to 126 ˚C for torrefied char blends and 8 to 67 ˚C for pyrolysed blends (90% char). Reduced T_{ig} enhanced earlier commencement of the co-combustion process. When the char combustion had minimal influence on coal combustion, it resulted in a prolonged co-combustion process with similar or reduced C_i values, as observed for 5-30% blends. The DTG curves from all the blends with 5 to 15% of char showed a similar pattern of profiles resembling the parent coals, generally with insignificant change of coal T_{bo}. For instance, the T_{bo} results for blends up to 15% for torrefied char blends with coal were not reduced by more than 8 ˚C and 18 ˚C for pyrolysed char with similar coal. The C_i values for coal were 3.2×10^{-7} for Phalanndwa and 3.8×10^{-7} for both Inyanda and Tshikondeni. As for the combustion performance with the three coals for the blends up to 15%, the C_i values were in the range of 3.0×10^{-7} to 3.7×10^{-7} for torrefied blends and 2.8×10^{-7} to 3.9×10^{-7} for pyrolysed char blends. As C_i values of the blending ratios up to 15% were close to those of the parent coal with a main peak corresponding to the combustion of coal, such blending ratios could be used for co-firing in current coal reactors to increase the amount of renewable fuel while reducing pollutant emissions [8–10]. Similarly, literature has shown that blending ratios less than 30% were acceptable for co-firing of lignocelluloses with coal, mainly dependent on unit process design and fuel requirements [5]. The main advantage of using pyrolysed chars for co-firing would be the higher energy output, due to their increased HHV in comparison with torrefied chars.

At 30% blends, the DTG curves were generally characterised by relatively low intensities with conversion extending over a wide range of temperature without real combustion peak, generally resulting into much decreased C_i values, a sign of poor performance for the blends. Such blending ratios may not be advantageous to use in co-combustion facilities, as the combustion characteristics of coal are drastically changed, showing a transition from coal into lignocellulosic char combustion region.

As the biomass char content in the fuel mixture increased to ≥ 60%, the main peaks on the DTG curves were observed in the combustion region of the biomass char. There was no clear peak observed for coal, as the coal combustion was shifted towards lower temperatures and the T_{bo} was significantly reduced (up to T_{bo} difference of 100 ˚C when compared to parent coal), showing that heat released by char combustion catalysed the coal conversion. Due to the shift of the main peak to lower temperatures and significant increase in C_i values (up to 75% at 60% blend and 244% at 90% blend), pilot tests would be necessary to check whether a new reactor design would be required for the optimal recovery of the energy output.

The influence of biomass char on coal combustion and possible interactions due to blending can be assessed in reference to reduced T_{bo}, an indication of quicker combustion of the parent coal. Figure 7-6 compares the evolution of T_{bo} values for the two different lignocellulosic samples, either torrefied or pyrolysed, when blended with Inyanda coal. For both LC and MP, pyrolysed char had more influence on lowering the T_{bo} of coal than torrefied char. For instance, when comparing LC300 with LC522 differences of 17 and 57 ˚C were obtained at 30 and 60% blend respectively. It was reported during co-combustion that similar combustion regions would result in increased interactions [21]. As combustion of pyrolysed char occurred at higher temperature than torrefied char (Figure 7-1), thus closer to the coal combustion temperature range, the T_{bo} evolution was as expected. As a consequence of increased fixed carbon content and impact on coal combustion, blends with pyrolysed chars generally gave higher values of C_i than with torrefied blends.

At both blending ratios of 30 and 60%, LC300 had a greater impact on T_{bo} reductions than MP300, while LC522 equally recorded greater T_{bo} reductions than MP578 with the same parent coal. Additionally, from Figure 7-6, at the blending ratio of 60%, it is worth noting that LC300 recorded a greater impact in lowering T_{bo} than MP578, despite a pre-treatment temperature difference of 278 ˚C. In this work, it was evidenced that lignocellulosic composition influenced the co-combustion performance of char with coal, with LC having a greater impact than MP. It appeared that the heat released by LC char combustion could have been substantial enough to influence coal conversion to such an extent that the resultant catalytic effect was stronger for LC than that for MP char. In this case, though LC char combustion region occurred at lower temperature than for MP (T_{bo} of 486 ˚C for LC522 and 514 ˚C for MP578), more interactions with coal and higher C_i were observed with LC (for all coal blends at 60 and 90%). For instance, LC522 char blend with Inyanda coal at 60% had a C_i value of 5.9 x 10^{-7} in comparison with 4.8 x 10^{-7} for MP578 at the same blending ratio with the same coal.

7.4 Conclusion

The combustibility parameters of blending torrefied and pyrolysed LC and MP chars with 3 coals were investigated in a thermogravimetric analyser. Co-combustion of the blends commenced earlier than the parent coals, mainly due to the addition of more reactive char in the fuel mixture. Mostly, lowered burnout temperatures of the blends during co-combustion indicated the interactions between char and coal. The combustion behaviours for blends up to 15% resembled those of the parent coals, with most of the conversion still occurring within the combustion zone of coal, resulting into limited impact on the combustion indices. Blends up to 15% could practically be utilised in reactors initially designed for coal use. Mainly, decreased combustion indices at 30% blends were obtained due to conversion occurring over a wide temperature range, transitioning into char combustion zone as char content increased. At 60 and 90% blends, interactions between char and coal resulted in decreased

burnout temperature and enhanced combustion indices. Char composition in relation with both pre-treatment temperature and composition of the lignocellulosic precursor were found to influence the co-combustion behaviours.

Acknowledgements

The authors acknowledge the material support in terms of three coal samples obtained from North West University, Potchefstroom campus of South Africa, as well as financial support from the Process Engineering Department of Stellenbosch University in South Africa and the Copperbelt University in Kitwe, Zambia.

7.5 References

[1] Van Loo J, Koppejan S. The handbook of biomass combustion & co-firing. first ed. Washington, DC: Earthscan; 2008.

[2] Parikka M. Global biomass fuel resources. Biomass and Bioenergy 2004;27:613–20.

[3] Schweinfurth SP. An introduction to coal quality. Virginia: 2009.

[4] Energy Information Administration (EIA). International Energy Outlook 2016. vol. 484. Washington, DC 20585: 2016.

[5] Suopajärvi H, Kemppainen A, Haapakangas J, Fabritius T. Extensive review of the opportunities to use biomass-based fuels in iron and steelmaking processes. J Clean Prod 2017;148:709–34.

[6] Suopajärvi H, Pongrácz E, Fabritius T. The potential of using biomass-based reducing agents in the blast furnace: A review of thermochemical conversion technologies and assessments related to sustainability. Renew Sustain Energy Rev 2013;25:511–28.

[7] Mousa E, Wang C, Riesbeck J, Larsson M. Biomass applications in iron and steel industry: An overview of challenges and opportunities. Renew Sustain Energy Rev 2016;65:1247–66.

[8] Smajevic I, Kazagic A, Music M, Becic K, Hasanbegovic I, Sokolovic S, Delihasanovic N, Skopljak A, Hodzic N. Co-firing bosnian coals with woody biomass: Experimental studies on a laboratory-scale furnace and 110 MW e power unit. Therm Sci 2012;16:789–804.

[9] Kubacki ML, Ross AB, Jones JM, Williams A. Small-scale co-utilisation of coal and biomass. Fuel 2012;101:84–9.

[10] Aho M, Gil A, Taipale R, Vainikka P, Vesala H. A pilot-scale fireside deposit study of co-firing Cynara with two coals in a fluidised bed. Fuel 2008;87:58–69.

[11] Liu Z, Hu W, Jiang Z, Mi B, Fei B. Investigating combustion behaviors of bamboo, torrefied

bamboo, coal and their respective blends by thermogravimetric analysis. Renew Energy 2016;87:346–52.

[12] Mellin P, Wei W, Yang W, Salman H, Hultgren A, Wang C. Biomass availability in Sweden for use in blast furnaces. Energy Procedia 2014;61:1352–5.

[13] Moon C, Sung Y, Ahn S, Kim T, Choi G, Kim D. Effect of blending ratio on combustion performance in blends of biomass and coals of different ranks. Exp Therm Fluid Sci 2013;47:232–40.

[14] Muthuraman M, Namioka T, Yoshikawa K. A comparison of co-combustion characteristics of coal with wood and hydrothermally treated municipal solid waste. Bioresour Technol 2010;101:2477–82.

[15] Arias B, Pevida C, Rubiera F, Pis JJ. Effect of biomass blending on coal ignition and burnout during oxy-fuel combustion. Fuel 2008;87:2753–9.

[16] Varol M, Atimtay AT, Bay B, Olgun H. Investigation of co-combustion characteristics of low quality lignite coals and biomass with thermogravimetric analysis. Thermochim Acta 2010;510:195–201.

[17] Liu X, Chen M, Yu D. Oxygen enriched co-combustion characteristics of herbaceous biomass and bituminous coal. Thermochim Acta 2013;569:17–24.

[18] Sahu SG, Sarkar P, Chakraborty N, Adak AK. Thermogravimetric assessment of combustion characteristics of blends of a coal with different biomass chars. Fuel Process Technol 2010;91:369–78.

[19] Gil M, Casal D, Pevida C, Pis J, Rubiera F. Thermal behaviour and kinetics of coal/biomass blends during co-combustion. Bioresour Technol 2010;101:5601–8.

[20] Haykiri-Acma, H Yaman S, Kucukbayrak S. Co-combustion of low rank coal / waste biomass blends using dry air or oxygen. Appl Therm Eng 2013;50:251–9.

[21] Kastanaki E, Vamvuka D. A comparative reactivity and kinetic study on the combustion of coal-biomass char blends. Fuel 2006;85:1186–93.

[22] Kumar R, Chandrashekar N. Study on chemical, elemental and combustion characteristics of Lantana camara wood charcoal. J Indian Acad Wood Sci 2013;10:134–9.

[23] Wongsiriamnuay T, Tippayawong N. Thermogravimetric analysis of giant sensitive plants under air atmosphere. Bioresour Technol 2010;101:9314–20.

[24] Mundike J, Collard F-X, Görgens JF. Torrefaction of Invasive Alien Plants: Influence of heating rate and other conversion parameters on mass yield and higher heating value. Bioresour Technol 2016;209:90–9.

[25] Neves D, Thunman H, Matos A, Tarelho L, Gómez-Barea A. Characterization and prediction of biomass pyrolysis products. Prog Energy Combust Sci 2011;37:611–30.

[26] Assis MR, Brancheriau L, Napoli A, Trugilho PF. Factors affecting the mechanics of carbonized wood: literature review. Wood Sci Technol 2016;50:1–18.

[27] Garcia R, Pizarro C, Lavin AG, Bueno JL. Characterization of Spanish biomass wastes for energy use. Bioresour Technol 2012;103:249–58.

[28] Di Blasi C. Combustion and gasification rates of lignocellulosic chars. Prog Energy Combust Sci 2009;35:121–40.

[29] Xiong S, Zhang S, Wu Q, Guo X, Dong A, Chen C. Investigation on cotton stalk and bamboo sawdust carbonization for barbecue charcoal preparation. Bioresour Technol 2014;152:86–92.

[30] Hasan Khan Tushar MS, Mahinpey N, Khan A, Ibrahim H, Kumar P, Idem R. Production, characterization and reactivity studies of chars produced by the isothermal pyrolysis of flax straw. Biomass and Bioenergy 2012;37:97–105.

[31] Daood SS, Munir S, Nimmo W, Gibbs BM. Char oxidation study of sugar cane bagasse,

cotton stalk and Pakistani coal under 1% and 3% oxygen concentrations. Biomass and Bioenergy 2010;34:263–71.

[32] Munir S, Daood SS, Nimmo W, Cunliffe AM, Gibbs BM. Thermal analysis and devolatilization kinetics of cotton stalk, sugar cane bagasse and shea meal under nitrogen and air atmospheres. Bioresour Technol 2009;100:1413–8.

[33] Haykiri-Acma H. Combustion characteristics of different biomass materials. Energy Convers Manag 2003;44:155–62.

[34] Garcia-Ibanez P, Sanchez M, Cabanillas A. Thermogravimetric analysis of olive-oil residue in air atmosphere. Fuel Process Technol 2006;87:103–7.

[35] Idris SS, Abd Rahman N, Ismail K, Alias AB, Abd Rashid Z, Aris MJ. Investigation on thermochemical behaviour of low rank Malaysian coal, oil palm biomass and their blends during pyrolysis via thermogravimetric analysis (TGA). Bioresour Technol 2010;101:4584–92.

[36] Mundike J, Collard F, Görgens JF. Pyrolysis of Lantana camara and Mimosa pigra : Influences of temperature , other process parameters and incondensable gas evolution on char yield and higher heating value. Bioresour Technol 2017;243:284–93.

Table 7-1: Proximate analysis, higher heating value (HHV) and combustion indices (C_i) of parent fuels used in this study (the sample char temperature between brackets corresponds to the pre-treatment temperature).

Sample	VM (%)	FC (%)	Ash (%)	HHV (MJ kg^{-1})	C_i (% min^{-1})^2 T^{-3}
MP char (300 °C)	50.9	45.9	3.1	24.4	7.3×10^{-7}
LC char (300 °C)	41.8	53.7	4.5	27.0	1.1×10^{-6}
LC char (522 °C)	16.4	76.7	6.9	29.1	1.2×10^{-6}
MP char (578 °C)	14.7	78.2	6.5	30.7	1.1×10^{-6}
Tshikondeni coal	22.8	62.4	14.8	29.6	3.8×10^{-7}
Phalanndwa coal	27.3	57.0	15.8	27.3	3.2×10^{-7}
Inyanda coal	22.2	60.4	17.5	26.5	3.8×10^{-7}

Note: VM: volatile matter; FC: fixed carbon; proximate analysis results are reported on dry basis

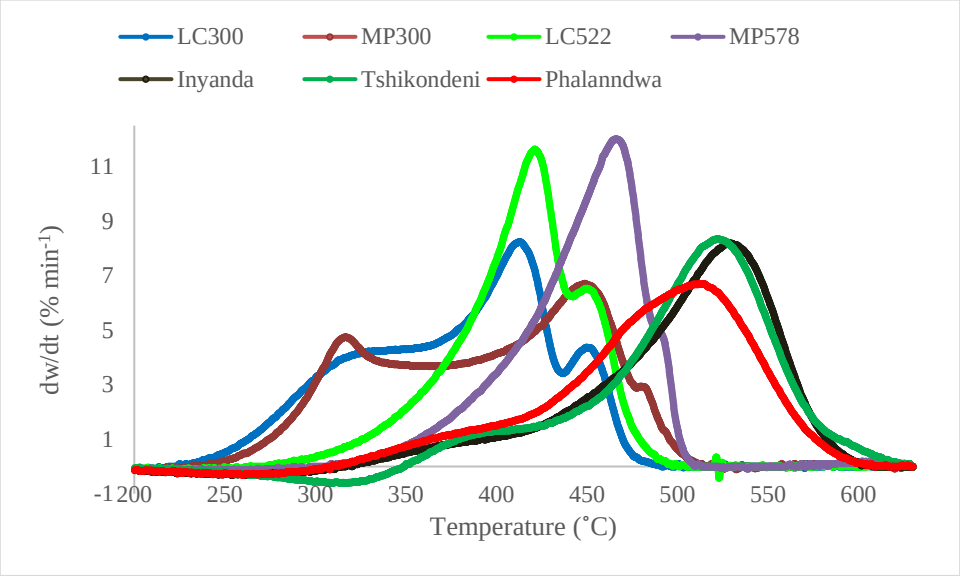

Figure 7-1: DTG curves showing the combustion profiles of the parent fuels (10 ˚C min^{-1}).

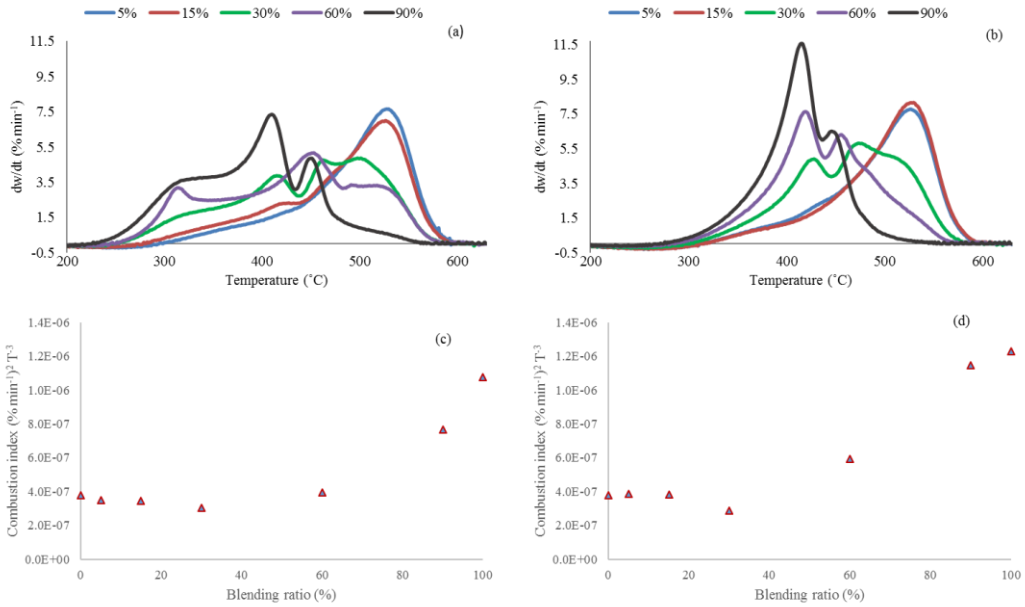

Figure 7-2: Combustion characteristics of *Lantana camara* (LC) char blends (wt.% of biomass) with Inyanda coal, showing (a) DTG curves for torrefied char at 300 ˚C (LC300), (c) influence of blending ratios on combustion indices for LC300 blends, (b) DTG curves for pyrolysed char at 522 ˚C (LC522) and (d) influence of blending ratios on combustion indices for LC522 blends.

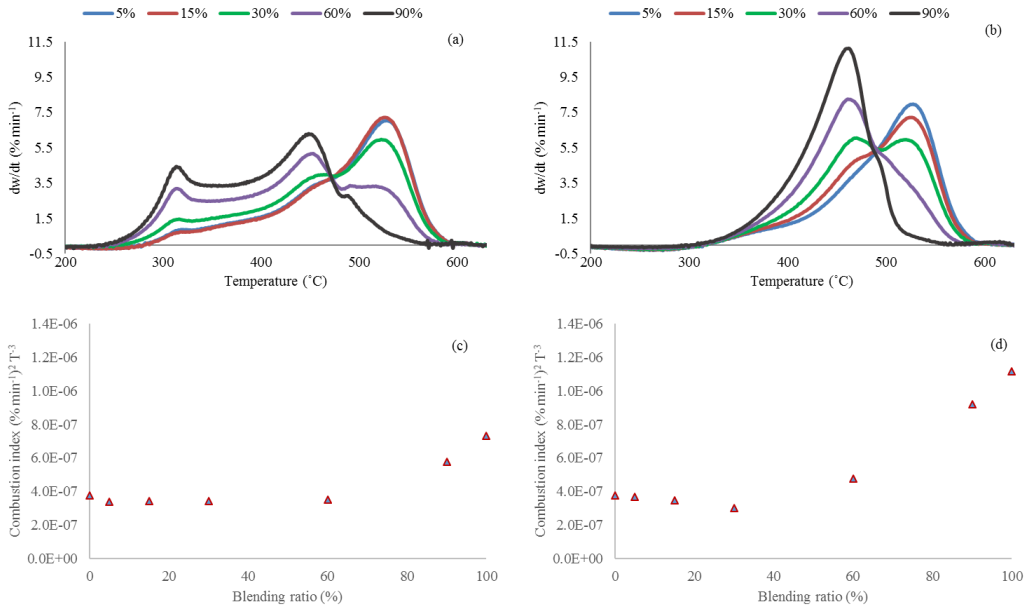

Figure 7-3: Combustion characteristics of *Mimosa pigra* (MP) char blends (wt.% of biomass) with Inyanda coal, showing (a) DTG curves for torrefied char at 300 ˚C (MP300), (c) influence of blending ratios on combustion indices for MP300 blends, (b) DTG curves for pyrolysed char at 578 ˚C (MP578) and (d) influence of blending ratios on combustion indices for MP578 blends.

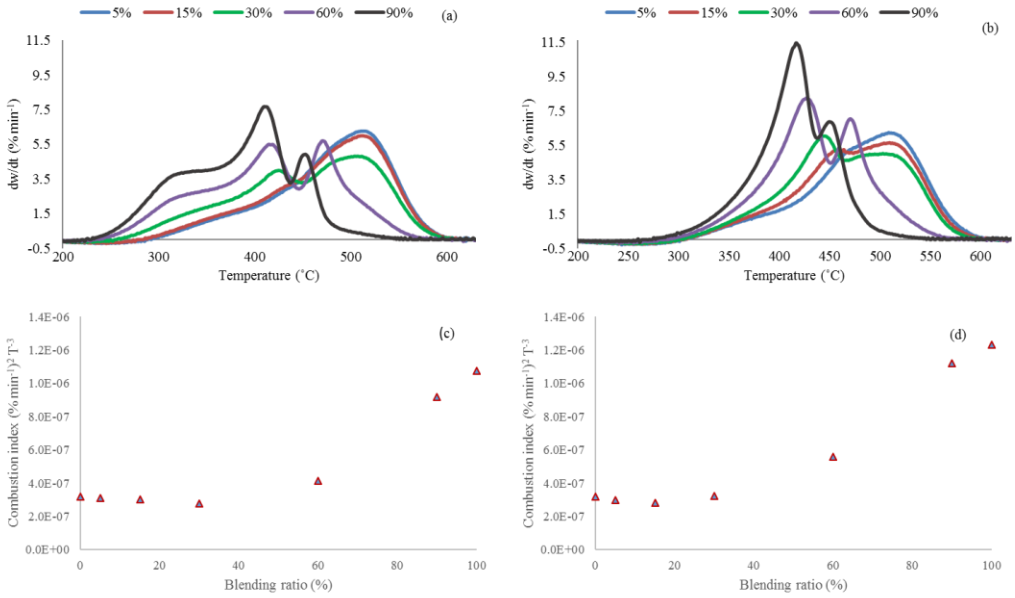

Figure 7-4: Combustion characteristics of *Lantana camara* (LC) char blends (wt.% of biomass) with Phalanndwa coal, showing (a) DTG curves for torrefied char at 300 ˚C (LC300), (c) influence of blending ratios on combustion indices for LC300 blends, (b) DTG curves for pyrolysed char at 522 ˚C (LC522) and (d) influence of blending ratios on combustion indices for LC522 blends.

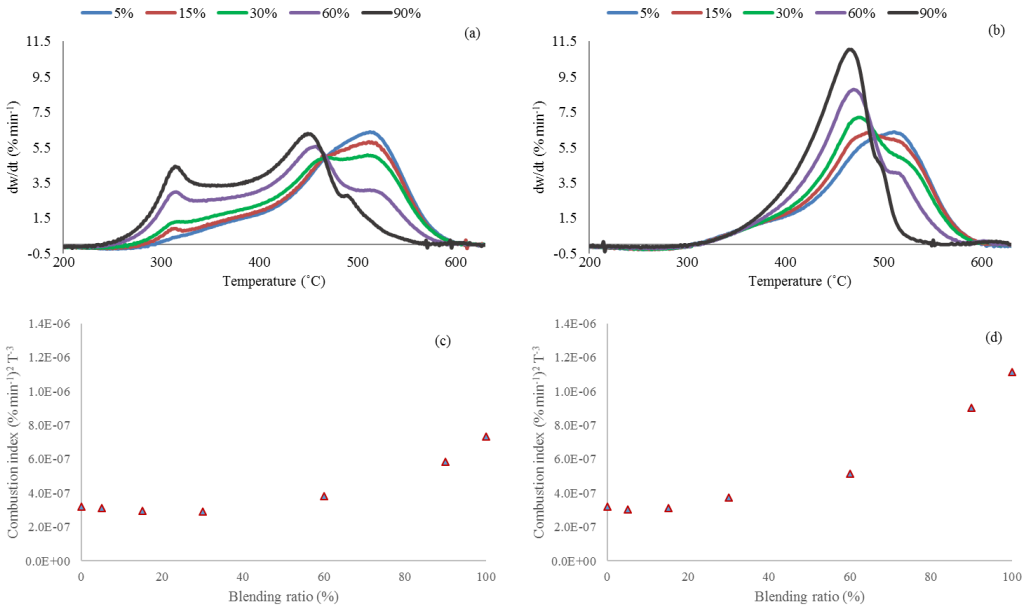

Figure 7-5: Combustion characteristics of *Mimosa pigra* (MP) char blends (wt.% of biomass) with Phalanndwa coal, showing (a) DTG curves for torrefied char at 300 ˚C (MP300), (c) influence of blending ratios on combustion indices for MP300 blends, (b) DTG curves for pyrolysed char at 578 ˚C (MP578) and (d) influence of blending ratios on combustion indices for MP578 blends.

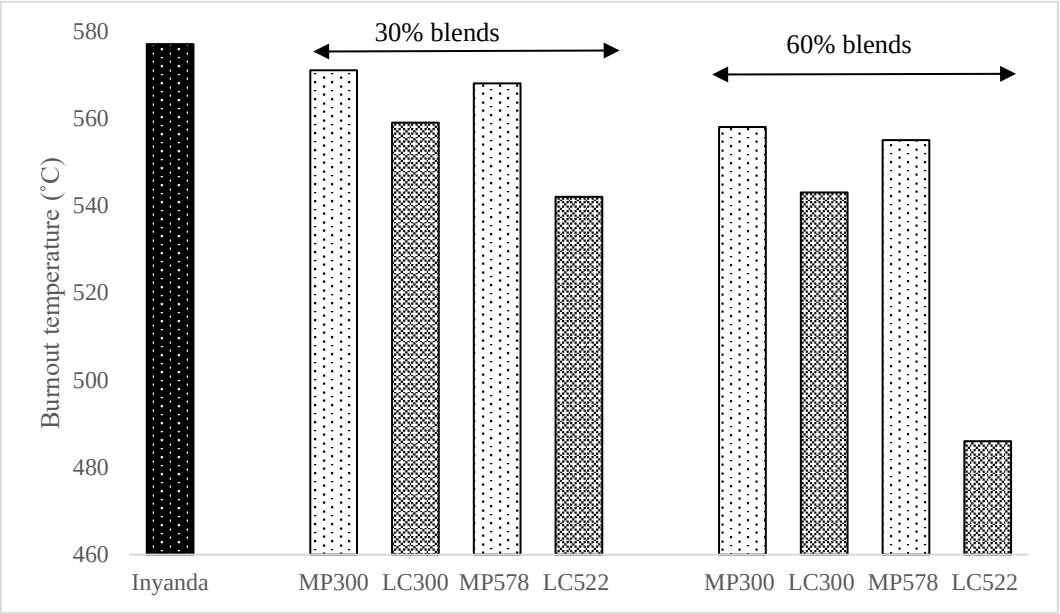

Figure 7-6: Influence of lignocellulosic char composition on burnout temperature reduction for Inyanda coal blended with *Mimosa pigra* (MP) and *Lantana camara* (LC), for torrefied chars, MP300 and LC300 and pyrolysed chars, MP578 and LC522, using char blending ratios of 30 and 60% with the parent coal.

Chapter 8 **Potential application of chars produced from LC and MP**

Objective of dissertation in this chapter

This chapter mainly addresses specific **objective four** that deals with the potential energy applications, based on some results from **Chapters 5 to 7** and additional relevant parameters measured according to some analytical techniques described in **Chapter 4.**

8.1 Introduction

Chapter 5 mainly addressed **objectives one and two,** dealing with the identification of fuel properties and determining the influence of thermal process variables on char yields and properties, respectively, at milligram-scale under torrefaction conditions, while **Chapter 6** answered issues related to **objectives one and two, as well as objective three** (determining heat and mass transfer effects on char yield and its properties) under slow pyrolysis, both at milligram-scale and gram-scale. **Chapter 7,** mainly addressed **objective four** (investigating combustion characteristics and assessing the potential applications), utilising char from gram-scale in order to study the combustion behaviour of selected parent chars, three South African coals and their blended samples. The results from **Chapter 7** were mainly biased towards co-firing of LC and MP with coal using selected samples prepared via torrefaction or slow pyrolysis.

Chars of different qualities were obtained from torrefaction and slow pyrolysis as described in **Chapters 5 and 6**, respectively. These chars have to be compared with other solid fuels in order to discuss their potential use. Among the solid fuels used in this dissertation, are two commercial charcoals for domestic use from Namibia and Zambia. Additionally, three South African coal samples (detailed in **Chapter 4**) were also used for comparative purposes in combustion study in order to assess the potential of using LC and MP chars for substituting Zambian coal, as outlined in (**Chapter**

2, Table 2-2). All these aspects of the study are included in this current chapter, specifically focussing on the aspect of potential applications.

8.2 Possible applications for LC and MP chars

The current section discusses the potential domestic and industrial energy applications of the chars from LC and MP, with reference to summarised fuel properties in Table 8-1 and combustion characteristics in Table 8-2.

Table 8-1: Compositions of various fuels used in this study in terms of bulk density (Bρ), volatile matter (VM), fixed carbon (FC), ash and higher heating value (HHV)

Sample	Bρ (kg m^{-3})	VM (%)	FC (%)	Ash (%)	HHV (MJ kg^{-1})
LC300	203	41.8	53.7	4.5	27.0
LC440	184	27.4	66.8	5.8	28.8
LC522	184	16.4	76.7	6.9	29.1
LC570	190	13.6	79.1	7.4	30.1
LC614	191	11.9	80.6	6.9	30.8
LC635	191	9.8	82.7	7.1	30.0
MP300	254	50.9	45.9	3.1	24.4
MP440	237	29.5	65.1	5.4	27.5
MP517	229	19.6	74.5	6.1	30.3
MP578	228	14.7	78.4	6.5	30.7
MP619	236	8.7	84.0	6.2	31.4
MP698	244	7.6	85.5	6.7	31.6
MP749	245	6.8	87.1	6.9	29.8
Nam-char[1]	315	18.0	73.1	8.9	27.1
Zam-char[2]	380	7.8	87.4	4.9	29.6
Zam-coal specs[A]	-	< 19.0	> 64.0	< 16.0	> 27.0
Zam-coal specs[B]	-	22.0 – 27.0	50.0 – 62.0	< 30.0	23.4 – 26.3
Zam-coal specs[C]	-	28.0 – 40.0	> 56.0	14.0 – 20.0	20.0 – 22.0
Inyanda coal	770	22.2	60.4	17.5	26.5
Tshikondeni coal	786	22.8	62.4	14.8	29.6
Phalanndwa coal	708	27.3	57.0	15.8	27.3

Note: [1]: Nam-char; Namibian charcoal prepared from local invasive plants; [2]: Zam-char; Zambia charcoal prepared from local miombo trees, **Chapter 4**, section 4.1.3; [A, B, C]: Zam-coal specs; Zambian coal specifications in **Chapter 2**, section 2.2.2.3. All the *Lantana camara* (LC) and *Mimosa pigra* (MP) chars were prepared at gram-scale using particle size distribution from 850 to 2800 µm. The values after each of the char samples correspond to the maximum sample temperature (˚C).

8.2.1 Use as domestic charcoal

Two commercial charcoals were considered for this study for comparisons with LC and MP chars, a Namibian charcoal produced from IAPs and a Zambian charcoal produced from indigenous miombo wood as earlier stated. Table 8-1 shows the compositions of various solid fuels used in this study. The Zambian charcoal is of better quality due to a lower ash content and VM, probably due to

conversion at higher temperature, resulting in an HHV of 29.6 MJ kg^{-1}. In order to produce a fuel similar to the Namibian charcoal (27.1 MJ kg^{-1} with VM of 18.0 wt.%), torrefaction conversion was not sufficient, as the produced chars are characterised by too high VM (> 40 wt.%), not desirable for domestic application. For both LC and MP, a pre-treatment temperature higher than 500 ˚C would be required to reduce the VM to less than 20 wt.% while obtaining an HHV above 27.0 MJ kg^{-1} (LC522 and MP517 for instance). For a higher quality charcoal with VM lower around 10 wt.% as the Zambian charcoal, a conversion temperature higher than 600 ˚C would be recommended. Such quality was observed for MP619 and LC614, together with HHVs above 30.0 MJ kg^{-1}. Table 8-2 shows the combustion characteristics of selected chars in comparison with the two commercial charcoals. T_{ig} for the chars prepared at T > 550 ˚C were similar to those of the Namibian and Zambian charcoals, showing that the commercial charcoals were certainly prepared at temperature higher than 550 ˚C.

Table 8-2: Combustion characteristics of selected char samples of *Lantana camara* (LC) and *Mimosa pigra* (MP) and two domestic charcoals

Sample	T_{ig} (˚C)	T_{bo} (˚C)	DTG_{max} (% min^{-1})	DTG_{mean} (% min^{-1})	C_i (% min^{-1})^2 T^{-3}
LC440	295	471	12.5	4.8	1.5 x 10^{-6}
MP440	308	502	10.0	4.5	9.4 x 10^{-7}
LC522	323	476	11.6	5.1	1.2 x 10^{-6}
MP578	354	500	12.0	5.7	1.1 x 10^{-6}
LC614	330	468	13.1	6.0	1.5 x 10^{-6}
MP698	375	513	12.8	5.1	9.1 x 10^{-7}
Nam-char[1]	359	505	13.5	5.2	1.1 x 10^{-6}
Zam-char[2]	383	509	14.3	6.5	1.2 x 10^{-6}

Note: [1]: Nam-char; Namibian charcoal prepared from local invasive plants; [2]: Zam-char; Zambia charcoal prepared from local miombo trees, **Chapter 4**, section 4.1.3. All the *Lantana camara* (LC) and *Mimosa pigra* (MP) chars were prepared at gram-scale using particle size distribution from 850 to 2800 µm. The values after each of the char samples correspond to the maximum sample temperature (˚C).T_{ig}: ignition temperature; T_{bo}: burnout temperature; $DTG_{max/mean:}$ maximum/average char combustion rate based on the percentage of the original sample C_i: combustion index as a measure of combustion efficiency.

The T_{bo} values for MP578 and MP698 were similar to the Namibian and Zambian charcoals, while a lower value was observed for LC614. As a consequence, the C_i for LC614 was found to be highest, which means that with this fuel the heat would be generated more quickly.

8.2.2 Use as coal substitute

From Table 8-1, char samples have lower bulk densities than coal which would require some adaptations in order to take into account the differences. In case of co-feeding with relatively low ratio of char, the blends between coal and char would generally result in a fuel mixture with homogeneous bulk density closer to that of coal.

Based on communications with some Zambian industries, three types of coal were considered for this study (Table 8-1). Company C has the least HHV requirements from 20.0 to 22.0 MJ kg^{-1}, which would require a torrefaction temperature < 300 ˚C, even though the VM was higher than the specifications and lower FC. Coal specifications for company B have HHV requirements falling in the range of sub-bituminous coal (23.4 to 26.3 MJ kg^{-1}). For both LC and MP, torrefaction would be suitable to prepare similar quality of fuel as torrefaction at 300 ˚C resulted in product with HHV above 24.0 MJ kg^{-1}. Based on HHV, MP300 (24.4 MJ kg^{-1}) had a suitable energy content while LC300 (27.0 MJ kg^{-1}) was characterised by a higher value. However, amongst these two samples, only LC300 was able to meet the specifications for FC requirements for company B, which ranged from 50.0 to 62.0 wt.%, while the FC for MP300 was far below the requirements. The VM contents from both torrefied chars were above the specified requirements for all the three Zambian companies, though LC300 was more by close to 2 wt.%. A similar trend was generally observed when comparing coal and char with similar HHV. In this study the ash content of coal was always higher than 14 wt.%, while lower than 9 wt.% for the biomass chars. As the VM has a positive effect on HHV (though lower than FC), at similar HHV, chars were generally characterised by higher VM and lower FC content.

In case of char HHVs obtained from slow pyrolysis, LC and MP samples pyrolysed at 440 ˚C were able to meet the energy requirements of company A, with FC content higher than 64 wt.% and HHV specifications > 27.0 MJ kg^{-1}.

Based on the co-combustion study in **Chapter 7,** the addition of biomass char at blending ratios lower than 30% would not affect significantly the combustion performance. This was observed for char prepared between 300 and 578 ˚C. As a consequence, for production of similar amount of heat with similar combustion performance in current combustion reactors, it appears that a pre-treatment temperature of 440 ˚C would be adequate to produce enough heat.

Chapter 9 Conclusions and recommendations

This work has shown that invasive alien plants (IAPs) namely *Lantana camara* (LC) and *Mimosa pigra* (MP), have the potential of being utilised as feedstock materials for char generation for domestic and industrial energy applications. The main conclusions and recommendations for future works, based on experimental results are discussed in this chapter.

9.1 Conclusions

Torrefaction and slow pyrolysis process optimisation for maximising char generation at milligram-scale showed that temperature played a major role in influencing char yields and the accompanying char quality in terms of energy properties for LC and MP samples. The use of IAPs, in this case, LC and MP as feedstocks, could offer an opportunity for producing char for domestic and industrial co-firing purposes. Based on optimised process conditions for torrefaction and slow pyrolysis, char yields increased by 2 to 4 wt.% due to the effects of scale-up from milligram-scale to gram-scale, with MP richer in lignin recording the highest char yield results. Scaling-up effects also resulted in increased fixed carbon and HHV, as the optimal temperature increased, with the highest optimal HHV temperature obtained from MP (698 ˚C). During torrefaction, LC richer in hemicelluloses produced a char of superior quality equivalent to that of high volatile bituminous *C* coal, with HHV up to 27 MJ kg^{-1}. However, the char fuel qualities were reversed during slow pyrolysis at optimised process conditions, with MP obtaining better char HHV of 31.6 MJ kg^{-1} compared with LC (30.8 MJ kg^{-1}).

The combustion characteristics of the parent fuels showed that lignocellulosic chars were more reactive than coal. LC char samples whether torrefied or pyrolysed, showed more reactivity than MP chars, with char maximum combustion rates increasing with an increase in pre-treatment temperature

for both samples. Similarly, LC char samples recorded a superior combustion efficiency than MP char samples. As a consequence, blended samples with coal showed that LC char had the greatest impact on lowering the combustibility temperatures of all the three coals than MP. Co-combustion characteristics for blends up to 15% showed similarities with those of the parent coals, with the combustion process occurring in the coal combustion region. Practically, for the short term use of renewable resources, blends up to 15% could have an advantage over higher blending ratios, as equipment design may not need any modifications as combustion occurs within coal combustion region for which the equipment was originally designed.

9.2 Recommendations

Based on the conclusions of this work, further research could be conducted on the following key areas to compliment the findings of this thesis.

During combustion study, it was observed that co-combustion characteristics for blends up to 30% were found to be closely related to those of the parent coal, especially in terms of combustion indices (measure of combustion performance). Additionally, the combustion process for these blends occurred in the coal combustion region. A further study at pilot-scale is hereby proposed to confirm these results. This study would be useful to confirm that the use of biomass char would not affect the energy efficiency of the process, while reducing the production of pollutant emissions.

Increased char yield and energy properties results were obtained due to increased particle size and sample bed (from milligram to gram-scale). A further study on scale-up of the processes from gram-scale to kg-scale is therefore recommended. The proposed kg-scale study would account for the expected effects of scale-up on char yields and the accompanying energy properties. The detailed study would allow the obtaining of more accurate results for mass and energy balances. In particular,

the composition and energy content of the bio-oil and gas products could be studied. From these results the techno-economics of the entire process could be evaluated. To make the process more viable, the combustion of the bio-oil and/or gas products could be considered in order to provide for the heat required for the torrefaction/pyrolysis conversion. Furthermore, with data available at kg-scale, a life cycle assessment for the entire process could be conducted.

Appendices

Appendix A Torrefaction

Table A-1 Average (Av) and standard deviation (SD) for *Lantana camara* (LC) char yield (wt.%) and higher heating value (HHV; MJ kg^{-1}) at each temperature, hold time (HT) and heating rate (HR)

Sample	Temperature (˚C)	HT (min)	HR (˚C min^{-1})	LC char (Av)	SD (±)	HHV (Av)	SD (±)
LC12	197.1	52.5	11.0	96.44	0.04	18.84	0.03
LC5	220.0	25.0	16.0	94.67	0.13	18.94	0.06
LC1	220.0	25.0	6.0	94.17	0.15	19.21	0.29
LC6	220.0	80.0	16.0	91.55	0.04	19.31	0.18
LC2	220.0	80.0	6.0	91.02	0.11	19.18	0.02
LC14	250.0	4.0	11.0	92.16	0.25	19.13	0.21
LC11	250.0	52.5	19.8	80.69	0.01	19.88	0.04
LC9.1	250.0	52.5	11.0	80.18	0.01	20.92	0.03
LC9.2	250.0	52.5	11.0	79.87	0.63	20.96	0.03
LC10	250.0	52.5	2.2	79.51	0.12	20.42	0.01
LC15	250.0	101.0	11.0	75.60	0.02	20.94	0.04
LC7	280.0	25.0	16.0	65.97	0.02	22.37	0.01
LC3	280.0	25.0	6.0	65.71	0.01	22.14	0.14
LC8	280.0	80.0	16.0	52.42	0.04	24.95	0.31
LC4	280.0	80.0	6.0	51.95	0.00	24.88	0.14
LC13	302.9	52.5	11.0	43.38	0.02	27.13	0.08
				Av.SD	0.10	Av. SD	0.10

Table A-2 Average (Av) and standard deviation (SD) for *Mimosa pigra* (MP) char yield (wt.%) and higher heating value (HHV; MJ kg^{-1}) at each temperature, hold time (HT) and heating rate (HR)

Sample	Temperature (˚C)	HT (min)	HR (˚C min^{-1})	MP char (Av)	SD (±)	HHV (Av)	SD (±)
MP12	197.1	52.5	11.0	97.85	0.00	18.43	0.03
MP5	220.0	25.0	16.0	96.24	0.00	18.93	0.45
MP1	220.0	25.0	6.0	95.67	0.01	19.05	0.15
MP6	220.0	80.0	16.0	93.04	0.15	19.42	0.03
MP2	220.0	80.0	6.0	92.60	0.11	19.05	0.01
MP14	250.0	4.0	11.0	94.72	0.02	19.16	0.01
MP11	250.0	52.5	19.8	82.76	0.11	20.76	0.04
MP9.1	250.0	52.5	11.0	82.61	0.07	19.99	0.06
MP9.2	250.0	52.5	11.0	82.67	0.11	19.85	0.03
MP10	250.0	52.5	2.2	82.30	0.05	20.04	0.04
MP15	250.0	101.0	11.0	79.53	0.08	20.92	0.18
MP7	280.0	25.0	16.0	72.84	0.06	21.80	0.06
MP3	280.0	25.0	6.0	72.68	0.00	21.11	0.07
MP8	280.0	80.0	16.0	66.04	0.10	22.15	0.04
MP4	280.0	80.0	6.0	65.69	0.10	21.93	0.04
MP13	302.9	52.5	11.0	52.14	0.07	24.54	0.27
				Av. SD	0.07	Av. SD	0.10

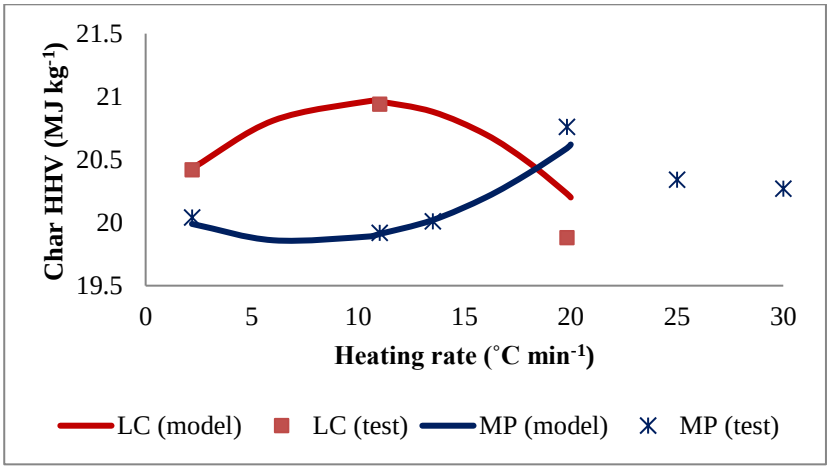

Figure A-1 Optimised heating rate conditions of the model and test results of *Lantana camara* (LC) and *Mimosa pigra* (MP) char HHV at 250 ˚C using HT (52.5 min)

Appendix B Slow pyrolysis

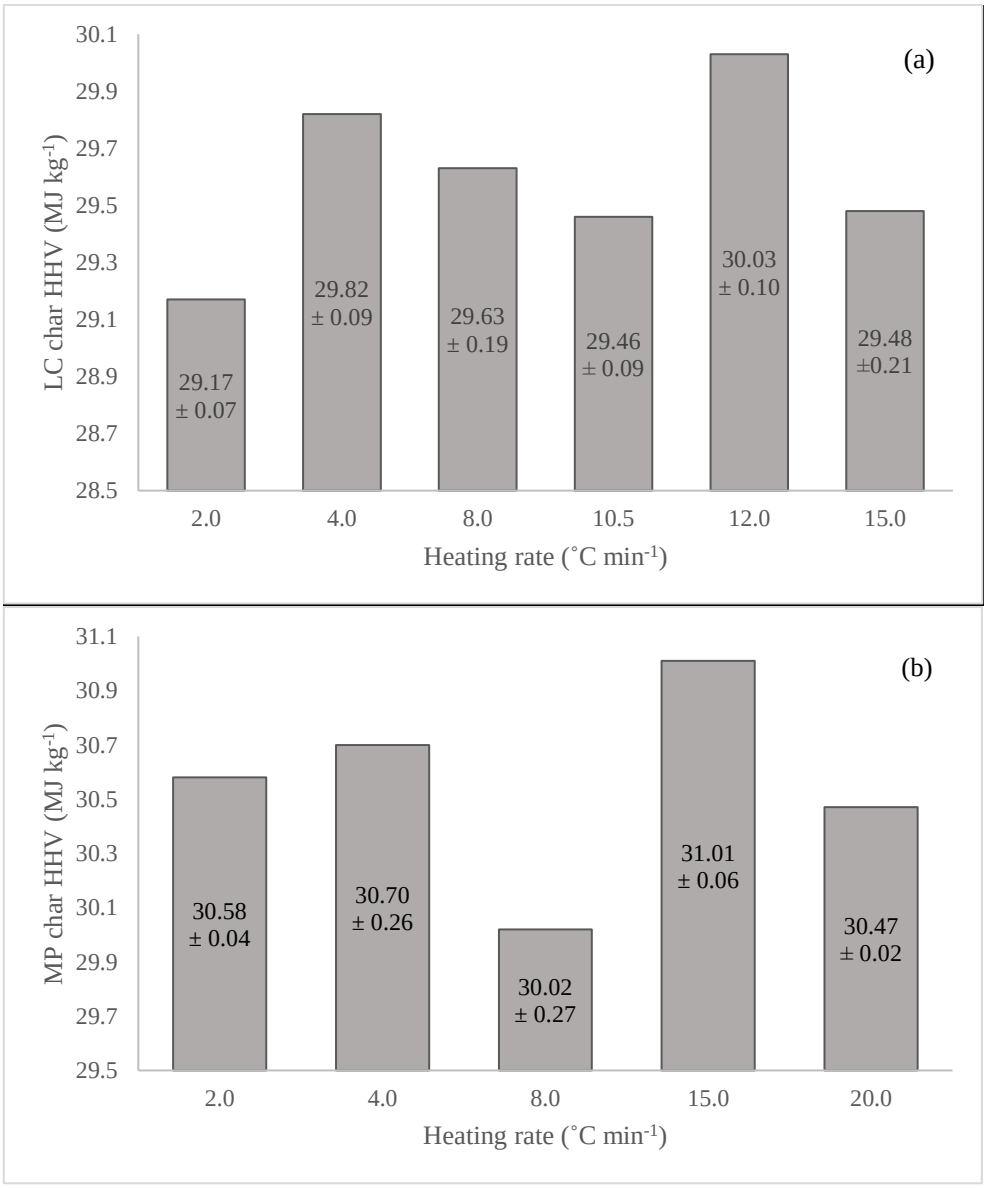

Figure B-1 Influence of heating rate on char higher heating value (HHV; MJ kg^{-1}) at milligram-scale for (a) *Lantana camara* (LC) at the optimal HHV temperature of 525 ˚C with variable heating rates from 2 to 15 ˚C min^{-1} (b) *Mimosa pigra* (MP) at the optimal HHV temperature of 580 ˚C with variable heating rates from 2 to 20 ˚C min^{-1}.

Appendix C Co-combustion characteristics of coal with Invasive Alien Plant chars prepared by torrefaction or slow pyrolysis

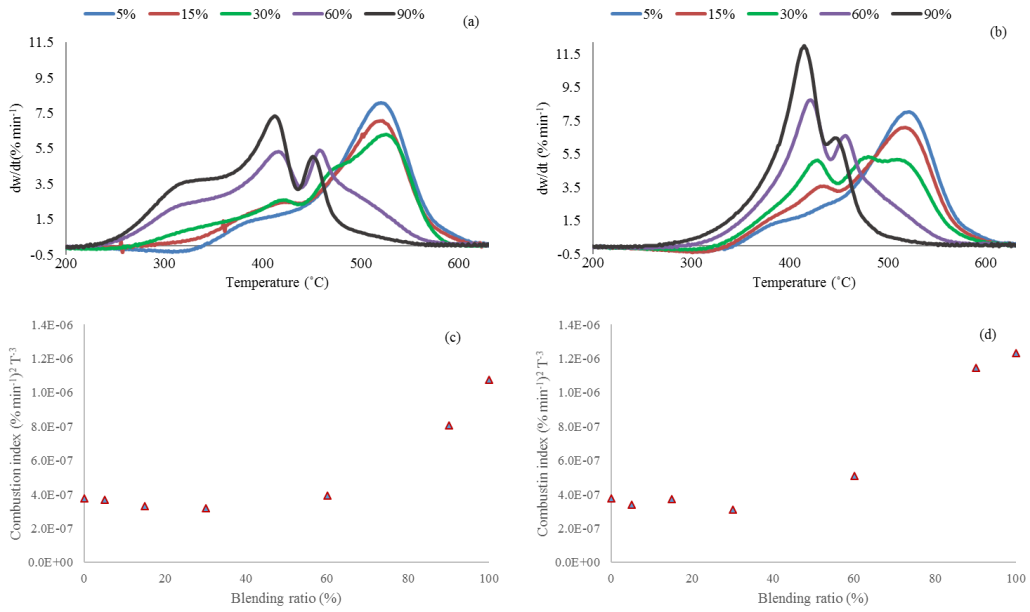

Figure C-2 Combustion characteristics of *Lantana camara* (LC) char blends (wt.% of biomass) with Tshikondeni coal, showing (a) DTG curves for torrefied char at 300 ˚C (LC300), (c) influence of blending ratios on combustion indices for LC300 blends, (b) DTG curves for pyrolysed char at 522 ˚C (LC522) and (d) influence of blending ratios on combustion indices for LC522 blends.

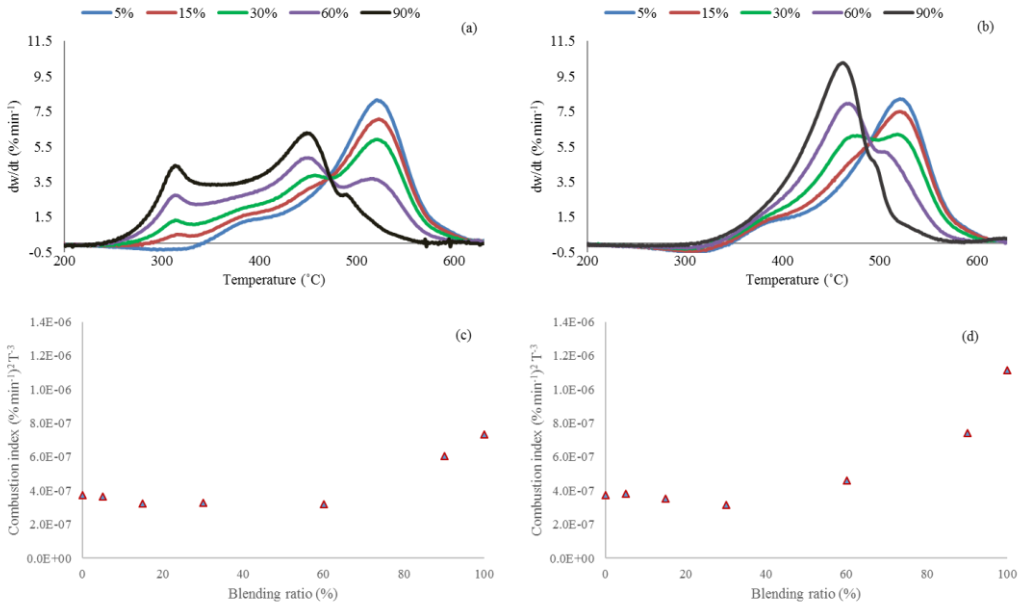

Figure C-3 Combustion characteristics of *Mimosa pigra* (MP) char blends (wt.% of biomass) with Tshikondeni coal, showing (a) DTG curves for torrefied char at 300 ˚C (MP300), (c) influence of blending ratios on combustion indices for MP300 blends, (b) DTG curves for pyrolysed char at 578 ˚C (MP578) and (d) influence of blending ratios on combustion indices for MP578 blends.